CAROTID ARTERY LONGITUDINAL WALL MOTION

CAROTID ARTERY LONGITUDINAL WALL MOTION: REGULATORY FACTORS AND IMPLICATIONS FOR ARTERIAL HEALTH

By JASON S. AU, Hon.B.Sc.Kin

A Thesis Submitted to the School of Graduate Studies In Partial Fulfillment of the Requirements for the Degree Doctor of Philosophy

McMaster University © Copyright by Jason S. Au, September 2017

DOCTOR OF PHILOSOPHY (2017) McMaster University
Kinesiology Hamilton, Ontario

TITLE: Carotid artery longitudinal wall motion: Regulatory factors and implications for arterial health

AUTHOR: Jason S. Au
Hon.B.Sc.Kin (McMaster University)

SUPERVISOR: Maureen J. MacDonald, Ph.D.

NUMBER OF PAGES: xvii, 173

LAY ABSTRACT

We have known for a long time that arteries expand in order to absorb pressure; however, only recently have we identified that arteries also move longitudinally along the length of the arterial wall. The overarching purpose of this dissertation was to study what causes carotid artery longitudinal wall motion (CALM), and how we can use this information to understand arterial health. We demonstrated that CALM is partly controlled through the forward blood velocity wave and left ventricular rotation of the heart, and that diastolic CALM is uniquely related to aging and health status, but is not impacted by exercise training in healthy men. There are many aspects of CALM that need to be examined before wide-spread use, though our results indicate that CALM represents a new way of studying arterial health, which has the potential to complement traditional measures of cardiovascular disease risk in humans.

ABSTRACT

The carotid artery wall moves longitudinally along the length of the vessel, although little is known about what causes this motion, or what health information it represents. The overarching purpose of this dissertation was to investigate the regulation of carotid artery longitudinal wall motion (CALM) in humans, as well as how CALM can be used to infer information about arterial health. Through observational and experimental designs, we tested evidence for a structural ventricular-vascular coupling effect, which postulates that systolic anterograde CALM is influenced by the forward blood shear rate while systolic retrograde CALM is influenced by left ventricular rotation, although the data suggests a moderate influence of left ventricular rotation, and minimal influence of shear rate. In cross-sectional analyses, we demonstrated that diastolic CALM variables are better related to age and health status compared to systolic CALM displacement and that this relationship was independent of traditional measures of arterial stiffness. These experimental and observational results directed the use of diastolic CALM as a potential indicator of arterial health in subsequent studies, due to the relative independence from systolic events. While there was no effect of 12-weeks of exercise training in healthy men on diastolic CALM variables, we observed increased systolic retrograde CALM and diastolic CALM acceleration in men with a history of resistance exercise training compared to sedentary men, suggesting an effect of habitual exercise training. Our novel findings suggest that CALM is regulated by a complex system, in part related to both arterial wall structure and ventricular-vascular coupling, and may have clinical value in complimenting measures of traditional arterial stiffness in humans. Future studies should

examine whether local changes to arterial wall structure or indirect changes in regulatory control dictate differences in CALM with aging and with chronic exercise training, before integrating CALM into routine measurement of arterial health.

ACKNOWLEDGEMENTS

This thesis would not be possible without the help of many individuals, who, through kindness and dedication, have supported me through my doctoral studies. First and foremost, I would like to thank Dr. Maureen MacDonald for supporting my development as a scientist from day one, and for all the opportunities you've offered me during my time at McMaster. We've come a long way to where we are today, and many of our accomplishments wouldn't be possible had you not supported my ideas and 'detours' along the way. I'm sincerely grateful for your mentorship and friendship and look forward to continuing to working with you throughout the rest of my academic career. My studies have also been supported by an excellent and engaging group of mentors, and would also like to thank Dr. Stöhr, Dr. Hughson, Dr. Hicks, and Dr. Ditor for their insight and suggestions for the design and interpretation of these studies. The foundation for this thesis would not be possible without your help, and I highly value our meetings early during this thesis as well as the intellectual challenges you posed during this last year.

My nine years at McMaster have been the best years of my life, in part due to the wonderful individuals I have met in kinesiology. In particular, I would like to thank Julia, Lisa and Jenna for setting me on the path of academia, and lab mates Patrick, Nicole, Ninette, Jem, Stacey, Johnny, Josie, Sydney, and Paula, for your friendship and support in science (and keeping me sane during the long analysis hours in the lab). Thank you Mark for keeping me grounded, Calvin and Alison for being the best officemates a guy could ask for, Skelly for being a wonderful human being, and Sara for always keeping me in line (and for pointing out every potential Hephy). The KGB has been a source of positive energy and moral support, and I want to thank every member that has made the last few years so special.

Thank you to the EMRG group for the collaboration that was essential to complete this thesis, in particular to Dr. Phillips and Dr. Gibala and their respective labs for allowing me to join their high quality trials to advance our knowledge of cardiovascular exercise physiology. Thank you to Todd, Dam, and John, for your patience in helping me being a better scientist and for everything you do for the EMRG group. Thank you to Rebecca, Glenna, Doris, Carol, and Lydia, who keep this ship afloat, and for your patience and kindness in managing every grad student that comes through those doors. None of us could do it without you.

Thank you to my family and friends outside the realm of science for supporting me in my studies, and putting up with my lame science facts and jokes over the last five years, and the countless more after this degree!

And finally, thank you Jem, for your love and support both in and out of the lab; I couldn't have finished this degree without you. Whether it's a last minute deadline, a series of injuries, or just a really awful day, you're always there for me when I need it most. I'm so proud of what we've both accomplished together and I'm so excited for what's in store for us in the future.

TABLE OF CONTENTS

LISTS OF FIGURES AND TABLES

FIGURES

CHAPTER 4: Cardiac and hemodynamic determinants of carotid artery longitudinal wall motion

CHAPTER 5: The effect of exercise training on carotid artery longitudinal wall motion

TABLES

CHAPTER 2: Carotid artery longitudinal wall motion is associated with local blood velocity and left ventricular rotational, but not longitudinal, mechanics

CHAPTER 3: Diastolic carotid artery longitudinal wall motion is sensitive to both aging and coronary artery disease status independent of arterial stiffness

CHAPTER 4: Cardiac and hemodynamic determinants of carotid artery longitudinal wall motion

CHAPTER 5: The effect of exercise training on carotid artery longitudinal wall motion

LIST OF ABBREVIATIONS

AET	aerobic exercise training
CAD	coronary artery disease
CALM	carotid artery longitudinal wall motion
CCA	common carotid artery
CPT	cold pressor test
CVD	cardiovascular disease
cfPWV	carotid-femoral pulse wave velocity
cIMT	carotid intima-media thickness
ECG	electrocardiogram
EX-CTL	exercising control group
HR	heart rate
HR-RET	higher-repetition resistance exercise training
IMT	intima-media thickness
LR-RET	lower-repetition resistance exercise training
LV	left ventricle
LVT	left ventricular twist
MBV	mean blood velocity
MDV	mean diastolic velocity
MICT	moderate-intensity continuous exercise training
MIDA	maximum instantaneous diastolic acceleration
MIDV	maximum instantaneous diastolic velocity
NTG	nitroglycerin
OHA	older healthy adults
PP	pulse pressure
PWV	pulse wave velocity
RET	resistance exercise training
SED-CTL	sedentary control group
SIT	sprint-interval exercise training
SST	serial subtraction test
VO_2max	maximal oxygen consumption
YHA	younger healthy adults

PREFACE
DECLARATION OF ACADEMIC ACHIEVEMENT

FORMAT AND ORGANIZATION OF THESIS

This thesis is prepared in the "sandwich" format as outlined in the School of Graduate Studies' Guide for the Preparation of Theses. It includes a general introduction, four independent studies prepared in journal article format, and an overall discussion. The candidate is the first author on all of the manuscripts. At the time of the thesis preparation, Chapters 2 and 3 were published in peer-reviewed journals, while Chapter 4 and Chapter 5 were in preparation for submission.

CONTRIBUTION TO PAPERS WITH MULTIPLE AUTHORSHIP

Chapter 2 (Study 1):
Au J.S., Ditor D.S., MacDonald M.J., Stöhr E.J. (2016). Carotid artery longitudinal wall motion is associated with local blood velocity and left ventricular rotational, but not longitudinal, mechanics. *Physiol Rep* 4(14): e12872.

Contributions:

Conceived and designed the research: JA, DD, MM, ES
Acquired the data: JA
Analyzed and interpreted the data: JA, MM, ES
Performed statistical analyses: JA
Drafted the manuscript: JA
Critical revision of the manuscript: JA, DD, MM, ES

Chapter 3 (Study 2):
Au J.S., Valentino S.E., McPhee P.G., MacDonald M.J. (2017). Diastolic carotid artery longitudinal wall motion is sensitive to both aging and coronary artery disease status independent of arterial stiffness. *Ultrasound Med Biol* [in press]; doi:10.1016/j.ultrasmedbio.2017.04.026

Contributions:

Conceived and designed the research: JA, MM
Acquired the data: JA, SV, PM
Analyzed and interpreted the data: JA, SV, MM
Performed statistical analyses: JA, PM
Drafted the manuscript: JA
Critical revision of the manuscript: JA, SV, PM, MM

Chapter 4 (Study 3):
Au J.S., Bochnak P.A., Valentino S.E., Cheng J.L., Stöhr E.J., MacDonald M.J. (2017). Cardiac and hemodynamic determinants of carotid artery longitudinal wall motion. *In preparation.*

Contributions:

Conceived and designed the research: JA, PB, SV, ES, MM
Acquired the data: JA, JC, PB, SV
Analyzed and interpreted the data: JA, JC, PB, SV, ES, MM
Performed statistical analyses: JA
Drafted the manuscript: JA
Critical revision of the manuscript: JA, PB, SV, JC, ES, MM

Chapter 5 (Study 4):
Au J.S., Shenouda N., Oikawa S.Y., Gillen J.B., Morton R.W., Gibala M.J., Phillips S.M., MacDonald M.J. (2017). The effect of exercise training on carotid artery longitudinal wall motion. *In preparation*.

Contributions:

Conceived and designed the research: JA, MM
Acquired the data: JA, NS, SO, JG, RM
Analyzed and interpreted the data: JA, MM
Performed statistical analyses: JA
Drafted the manuscript: JA
Critical revision of the manuscript: JA, NS, SO, JG, RM, MG, SP, MM

CHAPTER 1:

INTRODUCTION

1.1 PREAMBLE: PERIPHERAL ARTERY HEALTH AND CVD RISK PREDICTION

Peripheral arterial health has emerged as an independent predictor of cardiovascular disease (CVD) risk across a number of diverse populations, and has been suggested to provide information complementary to that obtained from the assessment of traditional indicators of risk, such as blood lipids, body composition and insulin resistance (15, 52). The predominant peripheral artery health indicators include non-invasive measures of endothelial function (156), carotid intima-media thickness (cIMT) (160) and arterial stiffness (161). Although endothelial function has been shown to have utility in delineating between populations at risk for CVD, as well as in predicting future CVD events (131, 179), it is technically difficult to perform, reliant on difficult methods and lengthy analysis and there are substantial concerns about the reliability of measures (118). cIMT measurement is an easier technique to perform, dependent on vascular ultrasound and simple wall tracking software, and is independently related to CVD endpoints in older populations (86). However, the utility in measuring cIMT progression over time and/or treatment is contested (87), with some work indicating the presence of carotid plaque and cardiac calcium score are superior for predicting coronary artery disease (47). Conversely, the feasibility of assessing arterial stiffness has increased due to the development of non-invasive and inexpensive pressure measuring devices. This relative ease of data acquisition has supported the inclusion of arterial stiffness measurements in several large scale, prospective population studies (5, 93, 147, 176), each offering high quality evidence for the role of arterial stiffness in CVD. Importantly, arterial stiffness is an independent predictor of both cardiovascular events and the development of CVD in

late adulthood (15), including coronary heart disease and stroke (91), first-onset cardiovascular disease events (93), and all-cause mortality (166).

Given the independent predictive capability of arterial stiffness, the transition from a tool used exclusively for scientific experimental measurement to a tool incorporated in clinical assessment has slowly been occurring over the last decade. Currently, there are multiple commercially available arterial stiffness measurement devices marketed towards clinicians for use in medical practice (e.g., Complior (9), SphygmoCor (108)), and even more recently, personal arterial stiffness measurement devices for home-based use (e.g., iHeart (51)). The advantages of including arterial stiffness in clinical assessments of CVD risk and progression include the relative simplicity in measurement, strong scientific rationale, and accessibility for repeated measurement over time. Although challenges remain in the adoption of measures of arterial stiffness into routine CVD risk assessment, recent recommendations by the European Society of Hypertension and the European Society of Cardiology advise for the measurement of arterial stiffness for enhanced stratification for CVD (89), thereby supporting its use in clinical practice.

The measurement of arterial stiffness is based on the fundamental properties of the arterial wall and how vascular researchers can infer precise mechanical information from wall motion. However, the use of arterial stiffness as a monitoring tool for cardiovascular health is not a perfect science, with many influencing aspects of arterial structure and function left ignored or understudied. The development of novel, non-invasive, imaging devices has allowed for the development of potentially superior indicators of arterial

stiffness, which can improve the quality of data acquisition, account for blood pressure-dependent effects, and simplify interpretation of outcomes. Specifically, while the pressure-buffering function of arterial wall distension has been studied in great depth, very little is known about axial (longitudinal) motion of the arterial wall, and its implications for vascular structure and function. The purpose of this review of the literature is to highlight the current standards in arterial stiffness measurement and to discuss the advancement of longitudinal, rather than radial, motion of conduit arteries as a novel indicator of arterial structure and function.

1.2 ARTERIAL WALL ANATOMY

The arterial wall is a dynamic organ, with functional responsibilities critical for distributing pressure stress evenly across the vasculature, as well as maintaining nutrient delivery to the peripheral organs. The arterial wall is made of three layers: the tunica intima, composed of endothelial cells attached to a basement membrane; the tunica media, which houses vascular smooth muscle needed for neural control of vasoconstriction and vasodilation; and the tunica adventitia, the structural foundation of the artery (129). As it is difficult to isolate the tunica intima from the tunica media, the layers are commonly studied as the intima-media complex for simplicity in imaging and tissue mechanics studies. When under experimental strain, the intima-media complex undergoes burst fragmentation at lower pressures than the adventitia (60 vs 250 kPa), supporting the structural role of the adventitia in mitigating cyclic distension of an artery (136). Tunica functions are largely determined by their structural composition, ranging in

different proportions of elastin fibres, collagen fibres and vascular smooth muscle cells, each of which have unique properties relevant to health of the vascular wall.

Together, elastin and collagen compose ~50% of the total dry weight of the central elastic arterial wall (55). At low intraluminal pressures, elastin is organized into wavy three dimensional lamellar sheets, which elongate and straighten at higher intraluminal pressures (175). In comparison, collagen is found in bundles throughout the extracellular matrix, and aligns circumferentially under high intraluminal pressures (175). Stress-strain experiments on porcine aortas also suggest collagen fibres are circumferentially aligned, as thoracic aorta segments are more likely to undergo circumferential crack propagation during force-extension ('tear') tests (121). The importance of these properties is seen in a two-phase stress-strain relationship, where the incremental Young's elastic modulus rapidly increases over a short range, indicating the shift between deformation of the elastin to collagen fibres in the extracellular matrix as pressure increases (16, 167). As the arterial wall is a heterogeneous structure, elastin and collagen properties act together to define the elastic properties of an arterial segment.

There is a gradual shift in arterial wall anatomy from the central elastic vasculature to the more peripheral muscular arteries closer to the capillaries. As neatly demonstrated in porcine models, the arterial wall of the aortic arch has a higher proportion of elastin (~30%) compared to collagen (~20%), which reverses in the lower abdominal aorta to a much lower proportion of elastin (~10%) compared to collagen (~40%). Smooth muscle makes up the remainder of the wall composition with a relatively high proportion in the aortic arch (135). Substantial elastin formation does not occur

beyond the first year of life (90), which predisposes a gradual shift towards a higher percentage of collagen in the central arteries. While an entire field of literature is devoted to the causes of arterial stiffening, there exists substantial evidence for the role of the collagen:elastin ratio in focal and diffuse arterial stiffness (24). The 'fatigue fracture' hypothesis of aging suggests that exposure to constant loading conditions on the elastin fibres (~30 million beats/year) gradually results in fragmentation over the lifespan, contributing to the age-related increase in arterial stiffness (107). Changes in elastin and collagen content may be related to elevated matrix metalloproteinases (e.g., MMP-2, MMP-9), which degrade both elastin and collagen, and are related to arterial stiffness in younger adults and adults with isolated systolic hypertension (177, 178). Increased collagen:elastin ratio has also been linked to arterial pulsatility (40), calcification (13), and inflammation (92), all of which are prominent features of vascular aging.

1.3 RADIAL ARTERIAL WALL MOTION

The vast majority of vascular physiology has focused on the pressure-buffering capacity of the vascular wall. Distension of the vascular wall acts as a multipurpose damping system in order to absorb the forward pressure wave to reduce high pressure-induced end-organ damage, as well as store a portion of the energy through the elastic wall fibres to release during diastole to reduce pulse pressure. This property is reflected by arterial stiffness and can be estimated from a propagative model, which assumes central generation of a forward pressure wave through a visco-elastic tube with branching points towards high levels of resistance (81). Arterial stiffness can be estimated from multiple

non-invasively measured variables (Figure 1), which all give an indication of the primary function of radial arterial wall motion - the pressure buffering capacity of an arterial segment. A wide range of these measurement variables have been shown to be associated with traditional risk factors for CVD and some have been further found to be independent predictors for CVD risk (161).

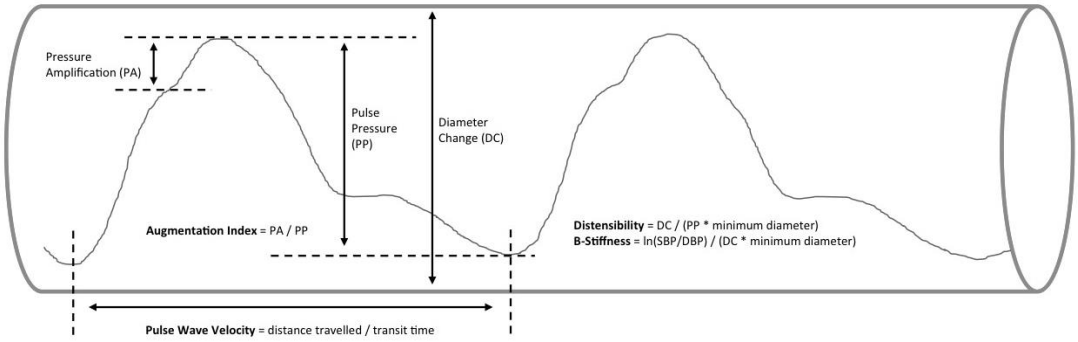

Figure 1. Non-invasive measures of arterial stiffness. Pulse wave velocity and augmentation index can be generated solely from the pressure wave, while distensibility and β-stiffness index also rely on the diameter change across the cardiac cycle.

1.3.1 Measurement of arterial stiffness

1.3.1.1 *Pulse Wave Velocity*

Carotid-femoral pulse wave velocity (cfPWV) is the reference standard for the assessment of central arterial stiffness, with standard guidelines clearly outlined by experts in the field (81, 161, 163). Working under the assumption of linear propagation of a pressure wave throughout the vascular tree, the speed of a pulse wave can be estimated

by measuring the time delay of pulse arrival at two arterial sites, and dividing by the distance between those sites [Eq1] (162):

$$PWV = \frac{Distance}{Pulse\ transit\ time} \quad \text{[Eq1]}$$

cfPWV has emerged as the standard for central arterial stiffness as it is easily measured, and estimates the stiffness of the large central elastic aorta. In order to account for the discrepancy in path length when the ascending aorta branches to the common carotid arteries, true path length is estimated as 80% of the total body surface distance between the carotid and femoral artery sites (67). However, distance estimation is the greatest limitation to cfPWV, as accurate path length measurement is difficult, especially in individuals with abdominal obesity.

PWV can also be measured at other arterial segments, most commonly measured as brachial-ankle PWV (baPWV) (145, 146). While baPWV has been used as a substitute for cfPWV, vascular inferences are limited by the inclusion of more muscular arteries along the measurement path, which have a smaller role in the pressure-buffering vascular system (128, 151). In comparison, central arteries are more clinically relevant to central hemodynamics, as the left ventricle of the heart works directly against the pressure in the proximal aorta (81). Furthermore, any changes in peripheral artery PWV may not necessarily be related to arterial stiffness, as sympathetic tone plays a much greater role in muscular arteries (58, 61). Indeed, between-limb differences may also confound systemic health inferences from peripheral PWV measurements. For example, significant

variability has been observed in affected *vs* non-affected limbs in individuals with diabetes (184), as well as patients with hemiparesis (110).

cfPWV has been touted as the reference standard for arterial stiffness measurement due to its simplicity, accessibility, and support from the literature, however, it is not without limitations (10). Palpation of the femoral artery can be difficult in some populations (e.g., obese individuals), or be perceived as an invasive method in others (e.g., children, Japanese culture). Furthermore, the pressure-dependent nature of PWV is a significant confounder in interpreting increasing PWV with age and hypertension. There is a direct relationship between PWV and blood pressure (77, 106), where increases in pressure are related to faster pulse wave transmissions. There is now enough evidence to reasonably suggest that arterial stiffening is a cause, rather than a consequence of hypertension (70, 85, 100), although it difficult to evaluate the direct effects of improving the arterial stiffness profile with concomitant improvements in the blood pressure profile. Development of pressure-independent metrics of arterial stiffness would be of value to directly assess the impact of arterial stiffening on CVD risk across different stages of hypertension and treatment.

1.3.1.2 *Arterial Distensibility*

While arterial stiffness can be estimated from the speed of a pulse wave, this is based on a propagative circulatory model (Moens-Korteweg equation) of which the pulse wave speed is directly proportional to the elastic modulus of the system (21). It is also possible to directly measure local stiffness of an arterial segment through calculation of arterial

distensibility, which can be estimated from a pulsatile model of the change in vessel cross-sectional area for a given change in blood pressure [Eq2] (48, 113):

$$Distensibility = \frac{CSA_{Max} - CSA_{Min}}{PP \times CSA_{Min}} \quad \text{[Eq2]}$$

where CSA_{Max} is the maximum cross-sectional area, CSA_{Min} is the minimum cross-sectional area and PP is pulse pressure. Local pulse pressure is estimated by local applanation tonometry, calibrated to simultaneous brachial or finger blood pressure. Calibration is valid in the supine position, as diastolic and mean arterial pressure are relatively consistent through the arterial tree, which can be used to forecast local systolic blood pressure from tonometry voltages (116).

Distensibility is inversely related to pulse wave velocity, but as it is a local index of vascular stiffness, the measure contributes unique information to CVD risk prediction. CCA distensibility is associated with increased risk of cardiovascular events, cardiovascular mortality and all-cause mortality (165, 186), with a notable association with risk of stroke in prospective longitudinal studies (109, 176).

The measurement of arterial distensibility is not without limitations. This technique requires a high amount of skill, as well as two trained operators to assess simultaneous diameters and pressures. Blood pressure should be measured locally at the carotid artery, rather than peripherally estimated from brachial sphygmomanometry or finger plethysmography (112). Furthermore, experiments eliciting different vascular

loading conditions indicate that differences in CCA distensibility may be driven by the distending pressure, rather than intrinsic stiffness of the arterial wall (112, 125). Due to the increasing stiffness of the arterial wall from central to peripheral arteries, distensibility of one arterial segment does not represent the whole system. For example, carotid distensibility is two times greater than that of femoral distensibility across a database of reference values in healthy adults (20, 42). While there is certainly a relationship between CCA distensibility and CVD risk, the limitations in operator skill and generalizability to the entire vascular tree make it unlikely that distensibility can be used in routine clinical practice for CVD risk assessment.

1.3.1.3 *β-Stiffness Index*

The noted limitations of local distensibility are problematic when observing a large range of blood pressures in cross-sectional analyses. In response to the pressure dependent limitations, Hirai et al. (1989) developed a pressure-independent index of vascular wall stiffness (64), building upon small sample pilot data from the same group [Eq3] (74):

$$\beta - Stiffness = \frac{ln\left(\frac{SBP}{DBP}\right)}{\left(\frac{LDmax - LDmin}{LDmin}\right)} \quad \text{[Eq3]}$$

where SBP is systolic blood pressure, DBP is diastolic blood pressure, LDmax is maximum lumen diameter and LDmin is minimum lumen diameter. To test pressure independence, the β-stiffness index was tested in eight patients post-myocardial infarction during intravenous nitroglycerin infusion, which yielded no change in β-stiffness across

all levels of systolic blood pressure (64). Although these results are widely cited by vascular physiologists, the blood pressure-independence of β-stiffness has recently been challenged (133, 139, 140) due to modification of the original formula (74), which can be corrected by subtraction the natural log of DBP/100mmHg .

The β-stiffness index is established as a validated measure of arterial structure, although it has not received as wide-spread attention as cfPWV or CCA distensibility. As its measurement uses the same techniques as distensibility, the limitations are the same, with the added complexity of interpreting the mathematical-based output of the equation.

1.3.1.4 *Augmentation Index*

While a typical blood pressure wave can be simplified as a single wave, in reality, it is composed of both a forward pressure wave originating from the left ventricle, as well as a backward compression wave caused by wave reflections from the distal arterial tree. The summation of these pressure waves in the central elastic arteries results in a complex waveform with an early systolic shoulder, and a clear systolic peak. The difference between the waveform shoulder and peak is termed pressure augmentation, and when expressed relative to the pulse pressure, represents the augmentation index (AIx) (76).

While AIx can be measured in any conduit artery (65), AIx estimated from central pressure waveforms (115) has been shown to be predictive of cardiovascular disease events, heart failure and all-cause mortality (25, 168). The relationship between AIx and arterial stiffness is primarily driven by differences in wave propagation, with reductions in reflection time being associate with higher PWV (119). However, other factors are also

likely to influence AIx, most notably heart rate, through a reduction in absolute systolic time (173). For this reason, AIx is typically standardized at 75bpm (AIx@75) to control for interindividual differences in heart rate. AIx is also influenced by age (43), thought to be due to a distal shift in the site of wave reflection caused by increasing stiffness of the central arteries (144), although this theory has recently been contested (119). Gender is also a consideration in measurement, though this is likely due to differences in height between men and women (57). Although the measurement of AIx and reflected waves have demonstrated success in predicting cardiovascular disease risk, current recommendations for the measurement of arterial stiffness do not include AIx as a surrogate for stiffness, as PWV is only one of many factors that may influence AIx (161). Even so, measurement of AIx@75 is not likely to fade from standard arterial assessments, as the ease of collection with peripheral tonometry waveform systems makes the study of central pressure augmentation both feasibly acquired and easily interpreted.

1.4 LONGITUDINAL ARTERIAL WALL MOTION

Longitudinal motion of an arterial wall segment was first observed *in vivo* by suturing reflective beads to the aorta in dogs in 1956 (82), although at the time it was largely disregarded as breathing artifact. In fact, the topic of longitudinal movement of the arterial wall has scarcely been acknowledged; for example, a single sentence on the topic can be found in *McDonald's Blood Flow in Arteries*: "*[Excised arterial retraction], together with the finding that there is very little, if any, longitudinal movement of the artery during passage of the pulse wave, led to the concept called* tethering *of arteries*"

(101). The first ultrasonic-based measurements did not re-assess this motion phenomenon until 2002, with the implementation of vascular speckle-tracking image analysis (117). In the first report by Persson et al. (2002), carotid artery longitudinal wall motion (CALM) was described as being of the same magnitude as radial wall motion, with a substantially different movement pattern. These observations form the first published suggestions of the complex regulatory factors likely dictating the CALM pattern. Since this first description, there has been increasing interest in developing more accurate measurement systems for the quantification of longitudinal motion (27, 153, 188), and more recently, decomposition of the pattern to base elements in order to infer arterial wall properties that may offer additional utility in the assessment and prediction of cardiovascular disease risk (150, 189).

In general, CALM has been described as being comprised of a cyclic biphasic movement pattern within each heart cycle, with motion occurring in both the anterograde (i.e., with the direction of blood flow) and retrograde (i.e., against the direction of blood flow) directions. Distinct from the pattern of radial arterial distension, there is significant inter-individual differences in CALM traces, which has contributed to the initial difficulty in interpreting motion traces in both healthy and chronic disease populations. Yli-Olilla et al. (2013) attempted to distinguish three general types of movement patterns observed in healthy adults: primarily anterograde motion patterns, with wall displacement consistently distal to the reference position at end-diastole; oscillatory patterns, with wall displacement equally spread both distal and proximal to the reference position; and primarily retrograde motion patterns, with wall displacement consistently proximal to the

reference position (180). These patterns are easily found within random samples of the healthy adult population (Figure 2), with no discernable method to stratify individual patterns based on anthropometrics or demographics. With respect to these observations, the majority of the literature has focused on developing methods to standardize quantification of CALM for comparison across a wide range of individuals.

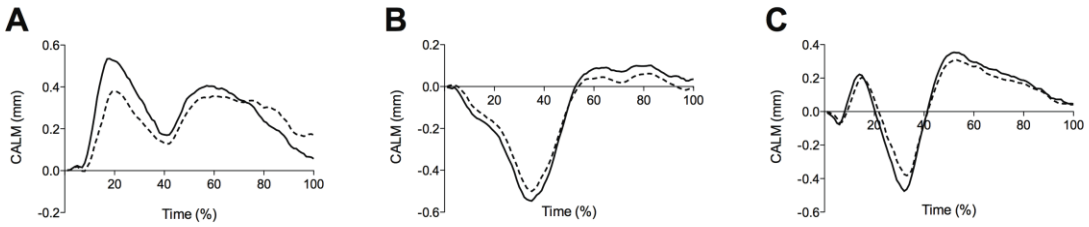

Figure 2. Carotid artery longitudinal wall motion patterns can be broadly categorized into primarily: A) anterograde; B) retrograde; or C) biphasic motion traces. The intima-media (IM) longitudinal wall motion is presented in solid lines, whereas the adventitial (ADV) longitudinal wall motion is presented in dashed lines. Shear strain is positive when the IM moves greater than the ADV in the anterograde direction, and is negative when the IM moves greater than the ADV in the retrograde direction. Each example represents a group-averaged trace (n_i=10) of healthy adults, normalized to a single cardiac cycle and gated to the R-spike of the ECG recording.

1.4.1 Measurement of CALM: Speckle-tracking algorithms

Arterial distension is typically assessed using edge-detection software, taking advantage of the distinct hyper- and hypo-echoic layers of the arterial wall (120) to identify long continuous sections of an arterial wall boundary (84). While this method is adequate for tracking one-dimensional arterial motion, it is unable to assess motion in other planes.

Therefore, speckle-tracking algorithms have primarily been employed to track two-dimensional movement, making use of the heterogeneous echogenicity of the arterial wall and surrounding tissue. Although speckle-tracking has been popularized by speckle echocardiography (97), there has recently been increased development of simple custom speckle-tracking software for 2D motion estimation of the arterial wall (27, 153, 188).

In brief, most speckle-tracking programs identify a region of interest (ROI) of a unique segment of the arterial wall (e.g., the intima-media or adventitial arterial wall layers), composed of a unique combination of greyscale pixels in an ultrasound image. A cross-correlation coefficient is then used to compare this reference ROI to subsequent frames in a cineloop, identifying a new ROI with the highest correlation coefficient. This shift in ROI is interpreted as wall motion in both the x (radial) and y (longitudinal) planes, which when pieced together across an entire heart cycle, gives a complete motion trace. The advantages of this method include excellent time resolution (depending on frame rate acquisition) and 2D motion variable estimation (i.e., position, velocity, acceleration). However, speckle-tracking has been criticized for potential of error due to 'speckle drift' with lengthy analysis windows. The cross-correlation method may become invalid should the coefficient drop below 0.7, indicating a severe departure from the reference ROI (44). Drift may be caused by low frame rates, increased lumen backscatter, or high velocity wall movements, all of which make it difficult to follow a specific set of pixels over time.

1.4.2 CALM Measurement Variables

While the general CALM pattern has now been well reported in recent literature, there is ongoing debate over which outcome variables best represent the complex motion over the duration of a cardiac cycle. Previously published CALM variables include different indexes of longitudinal displacement, a longitudinal attenuation coefficient, intramural shear strain, and motion complexity. Each variable is based on a set of assumptions, and has specific advantages and disadvantages in terms of standardizing the measurement of longitudinal wall motion for associations with arterial health.

1.4.2.1 *Displacement*

The simplest of CALM variables, the first description of the CALM pattern was conservatively made as absolute maximum wall displacement (117). While more complex indices have emerged, maximum wall displacement is commonly reported as a 'catch-all' description of CALM, with average values reported in the range of 0.42 mm to 0.64 mm (50, 188, 189). Maximum wall displacement is markedly lower in older individuals with diabetes (188), Indigenous Australians with periodontal disease (189), and adults with carotid plaque (149), compared to healthy younger adults. Segmented displacements have also been reported, including displacements during the initial anterograde (A1) phase, a retrograde (R1) phase, and a second anterograde (A2) phase (26). This segmented description of the CALM pattern is likely the smallest increment of motion that can be reliably measured in longitudinal motion traces from apparently healthy individuals. The segmented CALM method has been well described in younger healthy adults (1, 102,

103), although, there is a need for data in individuals with CVD or with high CVD risk to compare this measure to more established indicators of arterial health.

There is scarce information on the reproducibility of CALM displacement, with few reports in the last decade (1). Day-to-day coefficients of variation have been reported between ~10% to 30% depending on the phase of the CALM pattern (e.g., poorer CV% for anterograde motion) (28, 148, 153, 180, 181, 188). While these statistics are promising for the use of CALM as a vascular tool for longitudinal measurement of arterial health, additional long-term studies are needed to assess the stability in clinical populations, or the natural progression in CALM pattern across the lifespan.

Although displacements are a simple method to describe the CALM pattern, interpretation is limited by numerous factors. The tissue surrounding the CCA also moves in the same general pattern as the intima-media and adventitial layers (26), bringing into question whether intima-media displacement is a local descriptor of arterial structure, or is the product of large scale displacement of the entire vessel. There also appears to be a direct influence of arterial segment location, and an indirect influence of participant height, on absolute displacement magnitudes. Zahnd et al. (2014) demonstrated a gradual attenuation of motion along the length of the CCA, from 5 cm to 1 cm proximal to the carotid bifurcation (187), making comparison of single-location displacements difficult to interpret between individuals.

1.4.2.2 Longitudinal Attenuation Coefficient

In a small sample of healthy adults, Zahnd et al. (2014) reported a gradual attenuation of CALM displacement at three points along the length of the CCA, with an average attenuation coefficient of -2.5±2.0 %/mm distal to the left ventricle (187). These results have not been replicated in other participant populations, however, the authors speculate that the motion attenuation coefficient may be reflective of local arterial stiffness properties. Theoretically, motion could be reduced along the length of an artery due to two factors: a gradual loss of energy along the length of the artery, originating from a central source; or, attenuation related to the gradual shift in the vascular wall composition (i.e., smooth muscle, elastin, collagen) from the central elastic arteries to the peripheral muscular arteries (135). At this time, the regulation of arterial wall motion is not well understood and it is not clear whether why attenuation occurs, or whether attenuation represents local arterial stiffness properties. Although this measure appears to better capture the motion within an entire CCA segment rather than a discrete location, there have been no follow-up reports of attenuation coefficients in the literature, inviting both population comparisons and experimental investigation as to the relevance of the index to arterial health.

1.4.2.3 *Shear Strain*

Greater motion of the intima-media complex compared to the adventitia allows for the calculation of intramural shear strain as a variable of relative wall motion (26). Shear strain is independent from extravascular tissue motion, and is calculated as the shearing

angle between two parallel regions of interest in the intima-media and adventitial arterial wall layers [Eq4]:

$$shear\ strain = arctan\left\{\frac{[LPos_{IM} - LPos_{IM(ref)}] - [LPos_{Adv} - LPos_{Adv(ref)}]}{radial\ distance\ between\ ROI\ of\ IM\ and\ Adv}\right\} \quad \text{[Eq4]}$$

where LPos is longitudinal position, IM is intima-media, Adv is adventitia, and ref is reference frame. In humans, the absolute amount of longitudinal shear strain in healthy adults is comparable across studies (26, 28, 153), and is reduced in older individuals with spinal cord injuries (153).

While the measurement of shear strain appears to circumvent the limitations of measuring absolute wall motion, there is scarce data to support the validity of physiologically-relevant information in humans. The main limitation is that shear strain is dependent upon the pattern of CALM, and whether there is a primarily anterograde, retrograde, or biphasic displacement of the wall across a cardiac cycle. For example, it is unknown whether shear strain values from an individual with primarily anterograde CALM (and therefore only positive shear strain angles; Figure 2A) are comparable to an individual with primarily retrograde CALM (and therefore only negative shear strain angles; Figure 2B). As shear strain has only been investigated by two research groups (26, 153), these ambiguities are not clearly addressed in the literature. Further studies investigating other population groups are required to determine the added utility of measuring shear strain compared to other previously reported CALM variables.

1.4.2.4 *Motion Complexity*

Rather than separate the CALM pattern into segments, or take maximal values throughout the entire heart cycle, measures of motion complexity aim to characterize the entire CALM pattern with a single variable. The complex motion trace can be fitted to a higher-order polynomial (PolyDeg), with successful fitting of the data achieved at a Pearson's correlation coefficient of greater than 0.95 (180). The PolyDeg measure takes advantage of common local maxima and minima during the longitudinal cycle in order to circumvent the substantial interindividual variability reported in healthy adults. Due to the oscillatory diastolic period, CALM is typically fit to a 6^{th} to 8^{th} degree polynomial in healthy individuals (180, 181), with no data in older or unhealthy adults. In a small healthy sample (n=19), Yli-Ollila et al. (2015) reported moderate correlations between PolyDeg and estimated central vascular variables (i.e., AIx, aortic augmentation, systolic pressure time index) (181), although this relationship with arterial health was not replicated in a larger study (n = 292) with more established vascular variables (outcomes: flow-mediated dilation, PWV, IMT) (150). Given that the oscillatory longitudinal pattern in diastole would be heavily influenced by heart rate, it is unclear whether the PolyDeg measure is an appropriate representation of CALM in all individuals.

Arterial wall motion can also be quantified as the total wall displacement in both the radial and longitudinal directions within a single cardiac cycle (radial-axial length, [RAlength]) (180). Total wall excursion (measured as distance in mm) may be a better global measure of wall motion, as it fully takes into account 2D motion of the wall and can be easily visualized as a motion loop. RAlength decreases with age (181) and is

moderately related to CCA distensibility (150), although this is likely related to the radial component of RAlength, as distensibility is also measured in the radial direction. While the RAlength measure is able to fully capture 2D wall displacement across the cardiac cycle, it is difficult to separate the radial- *vs* longitudinal-specific vascular information from this global index.

1.4.3 Regulation of CALM: Experimental Evidence

Although the CALM pattern has been well described in several previous populations, little is known of the regulation of this wall motion. In particular, the determinants of the shape of the movement pattern and the large pattern variability in healthy populations remain unexplained. With the first observations of motion, multiple suggestions were put forward to explain the shape of the pattern, including: the shear force of the blood flow, the longitudinal tension and elastic recoil of the arterial wall, left ventricular basal displacement and the influence of reflective pressure waves from the periphery (26); however, no experimental evidence has been offered to test these hypotheses. In fact, there have only been three experimental studies reported by the same research group, performed in a porcine model of cardiovascular physiology to examine the regulation of CALM. In the first case report in a series of studies, Ahlgren et al. (2009) investigated the acute effects of epinephrine administration on absolute wall motion and shear strain index (3). These authors reported a ~200% increase in maximum CALM displacement and ~250% increase in intramural shear strain concurrent with a ~50 mmHg increase in intra-arterial mean blood pressure. While the acute increases in CALM were attributed to α-

adrenergic sympathetic activation, the authors were only able to acquire 2D wall motion, without measurement of either pressure waves or blood flow through the vessel, making it difficult to interpret the direct role of sympathetic activation on CALM.

In a first follow-up study, the authors investigated the effects of both low and high doses of epinephrine, combined epinephrine and norepinephrine, and β-blockade (metoprolol) on CALM in five additional pigs (2). During low-dose epinephrine infusion (relatively greater action on β_2-receptors *vs* α-receptors), pulse pressure decreased concurrent with reductions in maximal CALM displacement, whereas high-dose epinephrine (relatively greater action on α-receptors) greatly increased both pulse pressure and maximal CALM displacement. These effects were not reversed by the β_1-specific blocker metoprolol, indicating the effects were predominantly α-adrenergic mediated. The authors attributed these CALM modifications to the increases in blood pressure and α-adrenergic mediated constriction of vascular smooth muscle.

Finally, in a continuation report in the same group of pigs, the authors described a lack of a relationship between changes in arterial wall shear rate (the axial force of blood on the vessel wall) and maximal CALM displacement induced through catecholamine administration (4). While the authors concluded that changes in CALM can occur independent of blood flow wall shear rate, these results are largely qualitative in nature, relying on observations of beat-to-beat data. Furthermore, correlations between the change in shear rate and CALM were performed within an individual, and did not take into account other possible regulatory factors, such as vessel diameter, blood pressure or

left ventricular influence. Therefore, it may be premature to eliminate wall shear rate as a potential regulator of CALM.

The above animal models have laid the groundwork for further experimental studies in humans to investigate the regulatory control of CALM. However, there are major questions on the validity of the CALM observations in the porcine model, as well as the applicability to human studies. The porcine CALM traces presented in these studies are noticeably different from human recordings, characterized by a predominantly anterograde wall displacement with a much smaller diastolic anterograde displacement than that observed in many human carotid arteries (153, 180). In contrast, many healthy human CALM patterns present with a more biphasic trace, with large retrograde displacements in the systolic period (153, 180). Although porcine physiology is considered similar to that of humans (155), there are morphological differences between species that call into question the validity of a porcine CALM model. Anatomically, the 'valentine-shaped' porcine heart is suspended by the major blood vessels with the apex resting on the ventral wall of the thorax (34). Porcine hearts perform relatively higher work due to nearly twice the systemic vascular resistance (155), which is evident in the relatively thicker LV trabeculations and LV wall compared to humans (34). To further study the effects of acute sympathetic manipulation on CALM, these studies need to be reproduced in human participants, with concurrent measurement of other potential regulators of longitudinal motion.

1.4.4 Regulation of CALM: Mathematical Evidence

Recently, there has been increasing interest in the influence of the distending pressure wave in the shape of the CALM pattern in healthy humans. One current hypothesis proposes that the unique CALM pattern is dictated by the distending pressure wave, which is supported by a proof of concept study in healthy participants (182, 183). With principal component analysis, Yli-Ollila et al. (2016a) determined that there are two principal components of longitudinal wall motion; the first component being related to the biphasic pattern and pulse pressure, while the second component is potentially related to arterial stiffness (182). While intriguing, this study included a relatively small sample of healthy adults (n=19), likely with a limited range of arterial stiffness. Furthermore, principal component analysis is a fairly advanced regression method, which requires a large sample to be generalizable to population levels (30, 53). Future studies should expand the design to include participants at risk for CVD or with elevated arterial stiffness to confirm these findings.

In a separate report by the same group, transfer function analysis was also applied to a small sample of healthy adults in order to probe the energy transfer within the arterial wall (183). The authors reported a time delay between movement of the intima-media and adventitia, as well as a partly linear relationship between the diameter change and longitudinal wall motion. While the authors provided a tenuous relationship between longitudinal wall motion and blood pressure, this was based on the assumption that brachial blood pressure is equal to the carotid artery diameter change, which may not be an accurate representation of central blood pressure (116).

While it is of interest to continue mathematical analysis of the CALM pattern, it presents an isolated view of a physiological model that does not consider the additional control mechanisms previously suggested (i.e., shear rate, elastic recoil, or left ventricular motion). Left ventricular motion, in particular, is an interesting candidate to expand this hypothesis as it is the central driver of blood pressure waves and undergoes unique displacement in the same plane as CALM.

1.5 LEFT VENTRICULAR MECHANICS

The left ventricle (LV) is a powerful pump that controls the ejection of oxygenated blood from the heart to the rest of the body. LV motion has previously been theorized to influence the CALM pattern (26), potentially through displacement of the aortic root towards the LV apex (134). While intriguing, the relationships between either traditional LV functional indices (i.e., ejection fraction, longitudinal strain, LV volumes) or novel LV mechanics (i.e., LV rotation) with CALM have not been investigated.

1.5.1 Left ventricular anatomy

Compared to the low-pressure pulmonary system faced by the right ventricle, the LV must overcome the systemic pressure in the proximal aorta in order to open the aortic valve to eject blood. This difference in function is demonstrated through the orientation of the ventricular muscle band, which primarily coils around the left ventricle to provide three-dimensional control of contraction (159). The unique orientation of the ventricular muscle band forms three distinct myocardial layers: the deep subendocardium, the

midwall myocardium, and the superficial subepicardium. Myocardial fibres in the subendocardium are oriented in a right-handed helix, while fibres in the subepicardium are oriented in a left-handed helix, as if the fibres were tightly wrapped around a sphere. In comparison, the midwall layer is composed of concentric rings, similar to a stack of fibres wrapped around a cylinder (130).

The contraction of myocardial tissue determines the stroke volume of the LV, and provides an indication of cardiac function, which can be tracked through cardiovascular disease progression and treatment (79). LV function is traditionally described through ejection fraction, cardiac output, and more recently, longitudinal strain, which represents the relative shortening of the LV during systole. While these methods are all easily accessible through non-invasive techniques (79, 97), they disregard the important functional significance of measuring motion mechanics directly related to the helical anatomy of the LV myocardial fibres, known as LV rotation.

1.5.2 Left ventricular rotation mechanics

Although the helical anatomy of the LV has been known for some time (127), only more recently have LV rotation mechanics been highlighted in the literature. Rotation of the LV is measured in degrees or radians, and represents the angle between a radial line connecting a point on the short-axis myocardial wall to the center of mass, and the resulting position of that point during any part of the cardiac cycle (62). Viewed from the apex, the LV base rotates clockwise, while the LV apex rotates counter-clockwise, resulting in a net counter-clockwise twist of the LV due to stronger rotation of the apex

(Figure 3) (130). The net left ventricular twist (LVT) takes into account the two short-axis levels of the LV, as well as the different layers of the myocardium, providing a global index of LV rotation mechanics.

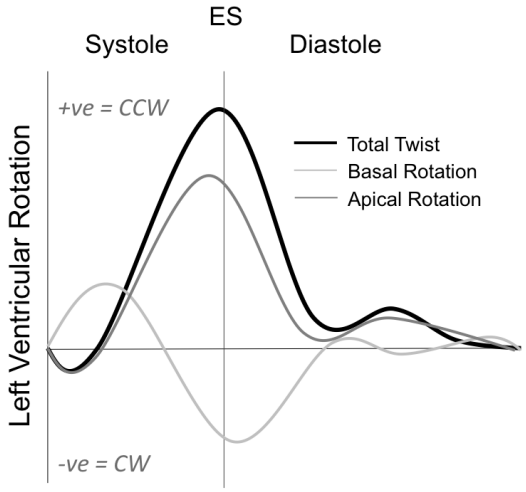

Figure 3. Schematic of left ventricular rotation separated into basal (light grey) and apical (dark grey) segments across a single cardiac cycle. The apex initially rotates in the clockwise direction during isovolumetric contraction and is followed by a large counter-clockwise rotation, whereas the base rotates in the opposite directions at lower magnitudes. At any point during the cardiac cycle, overall left ventricular rotation (black) is calculated as the instantaneous difference between apical and basal rotation, resulting in a net counter-clockwise rotation during end-systole (ES).

The study of LV rotation has become accessible to both basic and health researchers due to the development of speckle-tracking echocardiography and standard guidelines from experts in the field (97, 143). Functionally, LV rotation reduces the strain on endocardial fibres by offloading a portion of the myocardial work to the epicardial fibres, thereby improving systolic efficiency of the LV (7, 17). In fact, for only a 10-15%

shortening of a myofibre sarcomere, ~60% of blood is ejected from the LV, demonstrating a highly efficient functional mechanic (78, 143, 169).

While LVT represents a more accurate anatomical description of LV function, its regulation is poorly understood. Acutely, LVT is thought to be primarily controlled by afterload (the pressure the LV pumps against), preload (the loading pressure of the LV) and contractility (the strength of myocardial contraction) (143), although it has been difficult to isolate these factors in human research. Isometric handgrip exercise protocols have consistently been shown to reduce LV apical rotation by increasing blood pressure during exercise (171), although the independent effect of heart rate may confound interpretation of the results when using this model (12). The effect of increased preload on LVT has been tested using saline infusion models which increase plasma volume (170), peripheral heating models which increase venous return to the LV (142, 164), and experimental surgeries in dogs (38), all of which indicate increases in preload are related to increases in LVT. Reductions in preload have been tested using peripheral vasodilatory agents (e.g., glyceryl trinitrate, nitroprusside), and result in enhanced LVT, although these effects may be confounded by a concomitant reduction in afterload (22, 114). Further complicating the regulation, LV contractility has a positive effect on LVT (38, 105), though isolating increases in contractility without changes to afterload or preload in human models is challenging. The LV has an increasing β-adrenoreceptor density gradient from the base to the apex, which may explain the more consistent elevations in LV apical rotation with sympathetically-mediated increases in LV contractility (99). While it is not clear why LVT is affected by LV contractility independent of volume, it

may be due to a redistribution of forces along the oblique myocardial fibres, thereby increasing intramyocardial strain (38). Regardless, changes to LV contractility in humans will be confounded by simultaneous alterations to LV volumes and pressures, further complicating the assessment of the direct role of contractility on LVT.

1.5.3 Ventricular-Vascular Coupling: Traditional stiffness coupling

While it is possible to study the LV as an isolated organ, there is clear interaction with both the venous and arterial systems, requiring an integrative approach to studying the regulation and control of central hemodynamics. Classically referred to as ventricular-vascular coupling, structural and functional changes to the LV have been related to afterload in the proximal aorta (6). In this model, LV properties are linked to events in the proximal vasculature through direct coupling of tissue stiffness. For example, in normal aging, there is a progressive stiffening of the central elastic arteries, which is associated with increases in systolic blood pressure (154), and therefore increases in the afterload which the LV works against. Over time, this increase in myocardial work results in a stiffer LV in part due to myocardial fibrosis (68). Interestingly, early changes in arterial and ventricular stiffness result in no change in the arterial/LV stiffness ratio, indicating matching impairments between systems (72).

Moving beyond ventricular-vascular pressure coupling, there is also structural connectivity between the two systems, where the LV basal endocardium is attached to the proximal aorta by the aortic root (36). Both the functional and structural coupling between the ventricular and vascular systems supports the hypothesis that the LV might

be a regulator of CALM displacement. However, there is currently no data available to support this theory for the regulation of CALM.

1.6 EXERCISE TRAINING AND ARTERIAL STIFFNESS

Arterial stiffness variables have been considered viable candidates as monitoring tools for the assessment of improvements in cardiovascular risk profile with health interventions, such as exercise training (52). Although the effects of exercise training on CALM have never been investigated, the chronic effects of exercise training on traditional indicators of arterial stiffness have been well reported (66, 96). The effects of exercise training on arterial stiffness are complex, and appear to be modulated by exercise mode, intensity and baseline participant characteristics.

The main exercise models previously employed in the study of vascular physiology are variants of two types of exercise modes: aerobic (AET) and resistance (RET) exercise training. AET elicits a volume-loading response from the cardiovascular system to deliver a continuous supply of blood to the working muscles, with high elevations in heart rate, cardiac output, and cyclic elevations in vascular wall shear stress. In contrast, RET elicits a pressure-loading response, with large increases in blood pressure during effort, interspersed with rest periods with little, or no, activity. Compared to AET and RET, sprint interval training (SIT) may be considered a combination of the two exercise types from the perspective of the load on the vascular system as it is comprised of short bouts of supramaximal effort, likely eliciting high cardiac output and oscillatory shear stress on the vasculature, interspersed with short rest periods of light, or

no, activity. Each of these exercise modes has previously been associated with different vascular changes over training periods, which may be driven by differences in the hemodynamic stimulus generated during and after the exercise bouts.

1.6.1 Aerobic Exercise Training

Cross-sectional observations support an effect of AET on vascular remodelling, where arterial stiffness is reduced in athlete populations compared to sedentary controls (31, 41, 80). Stronger evidence stems from prospective exercise training studies, for which recent meta-analyses support a reduction in central PWV with AET (8, 66). Training effects are related to both the volume and intensity of aerobic exercise, with the greatest improvements in arterial stiffness accompanying the greatest improvements in VO_2max, and with vascular improvements more likely in individuals with higher baseline arterial stiffness (8). The majority of studies indicating improvements in PWV have been conducted in populations with poor health status (i.e., hypertension, type 2 diabetes, heart disease, chronic kidney disease). Studies in healthy men and women have also found improvements in central (56, 71, 98, 185) and peripheral (123) arterial stiffness. The effect of AET on IMT is limited with typical exercise training periods (≤16 weeks), with studies consistently demonstrated no change in wall thickness in otherwise healthy adults (152, 157).

The mechanisms by which arterial stiffness is improved with AET are understudied in human literature. As pulse wave-derived indices of arterial stiffness are related to mean arterial pressure (81, 141), AET may indirectly improve PWV or central

artery distensibility through exercise-related reductions in blood pressure (32, 75). A time course of vascular remodelling has also been observed with aerobic exercise training, with improvement in endothelial function preceding an increase in vessel diameter (158) reflective of the impact of elevated oscillatory shear stress at the vessel wall during a bout of aerobic exercise (18). Enhanced endothelial function may contribute to reductions in arterial stiffness by increased bioavailability of nitric oxide and reduced vasomotor tone (172, 174). While it is difficult to evaluate changes in the vascular extracellular matrix in humans, rodent models suggest exercise-related improvements in arterial stiffness are related to reductions in type I and type III collagen (46, 104), oxidative stress (39), and vascular inflammation (83), but not changes in elastin content (46). Although these mechanisms may not exactly mirror the responses in humans, pre-clinical animal models remain a critical component of the study of exercise-related improvements in vascular wall structure, and consequently, improvements in the functional viscoelastic behaviour of the arterial wall.

1.6.2 Resistance Exercise Training

RET has previously been suggested to have adverse effects on the vasculature, originally reported as reduced CCA distensibility in both cross-sectional observations of resistance-trained men (94), and with chronic RET protocols in sedentary men (73, 95). However, these findings have not been replicated since those initial reports, with more recent studies indicating no change (23, 33, 35, 45, 59, 69, 122, 126, 185) or reductions in arterial stiffness (11, 111) with RET. These findings are likely due to heterogeneity in

RET intensity, choice of arterial stiffness measurement, the age of participants, and baseline vascular stiffness (96). While there are no studies that have examined the mechanisms associated with the vascular responses to chronic RET, two reports suggests that conduit artery diameter also increases with RET along with improvements in endothelial function (122, 138), which may indicate changes to the extracellular matrix with training.

The hemodynamic stimulus of RET is likely driven by cyclic increases in blood pressure during a bout of exercise, although there are few studies examining the vascular environment during resistance exercise. In invasive pressure catheter studies, blood pressure increases upwards of 350/200 mmHg due to brief valsalva manoeuvres and high peripheral resistance caused by muscular contraction (88). Acute exercise studies suggest this pressure stimulus acutely increases arterial stiffness (37, 58) and systolic carotid strain (19), which may be due in part to the use of valsalva manoeuvres during intense lifts (60). Rodent models of RET are difficult to interpret, though a recent report suggests increased wall thickness, collagen thickness, and concentric LV hypertrophy following 12-weeks of ladder climbing in rats (137). Additional studies are needed to describe the structural changes to the vascular wall, in particular, the relationship between possible changes in the collagen and elastin with changes in arterial stiffness in both pre-clinical and human models.

1.6.3 Sprint interval training

From a practical standpoint, AET and RET are time-costly forms of exercise, with a single session lasting upwards of one to two hours including warm-up and cool-down periods. Recently, there has been renewed interest in developing very short, but highly effective exercise programs based on supramaximal intermittent exercise (sprint interval training, SIT) (49). Interval training has been shown to improve cardiorespiratory fitness in both healthy and overweight populations similar to that of traditional AET, albeit at a much lower time commitment (14). These exercise protocols have also demonstrated a positive effect on peripheral artery endothelial function (124) and, to a lesser extent, arterial stiffness in both clinical populations (29, 54) and healthy adults (63, 123), providing a similar degree of improvement compared to AET.

The mechanisms by which SIT enhances vascular structure and function are unknown. Similar to RET, very little is known about the hemodynamic stimulus during exercise; although it is likely characterized by short cyclic periods of high oscillatory shear stress in the conduit arteries. While it is currently unknown whether the magnitude or duration of exposure to vascular shear stress stimulates structural changes over time, our lab has recently demonstrated improved endothelial function following AET but not SIT after 12 weeks of training, suggesting that a prolonged duration of shear exposure may be necessary for chronic changes in vascular health (132). Additional studies examining the chronic vascular effects of SIT are warranted, with the need for characterizing the shear stress profile during a typical exercise bout.

1.7 STUDY OBJECTIVES AND HYPOTHESES

While the acquisition and measurement of 2D arterial wall motion is now readily available with non-invasive methods, there is a lack of knowledge of the physiological causes and consequences of CALM. The overarching objective of this dissertation is to examine the potential regulatory factors of CALM, and examine how a physiological control model may help interpret both cross-sectional and experimental differences in CALM across a range of vascular health in humans.

In Chapter 2, we establish a framework for a structural ventricular-vascular coupling theory through simultaneous imaging of the CCA and LV in healthy adults. In order to address the large interindividual differences in CALM patterns, we describe a standardized method of segmenting the CALM pattern based on consistent local maxima and minima during systolic and diastolic phases. We hypothesized that local shear stress and upstream LV rotation would be related to the anterograde and retrograde components of the CALM pattern, respectively.

In Chapter 3, we employed the segmentation method for the CALM pattern detailed in Chapter 2 in a large sample of healthy adults as well as in a small cohort of adults with coronary artery disease. We sought to examine the relationship between CALM variables and traditional measures of arterial stiffness, confirming their sensitivity to poor vascular health by using populations with known elevations in arterial stiffness. We hypothesized that diastolic CALM variables would be more strongly related to arterial stiffness, as systolic CALM variables would be confounded by local shear stress and LV rotation as per our structural ventricular-vascular coupling theory.

In Chapter 4, we sought to provide experimental evidence for the role of vascular shear stress and LV rotation in regulating the CALM pattern, accomplished through a series of stimulus-response studies in healthy humans. We hypothesized that acute interventions that generate alterations in shear stress would be related to systolic anterograde CALM variables, whereas interventions that impact LV rotation mechanics would be related to systolic retrograde CALM variables.

Finally, in Chapter 5, we examined the impact of four exercise interventions known to alter properties of vascular health (moderate-intensity continuous exercise training, sprint-interval exercise training, and high-repetition or low-repetition resistance exercise training) on systolic and diastolic CALM variables. We hypothesized that the CALM pattern would retain its general characteristics, but CALM magnitudes would increase over the 12-week training period.

1.8 REFERENCES

1. **Ahlgren AR**, **Cinthio M**, **Persson HW**, **Lindström K**. Different patterns of longitudinal displacement of the common carotid artery wall in healthy humans are stable over a four-month period. *Ultrasound Med Biol* 38: 916–925, 2012.

2. **Ahlgren AR**, **Cinthio M**, **Steen S**, **Nilsson T**, **Sjoberg T**, **Persson HW**, **Lindstrom K**. Longitudinal displacement and intramural shear strain of the porcine carotid artery undergo profound changes in response to catecholamines. *Am J Physiol Heart Circ Physiol* 302: H1102–H1115, 2012.

3. **Ahlgren AR**, **Cinthio M**, **Steen S**, **Persson HW**, **Sjöberg T**, **Lindström K**. Effects of adrenaline on longitudinal arterial wall movements and resulting intramural shear strain: a first report. *Clin Physiol Funct Imaging* 29: 353–359, 2009.

4. **Ahlgren AR**, **Steen S**, **Segstedt S**, **Erlöv T**, **Lindström K**, **Sjöberg T**, **Persson HW**, **Ricci S**, **Tortoli P**, **Cinthio M**. Profound increase in longitudinal displacements of the porcine carotid artery wall can take place independently of wall shear stress: A continuation report. *Ultrasound Med Biol* 41: 1342–1353, 2015.

5. **AlGhatrif M**, **Strait JB**, **Morrell CH**, **Canepa M**, **Wright J**, **Elango P**, **Scuteri A**, **Majjar SS**, **Ferrucci L**, **Lakatta EG**. Longitudinal Trajectories of Arterial Stiffness and the Role of Blood Pressure. *Hypertension* 62: 934–941, 2013.

6. **Antonini-Canterin F**, **Carerj S**, **Di Bello V**, **Di Salvo G**, **La Carrubba S**, **Vriz O**, **Pavan D**, **Balbarini A**, **Nicolosi GL**, **On behalf of the Research Group of the Italian Society of Cardiovascular Echography (SIEC)**. Arterial stiffness and ventricular stiffness: a couple of diseases or a coupling disease? A review from the cardiologist's point of view. *Eur J Echocardiogr* 10: 36–43, 2009.

7. **Arts T**, **Veenstra PC**, **Reneman RS**. Epicardial deformation and left ventricular wall mechanics during ejection in the dog. *Am J Physiol Heart Circ Physiol* 243: H379–H390, 1982.

8. **Ashor AW**, **Lara J**, **Siervo M**, **Celis-Morales C**, **Mathers JC**. Effects of Exercise Modalities on Arterial Stiffness and Wave Reflection: A Systematic Review and Meta-Analysis of Randomized Controlled Trials. *PLoS ONE* 9: e110034, 2014.

9. **Asmar R**, **Benetos A**, **Topouchian J**, **Laurent P**, **Pannier B**, **Brisac A-M**, **Target R**, **Levy BI**. Assessment of arterial distensibility by automatic pulse wave velocity measurement: Validation and clinical application studies. *Hypertension* 26: 485–490, 1995.

10. **Asmar R**, **Topouchian J**, **Pannier B**, **Benetos A**, **Safar M**. Pulse wave velocity as endpoint in large-scale intervention trial. The Complior® study. *J Hypertens* 19: 813–818, 2001.

11. **Au JS**, **Oikawa SY**, **Morton RW**, **MacDonald MJ**, **Phillips SM**. Arterial Stiffness Is Reduced Regardless of Resistance Training Load in Young Men. *Med Sci Sports Exerc* 49: 342–348, 2016.

12. **Balmain B**, **Stewart GM**, **Yamada A**, **Chan J**, **Haseler LJ**, **Sabapathy S**. The impact of an experimentally induced increase in arterial blood pressure on left ventricular twist mechanics. *Exp Physiol* 101: 124–134, 2015.

13. **Basalyga DM**, **Simionescu DT**, **Xiong W**, **Baxter T**, **Starcher BC**, **Vyavahare NR**. Elastin degradation and calcification in an abdominal aorta injury model: Role of matrix metalloproteinases. *Circulation* 110: 3480–3487, 2004.

14. **Batacan RB Jr**, **Duncan MJ**, **Dalbo VJ**, **Tucker PS**, **Fenning AS**. Effects of high-intensity interval training on cardiometabolic health: a systematic review and meta-analysis of intervention studies. *Br J Sports Med* 51: 494–503, 2017.

15. **Ben-Shlomo Y**, **Spears M**, **Boustred C**, **May M**, **Anderson SG**, **Benjamin EJ**, **Boutouyrie P**, **Cameron J**, **Chen C-H**, **Cruickshank JK**, **Hwang S-J**, **Lakatta EG**, **Laurent S**, **Maldonado J**, **Mitchell GF**, **Najjar SS**, **Newman AB**, **Ohishi M**, **Pannier B**, **Pereira T**, **Vasan RS**, **Shokawa T**, **Sutton-Tyrell K**, **Verbeke F**, **Wang K-L**, **Webb DJ**, **Willum Hansen T**, **Zoungas S**, **McEniery CM**, **Cockcroft JR**, **Wilkinson IB**. Aortic pulse wave velocity improves cardiovascular event prediction: an individual participant meta-analysis of prospective observational data from 17,635 subjects. *J Am Coll Cardiol* 63: 636–646, 2014.

16. **Bergel DH**. The dynamic elastic properties of the arterial wall. *J Physiol* 156: 458–469, 1961.

17. **Beyar R**, **Sideman S**. Left Ventricular Mechanics Related to the Local Distribution of Oxygen Demand Throughout the Wall. *Circ Res* 58: 664–677, 1986.

18. **Birk GK**, **Dawson EA**, **Atkinson C**, **Haynes A**, **Cable NT**, **Thijssen DHJ**, **Green DJ**. Brachial artery adaptation to lower limb exercise training: role of shear stress. *J Appl Physiol* 112: 1653–1658, 2012.

19. **Black JM**, **Stöhr EJ**, **Stone K**, **Pugh CJA**, **Stembridge M**, **Shave R**, **Esformes JI**. The effect of an acute bout of resistance exercise on carotid artery strain and strain rate. *Physiol Rep* 4: e12959, 2016.

20. **Bossuyt J**, **Engelen L**, **Ferreira I**, **Stehouwer CD**, **Boutouyrie P**, **Laurent S**, **Segers P**, **Reesink K**, **Van Bortel LM**. Reference values for local arterial stiffness. Part B: femoral artery. *J Hypertens* 33: 1997–2009, 2015.

21. **Bramwell JC**, **Hill AV**. The velocity of the pulse wave in man. *Proc Soc Lond (Biol)* 93: 298–306, 1922.

22. **Burns AT**, **Gerche AL**, **Prior DL**, **MacIsaac AI**. Left Ventricular Torsion Parameters are Affected by Acute Changes in Load. *Echocardiogr* 27: 407–414, 2010.

23. **Casey DP**, **Beck DT**, **Braith RW**. Progressive Resistance Training Without Volume Increases Does Not Alter Arterial Stiffness and Aortic Wave Reflection. *Exp Biol Med* 232: 1228–1235, 2007.

24. **Cecelja M**, **Chowienczyk P**. Arterial stiffening: Causes and consequences. *Artery Res* 7: 22–27, 2013.

25. **Chirinos JA**, **Kips JG**, **Jacobs DR**, **Brumback L**, **Duprez DA**, **Kronmal R**, **Bluemke DA**, **Townsend RR**, **Vermeersch S**, **Segers P**. Arterial wave reflections and incident cardiovascular events and heart failure: MESA (Multiethnic Study of Atherosclerosis). *J Am Coll Cardiol* 60: 2170–2177, 2012.

26. **Cinthio M**, **Ahlgren AR**, **Bergkvist J**, **Jansson T**, **Persson HW**, **Lindström K**. Longitudinal movements and resulting shear strain of the arterial wall. *Am J Physiol Heart Circ Physiol* 291: H394–H402, 2006.

27. **Cinthio M**, **Ahlgren AR**, **Jansson T**, **Eriksson A**, **Persson HW**, **Lindström K**. Evaluation of an ultrasonic echo-tracking method for measurements of arterial wall movements in two dimensions. *IEEE Trans Ultrason Ferroelectr Freq Control* 52: 1300–1311, 2005.

28. **Cinthio M**, **Ahlgren AR**. Intra-observer variability of longitudinal displacement and intramural shear strain measurements of the arterial wall using ultrasound noninvasively *in vivo*. *Ultrasound Med Biol* 36: 697–704, 2010.

29. **Ciolac EG**, **Bocchi EA**, **Bortolotto LA**, **Carvalho VO**, **Greve JM**, **Guimarães GV**. Effects of high-intensity aerobic interval training vs. moderate exercise on hemodynamic, metabolic and neuro-humoral abnormalities of young normotensive women at high familial risk for hypertension. *Hypertens Res* 33: 836–843, 2010.

30. **Comfrey AL**, **Lee HB**. *A First Course in Factor Analysis*. Hillsdale, NJ: Lawrence Erlbaum Associates, 1992.

31. **Cook JN**, **DeVan AE**, **Schleifer JL**, **Anton MM**, **Cortez-Cooper MY**, **Tanaka H**. Arterial compliance of rowers: implications for combined aerobic and strength training on arterial elasticity. *Am J Physiol Heart Circ Physiol* 290: H1596–H1600, 2005.

32. **Cornelissen VA**, **Smart NA**. Exercise Training for Blood Pressure: A Systematic Review and Meta-analysis. *J Am Heart Assoc* 2: e004473, 2012.

33. **Cortez-Cooper MY**, **Anton MM**, **DeVan AE**, **Neidre DB**, **Cook JN**, **Tanaka H**. The effects of strength training on central arterial compliance in middle-aged and older adults. *Eur J Cardiovasc Prev Rehabil* 15: 149–155, 2008.

34. **Crick SJ**, **Sheppard MN**, **Ho SY**, **Lior G**, **Anderson RH**. Anatomy of the pig heart: comparisons with normal human cardiac structure. *J Anat* 193: 105–119, 1998.

35. **Croymans DM**, **Krell SL**, **Oh CS**, **Katiraie M**, **Lam CY**, **Harris RA**, **Roberts CK**. Effects of resistance training on central blood pressure in obese young men. *J Hum Hypertens* 28: 157–164, 2013.

36. **de Kerchove L**, **Khoury El G**. Anatomy and pathophysiology of the ventriculo-aortic junction: implication in aortic valve repair surgery. *Ann Cardiothorac Surg* 2: 57–64, 2013.

37. **DeVan AE**, **Anton MM**, **Cook JN**, **Neidre DB**, **Cortez-Cooper MY**, **Tanaka H**. Acute effects of resistance exercise on arterial compliance. *J Appl Physiol* 98: 2287–2291, 2005.

38. **Dong S-J**, **Hees PS**, **Huang W-M**, **Buffer SA Jr**, **Weiss JL**, **Shapiro EP**. Independent effects of preload, afterload, and contractility on left ventricular torsion. *Am J Physiol Heart Circ Physiol* 277: H1053–H1060, 1999.

39. **Durrant JR**, **Seals DR**, **Connell ML**, **Russell MJ**, **Lawson BR**, **Folian BJ**, **Donato AJ**, **Lesniewski LA**. Vascular Effects of Exercise: Endothelial Adaptations Beyond Active Muscle Beds. *Physiology* 26: 132–145, 2011.

40. **Eberth JF**, **Gresham VC**, **Reddy AK**, **Popovic N**, **Wilson E**, **Humphrey JD**. Importance of pulsatility in hypertensive carotid artery growth and remodeling. *J Hypertens* 27: 2010–2021, 2009.

41. **Edwards DG**, **Lang JT**. Augmentation Index and Systolic Load Are Lower in Competitive Endurance Athletes. *Am J Hypertens* 18: 679–683, 2005.

42. **Engelen L**, **Bossuyt J**, **Ferreira I**, **Van Bortel LM**, **Reesink KD**, **Segers P**, **Stehouwer CD**, **Laurent S**, **Boutouyrie P**. Reference values for local arterial

stiffness. Part A: carotid artery. *J Hypertens* 33: 1981–1996, 2015.

43. **Fantin F**, **Mattocks A**, **Bulpitt CJ**, **Banya W**, **Rajkumar C**. Is augmentation index a good measure of vascular stiffness in the elderly? *Age Ageing* 36: 43–48, 2006.

44. **Farron J**, **Varghese T**, **Thelen DG**. Measurement of tendon strain during muscle twitch contractions using ultrasound elastography. *IEEE Trans Ultrason Ferroelectr Freq Control* 56: 27–35, 2009.

45. **Fjeldstad AS**, **Bemben MG**, **Bemben DA**. Resistance Training Effects on Arterial Compliance in Premenopausal Women. *Angiology* 60: 750–756, 2010.

46. **Fleenor BS**, **Marshall KD**, **Durrant JR**, **Lesniewski LA**, **Seals DR**. Arterial stiffening with ageing is associated with transforming growth factor-β1-related changes in adventitial collagen: reversal by aerobic exercise. *J Physiol-London* 588: 3971–3982, 2010.

47. **Gaibazzi N**, **Rigo F**, **Facchetti R**, **Carerj S**, **Giannattasio C**, **Moreo A**, **Mureddu GF**, **Salvetti M**, **Grolla E**, **Faden G**, **Cesana F**, **Faggiano P**. Differential incremental value of ultrasound carotid intima–media thickness, carotid plaque, and cardiac calcium to predict angiographic coronary artery disease across Framingham risk score strata in the APRES multicentre study. *Eur Heart J Cardiovasc Img* 17: 991–1000, 2016.

48. **Giannattasio C**, **Salvi P**, **Valbusa F**, **Kearney-Schwartz A**, **Capra A**, **Amigoni M**, **Failla M**, **Boffi L**, **Madotto F**, **Benetos A**, **Mancia G**. Simultaneous Measurement of Beat-to-Beat Carotid Diameter and Pressure Changes to Assess Arterial Mechanical Properties. *Hypertension* 52: 896–902, 2008.

49. **Gibala MJ**, **Hawley JA**. Sprinting Toward Fitness. *Cell Metabolism* 25: 988–990, 2017.

50. **Golemati S**, **Sassano A**, **Lever MJ**, **Bharath AA**, **Dhanjil S**, **Nicolaides AN**. Carotid artery wall motion estimated from b-mode ultrasound using region tracking and block matching. *Ultrasound Med Biol* 29: 387–399, 2003.

51. **Goodman S**. iHeart on Dragon's Den [Online]. *goiheart.com*: 1–1, 2016. https://goiheart.com/blog/iheart-on-dragon-s-den [22 Mar. 2017].

52. **Green DJ**. Exercise training as vascular medicine: Direct impacts on the vasculature in humans. *Exerc Sport Sci Rev* 37: 196–202, 2009.

53. **Guadagnoli E**, **Velicer WF**. Relation to sample size to the stability of component patterns. *Psychol Bull* 103: 265–275, 1988.

54. **Guimarães GV**, **Ciolac EG**, **Carvalho VO**, **D'Avila VM**, **Bortolotto LA**, **Bocchi EA**. Effects of continuous vs. interval exercise training on blood pressure and arterial stiffness in treated hypertension. *Hypertens Res* 33: 627–632, 2010.

55. **Harkness MLR**, **Harkness RD**, **McDonald DA**. The Collagen and Elastin Content of the Arterial Wall in the Dog. *Proc Soc Lond (Biol)* 146: 541–551, 1957.

56. **Hayashi K**, **Sugawara J**, **Komine H**, **Maeda S**, **Yokoi T**. Effects of aerobic exercise training on the stiffness of central and peripheral arteries in middle-aged sedentary men. *Jpn J Physiol* 55: 235–239, 2005.

57. **Hayward CS**, **Kelly RP**. Gender-Related Differences in the Central Arterial Pressure Waveform. *J Am Coll Cardiol* 30: 1863–1871, 1997.

58. **Heffernan K**, **Collier S**, **Kelly E**, **Jae S**, **Fernhall B**. Arterial Stiffness and Baroreflex Sensitivity Following Bouts of Aerobic and Resistance Exercise. *Int J Sport Med* 28: 197–203, 2007.

59. **Heffernan KS**, **Fahs CA**, **Iwamoto GA**, **Jae SY**, **Wilund KR**, **Woods JA**, **Fernhall B**. Resistance exercise training reduces central blood pressure and improves microvascular function in African American and white men. *Atherosclerosis* 207: 220–226, 2009.

60. **Heffernan KS**, **Jae SY**, **Edwards DG**, **Kelly EE**, **Fernhall B**. Arterial stiffness following repeated Valsalva maneuvers and resistance exercise in young men. *Appl Physiol Nutr Metab* 32: 257–264, 2007.

61. **Heffernan KS**, **Rossow L**, **Jae SY**, **Shokunbi HG**, **Gibson EM**, **Fernhall B**. Effect of single-leg resistance exercise on regional arterial stiffness. *Eur J Appl Physiol* 98: 185–190, 2014.

62. **Henson RE**, **Song SK**, **Pastorek JS**, **Ackerman JJH**, **Lorenz CH**. Left ventricular torsion is equal in mice and humans. *Am J Physiol Heart Circ Physiol* 278: H1117–H1123, 2000.

63. **Heydari M**, **Boutcher YN**, **Boutcher SH**. High-intensity intermittent exercise and cardiovascular and autonomic function. *Clin Aut Res* 23: 57–65, 2012.

64. **Hirai T**, **Sasayama S**, **Kawasaki T**, **Yagi S**. Stiffness of systemic arteries in patients with myocardial infarction. A noninvasive method to predict severity of coronary atherosclerosis. *Circulation* 80: 78–86, 1989.

65. **Hope SA**, **Tay DB**, **Meredith IT**, **Cameron JD**. Waveform dispersion, not reflection, may be the major determinant of aortic pressure wave morphology.

Am J Physiol Heart Circ Physiol 289: H2497–H2502, 2005.

66. **Huang C**, **Wang J**, **Deng S**, **She Q**, **Wu L**. The effects of aerobic endurance exercise on pulse wave velocity and intima media thickness in adults: A systematic review and meta-analysis. *Scand J Med Sci Sports* 26: 478–487, 2016.

67. **Huybrechts SAM**, **Devos DG**, **Vermeersch SJ**, **Mahieu D**, **Achten E**, **de Backer TLM**, **Segers P**, **Van Bortel LM**. Carotid to femoral pulse wave velocity: a comparison of real travelled aortic path lengths determined by MRI and superficial measurements. *J Hypertens* 29: 1577–1582, 2011.

68. **Iles L**, **Pfluger H**, **Phrommintikul A**, **Cherayath J**, **Aksit P**, **Gupta SN**, **Kaye DM**, **Taylor AJ**. Evaluation of diffuse myocardial fibrosis in heart failure with cardiac magnetic resonance contrast-enhanced T1 mapping. *J Am Coll Cardiol* 52: 1574–1580, 2008.

69. **Jefferson ME**, **Nicklas BJ**, **Chmelo EA**, **Crotts CI**, **Shaltout HA**, **Diz DI**, **Marsh AP**, **Brinkley TE**. Effects of Resistance Training With and Without Caloric Restriction on Arterial Stiffness in Overweight and Obese Older Adults. *Am J Hypertens* 29: 494–500, 2015.

70. **Kaess BM**, **Rong J**, **Larson MG**, **Hamburg NM**, **Vita JA**, **Levy D**, **Benjamin EJ**, **Vasan RS**, **Mitchell GF**. Aortic stiffness, blood pressure progression, and incident hypertension. *J Am Med Assoc* 308: 875–881, 2012.

71. **Kakiyama T**, **Sugawara J**, **Murakami H**, **Maeda S**, **Kuno S**, **Matsuda M**. Effects of Short-Term Endurance Training on Aortic Distensibility in Young Males. *Med Sci Sports Exerc* 37: 267–271, 2005.

72. **Kass DA**. Age-related Changes in Venticular–Arterial Coupling: Pathophysiologic Implications. *Heart Fail Rev* 7: 51–62, 2002.

73. **Kawano H**, **Tanaka H**, **Miyachi M**. Resistance training and arterial compliance: keeping the benefits while minimizing the stiffening. *J Hypertens* 24: 1753–1759, 2006.

74. **Kawasaki T**, **Sasayama S**, **Yagi S**, **Asakawa T**, **Hirai T**. Non-invasive assessment of the age related changes in stiffness of major branches of the human arteries. *Cardiovasc Res* 21: 678–687, 1987.

75. **Kelley GA**, **Kelley KA**, **Tran ZV**. Aerobic Exercise and Resting Blood Pressure: A Meta-Analytic Review of Randomized, Controlled Trials. *Prev Cardiol* 4: 73–80, 2001.

76. **Kelly R**, **Hayward C**, **Avolio A**, **O'Rourke M**. Noninvasive determination of

age-related changes in the human arterial pulse. *Circulation* 80: 1652–1659, 1989.

77. **Kim EJ**, **Park CG**, **Park JS**, **Suh SY**, **Choi CU**, **Kim JW**, **Kim SH**, **Lim HE**, **Rha SW**, **Seo HS**, **Oh DJ**. Relationship between blood pressure parameters and pulse wave velocity in normotensive and hypertensive subjects: invasive study. *J Hum Hypertens* 21: 141–148, 2006.

78. **Krueger JW**, **Pollack GH**. Myocardial sarcomere synamics during isometric contraction. *J Physiol* 251: 627–643, 1975.

79. **Lang RM**, **Badano LP**, **Mor-Avi V**, **Afilalo J**, **Armstrong A**, **Ernande L**, **Flachskampf FA**, **Foster E**, **Goldstein SA**, **Kuznetsova T**, **Lancellotti P**, **Muraru D**, **Picard MH**, **Rietzschel ER**, **Rudski L**, **Spencer KT**, **Tsang W**, **Voigt JU**. Recommendations for Cardiac Chamber Quantification by Echocardiography in Adults: An Update from the American Society of Echocardiography and the European Association of Cardiovascular Imaging. *Eur Heart J Cardiovasc Img* 16: 233–271, 2015.

80. **Laurent P**, **Marenco P**, **Castagna O**, **Smulyan H**, **Blacher J**, **Safar ME**. Differences in central systolic blood pressure and aortic stiffness between aerobically trained and sedentary individuals. *J Am Soc Hypertens* 5: 85–93, 2011.

81. **Laurent S**, **Cockcroft J**, **Van Bortel L**, **Boutouyrie P**, **Giannattasio C**, **Hayoz D**, **Pannier B**, **Vlachopoulos C**, **Wilkinson I**, **Struijker-Boudier H**, **on behalf of the European Network for Non-invasive Investigation of Large Arteries**. Expert consensus document on arterial stiffness: methodological issues and clinical applications. *Eur Heart J* 27: 2588–2605, 2006.

82. **Lawton RW**, **Greene LC**. *A method for the in situ study of aortic elasticity in the dog*. AMAL, U.S. Naval and Air Development Center, 1956.

83. **Lesniewski LA**, **Durrant JR**, **Connell ML**, **Henson GD**, **Black AD**, **Donato AJ**, **Seals DR**. Aerobic exercise reverses arterial inflammation with aging in mice. *Am J Physiol Heart Circ Physiol* 301: H1025–H1032, 2011.

84. **Liang Q**, **Wendelhag I**, **Wikstrand J**, **Gustavsson T**. A multiscale dynamic programming procedure for boundary detection in ultrasonic artery images. *IEEE Trans Med Img* 19: 127–142, 2000.

85. **Liao D**, **Arnett DK**, **Tyroler HA**, **Riley WA**, **Chambless LE**, **Szklo M**, **Heiss G**. Arterial Stiffness and the Development of Hypertension : The ARIC Study. *Hypertension* 34: 201–206, 1999.

86. **Lorenz MW**, **Markus HS**, **Bots ML**, **Rosvall M**, **Sitzer M**. Prediction of Clinical Cardiovascular Events With Carotid Intima-Media Thickness: A Systematic Review and Meta-Analysis. *Circulation* 115: 459–467, 2007.

87. **Lorenz MW**, **Polak JF**, **Kavousi M**, **Mathiesen EB**, **Völzke H**, **Tuomainen T-P**, **Sander D**, **Plichart M**, **Catapano AL**, **Robertson CM**, **Kiechl S**, **Rundek T**, **Desvarieux M**, **Lind L**, **Schmid C**, **DasMahapatra P**, **Gao L**, **Ziegelbauer K**, **Bots ML**, **Thompson SG**, **Group OBOTP-IS**. Carotid intima-media thickness progression to predict cardiovascular events in the general population(the PROG-IMT collaborative project): a meta-analysis of individual participant data. *Lancet* 379: 2053–2062, 2012.

88. **MacDougall JD**, **McKelvie RS**, **Moroz DE**, **Sale DG**, **McCartney N**, **Buick F**. Factors affecting blood pressure during heavy weight lifting and static contractions. *J Appl Physiol* 73: 1590–1597, 1992.

89. **Mancia G**, **Fagard R**, **Narkiewicz K**, **Redon J**, **Zanchetti A**, **Böhm M**, **Christiaens T**, **Cífková R**, **De Backer G**, **Dominiczak A**, **Galderisi M**, **Grobbee DE**, **Jaarsma T**, **Kirchhof P**, **Kjeldsen SE**, **Laurent S**, **Manolis AJ**, **Nilsson PM**, **Ruilope LM**, **Schmieder RE**, **Sirnes PA**, **Sleight P**, **Viigimaa M**, **Waeber B**, **Zannad F**. 2013 ESH/ESC Guidelines for the management of arterial hypertension. *Blood Press* 22: 193–278, 2013.

90. **Martyn CN**, **Greenwald SE**. Impaired synthesis of elastin in walls of aorta and large conduit arteries during early development as an initiating event in pathogenesis of systemic hypertension. *The Lancet* 350: 953–955, 1997.

91. **Mattace-Raso FUS**, **van der Cammen TJM**, **Hofman A**, **van Popele NM**, **Bos ML**, **Schalekamp MADH**, **Asmar R**, **Reneman RS**, **Hoeks APG**, **Breteler MMB**, **Witteman JCM**. Arterial Stiffness and Risk of Coronary Heart Disease and Stroke: The Rotterdam Study. *Circulation* 113: 657–663, 2006.

92. **Mäki-Petäjä KM**, **Wilkinson IB**. Inflammation and large arteries: Potential mechanisms for inflammation-induced arterial stiffness. *Artery Res* 6: 59–64, 2012.

93. **Mitchell GF**, **Hwang SJ**, **Vasan RS**, **Larson MG**, **Pencina MJ**, **Hamburg NM**, **Vita JA**, **Levy D**, **Benjamin EJ**. Arterial Stiffness and Cardiovascular Events: The Framingham Heart Study. *Circulation* 121: 505–511, 2010.

94. **Miyachi M**, **Donato AJ**, **Yamamoto K**, **Takahashi K**, **Gates PE**, **Moreau KL**, **Tanaka H**. Greater Age-Related Reductions in Central Arterial Compliance in Resistance-Trained Men. *Hypertension* 41: 130–135, 2003.

95. **Miyachi M**, **Kawano H**, **Sugawara J**, **Takahashi K**, **Hayashi K**, **Yamazaki K**,

Tabata I, **Tanaka H**. Unfavorable Effects of Resistance Training on Central Arterial Compliance: A Randomized Intervention Study. *Circulation* 110: 2858–2863, 2004.

96. **Miyachi M**. Effects of resistance training on arterial stiffness: a meta-analysis. *Brit J Sport Med* 47: 393–396, 2013.

97. **Mor-Avi V**, **Lang RM**, **Badano LP**, **Belohlavek M**, **Cardim NM**, **Derumeaux G**, **Marwick T**, **Nagueh SF**, **Sengupta PP**, **Sicari R**, **Smiseth OA**, **Galderisi M**, **Smulevitz B**, **Takeuchi M**, **Thomas JD**, **Vannan M**, **Voigt J-U**, **Zamorano JL**. Current and evolving echocardiographic techniques for the quantitative evaluation of cardiac mechanics: ASE/EAE consensus statement on methodology and indications. *J Am Soc Echocardiogr* 24: 277–313, 2011.

98. **Moreau KL**, **Donato AJ**, **Seals DR**, **DeSouza CA**, **Tanaka H**. Regular exercise, hormone replacement therapy and the age-related decline in carotid arterial compliance in healthy women. *Cardiovasc Res* 57: 861–868, 2003.

99. **Mori H**, **Ishikawa S**, **Kojima S**, **Hayashi J**, **Watanabe Y**, **Hoffman JIE**, **Okino H**. Increased responsiveness of left ventricular apical myocardium to adrenergic stimuli. *Cardiovasc Res* 27: 192–198, 1993.

100. **Najjar SS**, **Scuteri A**, **Shetty V**, **Wright JG**, **Muller DC**, **Fleg JL**, **Spurgeon HP**, **Ferrucci L**, **Lakatta EG**. Pulse Wave Velocity Is an Independent Predictor of the Longitudinal Increase in Systolic Blood Pressure and of Incident Hypertension in the Baltimore Longitudinal Study of Aging. *J Am Coll Cardiol* 51: 1377–1383, 2008.

101. **Nichols WW**, **O'Rourke MF**. *McDonald's Blood Flow in Arteries: Theoretical, experimental and clinical principles*. 5 ed. London: Hodder Arnold, 2005.

102. **Nilsson T**, **Ahlgren AR**, **Jansson T**, **Persson HW**, **Nilsson J**, **Lindström K**, **Cinthio M**. A method to measure shear strain with high spatial resolution in the arterial wall non-invasively *in vivo* by tracking zero-crossings of B-mode intensity gradients. *Proc IEEE Ultrason Symp* (May 10, 2010). doi: 10.1109/ULTSYM.2010.0121.

103. **Nilsson T**, **Ricci S**, **Ahlgren AR**, **Jansson T**, **Lindström K**, **Tortoli P**, **Persson HW**, **Cinthio M**. Methods for measurements of the longitudinal movement and the shear-induced longitudinal elastic modulus of the arterial wall. *Proc IEEE Ultrason Symp* (September 20, 2009). doi: 10.1109/ULTSYM.2009.0079.

104. **Nosaka T**, **Tanaka H**, **Watanabe I**, **Sato M**, **Matsuda M**. Influence of regular exercise on age-related changes in arterial elasticity: Mechanistic insights from wall compositions in rat aorta. *Can J Appl Physiol* 28: 204–212, 2003.

105. **Notomi Y**, **Popović ZB**, **Yamada H**, **Wallick DW**, **Martin MG**, **Oryszak SJ**, **Shiota T**, **Greenberg NL**, **Thomas JD**. Ventricular untwisting: a temporal link between left ventricular relaxation and suction. *Am J Physiol Heart Circ Physiol* 294: H505–H513, 2007.

106. **Nürnberger J**, **Dammer S**, **Opazo Saez A**, **Philipp T**, **Schäfers RF**. Diastolic blood pressure is an important determinant of augmentation index and pulse wave velocity in young, healthy males. *J Hum Hypertens* 17: 153–158, 2003.

107. **O'Rourke MF**, **Hashimoto J**. Mechanical Factors in Arterial Aging. *J Am Coll Cardiol* 50: 1–13, 2007.

108. **O'Rourke MF**, **Pauca A**, **Jiang X-J**. Pulse wave analysis. *Brit J Clin Pharmacol* 51: 507–522, 2001.

109. **O'Rourke MF**, **Safar ME**. Relationship Between Aortic Stiffening and Microvascular Disease in Brain and Kidney: Cause and Logic of Therapy. *Hypertension* 46: 200–204, 2005.

110. **Okabe R**, **Inaba M**, **Sakai S**, **Ishimura E**, **Morisuchi A**, **Shoji T**, **Nishizawa Y**. Increased arterial stiffening and thickening in the paretic lower limb in patients with hemiparesis. *Clin Sci* 106: 613–618, 2004.

111. **Okamoto T**, **Masuhara M**, **Ikuta K**. Effect of low-intensity resistance training on arterial function. *Eur J Appl Physiol* 111: 743–748, 2011.

112. **Oliver JJ**, **Webb DJ**. Noninvasive Assessment of Arterial Stiffness and Risk of Atherosclerotic Events. *Arterioscler Throm Vas* 23: 554–566, 2003.

113. **Pannier BM**, **Avolio AP**, **Hoeks A**, **Mancia G**, **Takazawa K**. Methods and devices for measuring arterial compliance in humans. *Am J Hypertens* 15: 743–753, 2002.

114. **Park SJ**, **Nishimura RA**, **Borlaug BA**, **Sorajja P**, **Oh JK**. The effect of loading alterations on left ventricular torsion: a simultaneous catheterization and two-dimensional speckle tracking echocardiographic study. *Eur J Echocardiogr* 11: 770–777, 2010.

115. **Pauca AL**, **O'Rourke MF**, **Kon ND**. Prospective Evaluation of a Method for Estimating Ascending Aortic Pressure From the Radial Artery Pressure Waveform. *Hypertension* 38: 932–937, 2001.

116. **Pauca AL**, **Wallenhaupt SL**, **Kon ND**, **Tucker WY**. Does Radial Artery Pressure Accurately Reflect Aortic Pressure? *Chest* 102: 1193–1198, 1992.

117. **Persson M**, **Ahlgren AR**, **Eriksson A**, **Jansson T**, **Persson HW**, **Lindström K**.

Non-invasive measurement of arterial longitudinal movement. *Proc IEEE Ultrason Symp* 2: 1783–1786, 2002.

118. **Peters SAE**, **Ruijter den HM**, **Bots ML**, **Moons KGM**. Improvements in risk stratification for the occurrence of cardiovascular disease by imaging subclinical atherosclerosis: a systematic review. *Heart* 98: 177–184, 2011.

119. **Phan TS**, **Li JK-J**, **Segers P**, **Reddy Koppula M**, **Akers SR**, **Kuna ST**, **Gislason T**, **Pack AI**, **Chirinos JA**. Aging is Associated With an Earlier Arrival of Reflected Waves Without a Distal Shift in Reflection Sites. *J Am Heart Assoc* 5: e003733, 2016.

120. **Pignoli P**, **Tremoli E**, **Poli A**, **Oreste P**, **Paoletti R**. Intimal plus medial thickness of the arterial wall: a direct measurement with ultrasound imaging. *Circulation* 74: 1399–1406, 1986.

121. **Purslow PP**. Positional variations in fracture toughness, stiffness and strength of descending thoracic pig aorta. *J Biomechanics* 16: 947–953, 1983.

122. **Rakobowchuk M**, **McGowan CL**, **de Groot PC**, **Bruinsma D**, **Hartman JW**, **Phillips SM**, **MacDonald MJ**. Effect of whole body resistance training on arterial compliance in young men. *Exp Physiol* 90: 645–651, 2005.

123. **Rakobowchuk M**, **Tanguay S**, **Burgomaster KA**, **Howarth KR**, **Gibala MJ**, **MacDonald MJ**. Sprint interval and traditional endurance training induce similar improvements in peripheral arterial stiffness and flow-mediated dilation in healthy humans. *Am J Physiol Regul Integr Comp Physiol* 295: R236–R242, 2008.

124. **Ramos JS**, **Dalleck LC**, **Tjonna AE**, **Beetham KS**, **Coombes JS**. The Impact of High-Intensity Interval Training Versus Moderate-Intensity Continuous Training on Vascular Function: a Systematic Review and Meta-Analysis. *Sports Med* 45: 679–692, 2015.

125. **Roman MJ**, **Pini R**, **Pickering TG**, **Devereux RB**. Non-invasive measurements of arterial compliance in hypertensive compared with normotensive adults. *J Hypertens* 10: S115–S118, 1992.

126. **Rossow LM**, **Fahs CA**, **Thiebaud RS**, **Loenneke JP**, **Kim D**, **Mouser JG**, **Shore EA**, **Beck TW**, **Bemben DA**, **Bemben MG**. Arterial stiffness and blood flow adaptations following eight weeks of resistance exercise training in young and older women. *Exp Gerontol* 53: 48–56, 2014.

127. **Rushmer RF**, **Crystal DK**, **Wagner C**. The Functional Anatomy of Ventricular Contraction. *Circ Res* 1: 162–171, 1953.

128. **Schillaci G**, **Pucci G**. Lower-limb pulse wave velocity: correlations and clinical value. *Hypertens Res* 36: 679–681, 2013.

129. **Seeley R**, **Stephens T**, **Tate P**. *Anatomy & Physiology*. 7 ed. New York: McGraw-Hill Companies, Inc, 2007.

130. **Sengupta PP**, **Tajik AJ**, **Chandrasekaran K**, **Khandheria BK**. Twist mechanics of the left ventricle. *J Am Coll Cardiol Img* 1: 366–376, 2008.

131. **Shechter M**, **Issachar A**, **Marai I**, **Koren-Morag N**, **Freinark D**, **Shahar Y**, **Shechter A**, **Feinberg MS**. Long-term association of brachial artery flow-mediated vasodilation and cardiovascular events in middle-aged subjects with no apparent heart disease. *Int J Cardiol* 134: 52–58, 2009.

132. **Shenouda N**, **Gillen JB**, **Gibala MJ**, **MacDonald MJ**. Changes in brachial artery endothelial function and resting diameter with moderate-intensity continuous but not sprint interval training in sedentary men. *J Appl Physiol* (May 25, 2017). doi: 10.1152/japplphysiol.00058.2017.

133. **Shirai K**, **Shimizu K**, **Takata M**, **Suzuki K**. Independency of the cardio-ankle vascular index from blood pressure at the time of measurement. *J Hypertens* 35: 1521–1526, 2017.

134. **Simonson JS**, **Schiller NB**. Descent of the base of the left ventricle: An echocardiographic index of left ventricular function. *J Am Soc Echocardiogr* 2: 25–35, 1989.

135. **Sokolis DP**. Passive mechanical properties and structure of the aorta: segmental analysis. *Acta Physiol* 190: 277–289, 2007.

136. **Sommer G**, **Regitnig P**, **Koltringer L**, **Holzapfel GA**. Biaxial mechanical properties of intact and layer-dissected human carotid arteries at physiological and supraphysiological loadings. *Am J Physiol Heart Circ Physiol* 298: H898–H912, 2010.

137. **Souza RR**, **de França E**, **Madureira D**, **Pontes CCR**, **Santana JO**, **Caperuto EC**. Resistance training improves aortic structure in Wistar rats. *Braz J Phys Ther* (May 20, 2017). doi: 10.1016/j.bjpt.2017.05.001.

138. **Spence AL**, **Carter HH**, **Naylor LH**, **Green DJ**. A prospective randomized longitudinal study involving 6 months of endurance or resistance exercise. Conduit artery adaptation in humans. *J Physiol-London* 591: 1265–1275, 2013.

139. **Spronck B**, **Avolio AP**, **Tan I**, **Butlin M**, **Reesink KD**, **Delhaas T**. Arterial stiffness index beta and cardio-ankle vascular index inherently depend on blood

pressure but can be readily corrected. *J Hypertens* 35: 98–104, 2017.

140. **Spronck B**, **Avolio AP**, **Tan I**, **Butlin M**, **Reesink KD**, **Delhaas T**. Reply: physics cannot be disputed. *J Hypertens* 35: 1521–1526, 2017.

141. **Steptoe A**, **Smulyan H**, **Gribbin B**. Pulse wave velocity and blood pressure change: Calibration and applications. *Psychophysiol* 13: 488–496, 1976.

142. **Stöhr EJ**, **González-Alonso J**, **Pearson J**, **Low DA**, **Ali L**, **Barker H**, **Shave R**. Effects of graded heat stress on global left ventricular function and twist mechanics at rest and during exercise in healthy humans. *Exp Physiol* 96: 114–124, 2011.

143. **Stöhr EJ**, **Shave RE**, **Baggish AL**, **Weiner RB**. Left Ventricular Twist Mechanics in the Context of Normal Physiology and Cardiovascular Disease: A Review of Studies using Speckle Tracking Echocardiography. *Am J Physiol Heart Circ Physiol* 311: H633-H644.

144. **Sugawara J**, **Hayashi K**, **HH T**. Distal Shift of Arterial Pressure Wave Reflection Sites With Aging. *Hypertension* 56: 920–925, 2010.

145. **Sugawara J**, **Hayashi K**, **Yokoi T**, **Cortez-Cooper MY**, **DeVan AE**, **Anton MA**, **HH T**. Brachial–ankle pulse wave velocity: an index of central arterial stiffness? *J Hum Hypertens* 19: 401–406, 2005.

146. **Sugawara J**, **Tanaka H**. Brachial-Ankle Pulse Wave Velocity: Myths, Misconceptions, and Realities. *Pulse* 3: 106–113, 2015.

147. **Sutton-Tyrrell K**, **Najjar SS**, **Boudreau RM**, **Venkitachalam L**, **Kupelian V**, **Simonsick EM**, **Havlik R**, **Lakatta EG**, **Spurgeon H**, **Kritchevsky S**, **Pahor M**, **Bauer D**, **Newman A**, **Study FTHA**. Elevated aortic pulse wave velocity, a marker of arterial stiffness, predicts cardiovascular events in well-functioning older adults. *Circulation* 111: 3384–3390, 2005.

148. **Svedlund S**, **Gan L-M**. Longitudinal wall motion of the common carotid artery can be assessed by velocity vector imaging. *Clin Physiol Funct Imaging* 31: 32–38, 2010.

149. **Svedlund S**, **Gan L-M**. Longitudinal common carotid artery wall motion is associated with plaque burden in man and mouse. *Atherosclerosis* 217: 120–124, 2011.

150. **Taivainen SH**, **Yli-Ollila H**, **Juonala M**, **Kähönen M**, **Raitakari OT**, **Laitinen TM**, **Laitinen TP**. Interrelationships between indices of longitudinal movement of the common carotid artery wall and the conventional measures of subclinical

arteriosclerosis. *Clin Physiol Funct Imaging* 37: 305–313, 2017.

151. **Tanaka H**, **Munakata M**, **Kawano Y**, **Ohishi M**, **Shoji T**, **Sugawara J**, **Tomiyama H**, **Yamashina A**, **Yasuda H**, **Sawayama T**, **Ozawa T**. Comparison between carotid-femoral and brachial-ankle pulse wave velocity as measures of arterial stiffness. *J Hypertens* 27: 2022–2027, 2009.

152. **Tanaka H**, **Seals DR**, **Monahan KD**, **Clevenger CM**, **DeSouza CA**, **Dinenno FA**. Regular aerobic exercise and the age-related increase in carotid artery intima-media thickness in healthy men. *J Appl Physiol* 92: 1458–1464, 2001.

153. **Tat J**, **Au JS**, **Keir PJ**, **MacDonald MJ**. Reduced common carotid artery longitudinal wall motion and intramural shear strain in individuals with elevated cardiovascular disease risk using speckle tracking. *Clin Physiol Funct Imaging* 37: 106–116, 2015.

154. **The Reference Values for Arterial Stiffness' Collaboration**. Determinants of pulse wave velocity in healthy people and in the presence of cardiovascular risk factors: "establishing normal and reference values." *Eur Heart J* 31: 2338–2350, 2010.

155. **Thein E**, **Hammer C**. Physiologic barriers to xenotransplantation. *Curr Opin Organ Tran* 9: 186–189, 2004.

156. **Thijssen DHJ**, **Black MA**, **Pyke KE**, **Padilla J**, **Atkinson G**, **Harris RA**, **Parker B**, **Widlansky ME**, **Tschakovsky ME**, **Green DJ**. Assessment of flow-mediated dilation in humans: a methodological and physiological guideline. *Am J Physiol Heart Circ Physiol* 300: H2–H12, 2011.

157. **Thijssen DHJ**, **Cable NT**, **Green DJ**. Impact of exercise training on arterial wall thickness in humans. *Clin Sci* 122: 311–322, 2012.

158. **Tinken TM**, **Thijssen DHJ**, **Black MA**, **Cable NT**, **Green DJ**. Time course of change in vasodilator function and capacity in response to exercise training in humans. *J Physiol-London* 586: 5003–5012, 2008.

159. **Torrent-Guasp F**, **Ballester M**, **Buckberg GD**, **Carreras F**, **Flotats A**, **Carrió I**, **Ferreira A**, **Samuels LE**, **Narula J**. Spatial orientation of the ventricular muscle band: Physiologic contribution and surgical implications. *J Thorac Cardiovasc Surg* 122: 389–392, 2001.

160. **Touboul PJ**, **Hennerici MG**, **Meairs S**, **Adams H**, **Amarenco P**, **Bornstein N**, **Csiba L**, **Desvarieux M**, **Ebrahim S**, **Fatar M**, **Hernandez Hernandez R**, **Jaff M**, **Kownator S**, **Prati P**, **Rundek T**, **Sitzer M**, **Schminke U**, **Tardif JC**, **Taylor A**, **Vicaut E**, **Woo KS**, **Zannad F**, **Zureik M**. Mannheim Carotid

Intima-Media Thickness Consensus (2004-2006). *Cerebrovasc Dis* 23: 75–80, 2007.

161. **Townsend RR**, **Wilkinson IB**, **Schiffrin EL**, **Avolio AP**, **Chirinos JA**, **Cockcroft JR**, **Heffernan KS**, **Lakatta EG**, **McEniery CM**, **Mitchell GF**, **Naijar SS**, **Nichols WW**, **Urbina EM**, **Weber T**. Recommendations for improving and standardizing vascular research on arterial stiffness. *Hypertension* 66: 698–722, 2015.

162. **Van Bortel LM**, **De Backer T**, **Segers P**. Standardization of arterial stiffness measurements make them ready for use in clinical practice. *Am J Hypertens* 29: 1234–1236, 2016.

163. **Van Bortel LM**, **Laurent S**, **Boutouyrie P**, **Chowienczyk P**, **Cruickshank JK**, **De Backer T**, **Filipovsky J**, **Huybrechts S**, **Mattace-Raso FUS**, **Protogerou AD**, **Schillaci G**, **Segers P**, **Vermeersch S**, **Weber T**. Expert consensus document on the measurement of aortic stiffness in daily practice using carotid-femoral pulse wave velocity. *J Hypertens* 30: 445–448, 2012.

164. **van Mil ACCM**, **Pearson J**, **Drane AL**, **Cockcroft JR**, **McDonnell BJ**, **Stöhr EJ**. Interaction between left ventricular twist mechanics and arterial haemodynamics during localised, non-metabolic hyperaemia with and without blood flow restriction. *Exp Physiol* 101: n/a–n/a, 2016.

165. **van Sloten TT**, **Sedaghat S**, **Laurent S**, **London GM**, **Pannier B**, **Ikram MA**, **Kavousi M**, **Mattace-Raso F**, **Franco OH**, **Boutouyrie P**, **Stehouwer CDA**. Carotid Stiffness Is Associated With Incident Stroke: A systematic review and individual participant data meta-analysis. *J Am Coll Cardiol* 66: 2116–2125, 2015.

166. **Vlachopoulos C**, **Aznaouridis K**, **Stefanadis C**. Prediction of cardiovascular events and all-cause mortality with arterial stiffness: A systematic review and meta-analysis. *J Am Coll Cardiol* 55: 1318–1327, 2010.

167. **Wagenseil JE**, **Mecham RP**. Vascular Extracellular Matrix and Arterial Mechanics. *Physiol Rev* 89: 957–989, 2009.

168. **Wang KL**, **Cheng H-M**, **Sung SH**, **Chuang S-Y**, **Li CH**, **Spurgeon HA**, **Ting CT**, **Najjar SS**, **Lakatta EG**, **Yin FCP**, **Chou P**, **Chen C-H**. Wave Reflection and Arterial Stiffness in the Prediction of 15-Year All-Cause and Cardiovascular Mortalities: A Community-Based Study. *Hypertension* 55: 799–805, 2010.

169. **Watson LE**, **Sheth M**, **Denyer RF**, **Dostal DE**. Baseline Echocardiographic Values For Adult Male Rats. *J Am Soc Echocardiogr* 17: 161–167, 2004.

170. **Weiner RB**, **Weyman AE**, **Khan AM**, **Reingold JS**, **Chen-Tournoux AA**, **Scherrer-Crosbie M**, **Picard MH**, **Wang TJ**, **Baggish AL**. Preload Dependency of Left Ventricular Torsion: The Impact of Normal Saline Infusion. *Circ Cardiovasc Img* 3: 672–678, 2010.

171. **Weiner RB**, **Weyman AE**, **Kim JH**, **Wang TJ**, **Picard MH**, **Baggish AL**. The impact of isometric handgrip testing on left ventricular twist mechanics. *J Physiol* 590: 5141–5150, 2012.

172. **Wilkinson IB**, **Franklin SS**, **Cockcroft JR**. Nitric Oxide and the Regulation of Large Artery Stiffness: From Physiology to Pharmacology. *Hypertension* 44: 112–116, 2004.

173. **Wilkinson IB**, **MacCallum H**, **Flint L**, **Cockcroft JR**, **Newby DE**, **Webb DJ**. The influence of heart rate on augmentation index and central arterial pressure in humans. *J Physiol* 525: 263–270, 2000.

174. **Wilkinson IB**, **Qasem A**, **McEniery CM**, **Webb DJ**, **Avolio AP**, **Cockcroft JR**. Nitric Oxide Regulates Local Arterial Distensibility In Vivo. *Circulation* 105: 213–217, 2002.

175. **Wolinsky H**, **Glagov S**. Structural Basis for the Static Mechanical Properties of the Aortic Media. *Circ Res* 14: 400–414, 1964.

176. **Yang EY**, **Chambless L**, **Sharrett AR**, **Virani SS**, **Liu X**, **Tang Z**, **Boerwinkle E**, **Ballantyne CM**, **Nambi V**. Carotid Arterial Wall Characteristics Are Associated With Incident Ischemic Stroke But Not Coronary Heart Disease in the Atherosclerosis Risk in Communities (ARIC) Study. *Stroke* 43: 103–108, 2012.

177. **Yasmin**, **McEniery CM**, **O'Shaughnessy KM**, **Harnett P**, **Arshad A**, **Wallace S**, **Maki-Petaja K**, **McDonnell B**, **Ashby MJ**, **Brown J**, **Cockcroft JR**, **Wilkinson IB**. Variation in the Human Matrix Metalloproteinase-9 Gene Is Associated With Arterial Stiffness in Healthy Individuals. *Arterioscler Throm Vas* 26: 1799–1805, 2006.

178. **Yasmin**, **Wallace S**, **McEniery CM**, **Dakham Z**, **Pusalkar P**, **Maki-Petaja K**, **Ashby MJ**, **Cockcroft JR**, **Wilkinson IB**. Matrix Metalloproteinase-9 (MMP-9), MMP-2, and Serum Elastase Activity Are Associated With Systolic Hypertension and Arterial Stiffness. *Arterioscler Throm Vas* 25: 372–378, 2004.

179. **Yeboah J**, **Crouse JR**, **Hsu FC**, **Burke GL**, **Herrington DM**. Brachial Flow-Mediated Dilation Predicts Incident Cardiovascular Events in Older Adults: The Cardiovascular Health Study. *Circulation* 115: 2390–2397, 2007.

180. **Yli-Ollila H**, **Laitinen T**, **Weckström M**, **Laitinen TM**. Axial and radial

waveforms in common carotid artery: An advanced method for studying arterial elastic properties in ultrasound imaging. *Ultrasound Med Biol* 39: 1168–1177, 2013.

181. **Yli-Ollila H**, **Laitinen T**, **Weckström M**, **Laitinen TM**. New indices of arterial stiffness measured from longitudinal motion of common carotid artery in relation to reference methods, a pilot study. *Clin Physiol Funct Imaging* 36: 376–388, 2015.

182. **Yli-Ollila H**, **Tarvainen MP**, **Laitinen TP**, **Laitinen TM**. Principal component analysis of the longitudinal carotid wall motion in association with vascular stiffness: a pilot study. *Ultrasound Med Biol* 42: 2873–2886, 2016.

183. **Yli-Ollila H**, **Tarvainen MP**, **Laitinen TP**, **Laitinen TM**. Transfer function analysis of the longitudinal motion of the common carotid artery wall. *Front Physiol* 7, 2016.

184. **Yokoyama H**, **Shoji T**, **Kimoto E**, **Shinohara K**, **Tanaka S**, **Koyama H**, **Emoto M**, **Nishizawa Y**. Pulse wave velocity in lower-limb arteries among diabetic patients with peripheral artery disease. *J Atheroscler Throm* 10: 253–258, 2003.

185. **Yoshizawa M**, **Maeda S**, **Miyaki A**, **Misono M**, **Saito Y**, **Tanaka H**, **Kuno S**, **Ajisaka R**. Effect of 12 weeks of moderate-intensity resistance training on arterial stiffness: a randomised controlled trial in women aged 32-59 years. *Brit J Sport Med* 43: 615–618, 2009.

186. **Yuan C**, **Wang J**, **Ying M**. Predictive Value of Carotid Distensibility Coefficient for Cardiovascular Diseases and All-Cause Mortality: A Meta-Analysis. *PLoS ONE* 11: e0152799, 2016.

187. **Zahnd G**, **Balocco S**, **Sérusclat A**, **Moulin P**, **Orkisz M**, **Vray D**. Progressive attenuation of the longitudinal kinetics in the common carotid artery: Preliminary in vivo assessment. *Ultrasound Med Biol* 41: 339–345, 2014.

188. **Zahnd G**, **Boussel L**, **Marion A**, **Durand M**, **Moulin P**, **Sérusclat A**, **Vray D**. Measurement of two-dimensional movement parameters of the carotid artery wall for early detection of arteriosclerosis: A preliminary clinical study. *Ultrasound Med Biol* 37: 1421–1429, 2011.

189. **Zahnd G**, **Vray D**, **Sérusclat A**, **Alibay D**, **Bartold M**, **Brown A**, **Durand M**, **Jamieson LM**, **Kapellas K**, **Maple-Brown LJ**, **O'Dea K**, **Moulin P**, **Celermajer DS**, **Skilton MR**. Longitudinal displacement of the carotid wall and cardiovascular risk factors: Associations with aging, adiposity, blood pressure and periodontal disease independent of cross-sectional distensibility and intima-

media thickness. *Ultrasound Med Biol* 38: 1705–1715, 2012.

CHAPTER 2:

CAROTID ARTERY LONGITUDINAL WALL MOTION IS ASSOCIATED WITH LOCAL BLOOD VELOCITY AND LEFT VENTRICULAR ROTATIONAL, BUT NOT LONGITUDINAL, MECHANICS

Published in *Physiological Reports*, 4(14):e12872, 2016.

Published under a Creative Commons Attribution License 3.0.

Physiological Reports

Open Access

Physiological Reports ISSN 2051-817X

ORIGINAL RESEARCH

Carotid artery longitudinal wall motion is associated with local blood velocity and left ventricular rotational, but not longitudinal, mechanics

Jason S. Au[1], David S. Ditor[2], Maureen J. MacDonald[1] & Eric J. Stöhr[3]

1 Department of Kinesiology, McMaster University, Hamilton, Ontario, Canada
2 Department of Kinesiology, Brock University, St. Catharines, Ontario, Canada
3 Discipline of Physiology & Health, Cardiff School of Sport, Cardiff Metropolitan University, Cardiff, Wales, UK

Keywords
Carotid artery longitudinal wall motion, left ventricular rotation, ultrasound.

Correspondence
Maureen J. MacDonald, McMaster University, Department of Kinesiology, IWC E207, 1280 Main Street West, Hamilton, ON, Canada, L8S 4K1.
Telephone: 905-525-9140 ext. 23580
Fax: 905-523-6011
E-mail: macdonmj@mcmaster.ca

Funding Information
This study was supported by funding from the Natural Sciences and Engineering Research Council to Maureen MacDonald (DG # 238819-13, and RTI # 406308-11).

Received: 26 June 2016; Accepted: 28 June 2016

doi: 10.14814/phy2.12872

Physiol Rep, 4 (14), 2016, e12872, doi: 10.14814/phy2.12872

Abstract

Recent studies have identified a predictable movement pattern of the common carotid artery wall in the longitudinal direction. While there is evidence that the magnitude of this carotid artery longitudinal wall motion (CALM) is sensitive to cardiovascular health status, little is known about the determinants of CALM. The purpose of this integrative study was to evaluate the contribution of left ventricular (LV) cardiac motion and local blood velocity to CALM. Simultaneous ultrasound measurements of CALM, common carotid artery mean blood velocity (MBV), and left ventricular motion were performed in ten young, healthy individuals (6 males; 22 ± 1 years). Peak anterograde CALM occurred at a similar time as peak MBV (18.57 ± 3.98% vs. 18.53 ± 2.81% cardiac cycle; *t*-test: $P = 0.94$; ICC: 0.79, $P < 0.01$). The timing of maximum retrograde CALM displacement was different, but related, to both peak apical (41.00 ± 7.81% vs. 35.33 ± 5.79% cardiac cycle; *t*-test: $P < 0.01$; ICC: 0.79, $P < 0.01$) and basal rotation (41.80 ± 6.12% vs. 37.30 ± 5.66% cardiac cycle; *t*-test: $P < 0.01$; ICC: 0.74, $P < 0.01$) with peak cardiac displacements preceding peak CALM displacements in both cases. The association between basal rotation and retrograde CALM was further supported by strong correlations between their peak magnitudes ($r = -0.70$, $P = 0.02$), whereas the magnitude of septal longitudinal displacement was not associated with peak CALM ($r = 0.11$, $P = 0.77$). These results suggest that the rotational mechanical movement of the LV base may be closely associated with longitudinal mechanics in the carotid artery. This finding may have important implications for interpreting the complex relationship between ventricular and vascular function.

Introduction

Recent investigations have revealed a predictable and stable carotid artery longitudinal wall motion (CALM) pattern in healthy individuals, which retains both its pattern and magnitude over time (Ahlgren et al. 2012). Once thought to be breathing artifact, arterial motion in the longitudinal plane was first confirmed by cinematography of reflective beads sutured to the pig abdominal aorta (Tozzi et al. 2001), and has since been reported in the human common carotid artery (CCA) (Golemati et al. 2003; Persson et al. 2003; Soleimani et al. 2011). Due to the low motion velocities and thin arterial wall thickness, it has been difficult to accurately quantify CALM using standard techniques. With the use of more advanced 2D speckle tracking algorithms (O'Donnell et al. 1991, 1994; Larsson et al. 2011; Tat et al. 2015), longitudinal motion can be accurately quantified and has been shown to be of equal magnitude as radial expansion in both elastic (Cinthio et al.

© 2016 The Authors. *Physiological Reports* published by Wiley Periodicals, Inc. on behalf of the American Physiological Society and The Physiological Society.
This is an open access article under the terms of the Creative Commons Attribution License, which permits use, distribution and reproduction in any medium, provided the original work is properly cited.

2006; Tat et al. 2015) and muscular arteries (Cinthio and Ahlgren 2010).

Following initial descriptions of CALM, it is now apparent that the walls of the CCA move longitudinally, both in the direction of blood flow (anterograde) as well as in the direction opposing blood flow (retrograde), at different time points throughout the cardiac cycle (Golemati et al. 2003; Cinthio et al. 2006). Although the movement pattern may vary greatly between individuals, CALM has been demonstrated to remain stable within an individual over time (Ahlgren et al. 2012), making it a potential target for the noninvasive assessment of arterial properties in humans. The gold standard for the assessment of arterial stiffness, pulse wave velocity, has been extensively examined as a predictor for cardiovascular disease risk (The Reference Values for Arterial Stiffness' Collaboration, 2010; Van Bortel et al. 2012; Townsend et al. 2015), and has been shown to correlate to the magnitude of CALM displacements (Taivainen et al. 2015; Yli-Ollila et al. 2015). Preliminary cross-sectional studies have reported differences in the magnitude of CALM in populations at high risk of developing cardiovascular disease, including older adults with diabetes, Indigenous Australians with periodontal disease and individuals with spinal cord injury (Zahnd et al. 2011, 2012; Tat et al. 2015). These studies indicate promise in CALM as a measurement of arterial health that is noninvasive, and feasible in a clinical setting.

Despite preliminary evidence of a link between CALM and cardiovascular health, the determinants of the phases of CALM remain unknown. Ahlgren et al. (2015) found no correlation between maximal longitudinal displacement of the porcine CCA intima-media and wall shear rate. However, the authors did not separate CALM into anterograde and retrograde phases, and it may be that the forward shear stimulus can only explain the anterograde phase of motion. Likewise, the retrograde CALM phase is likely not determined by the local mechanical stimuli such as the frictional forces due to blood flow and transmural pressure forces, as anterograde shear stress would push the arterial wall in the forward direction. We have, therefore, approached this problem at an integrative systems level where we hypothesized that cardiac contraction would induce retrograde motion during early systole through a structural ventricular-vascular coupling effect. Recent work by Zahnd et al. (2014) has demonstrated regional differences in CALM along the length of the CCA, quantifying an attenuation in movement with a coefficient of $-2.5 \pm 2.0\%\ mm^{-1}$ distal to the heart. With a clear distal loss of motion magnitude along the CCA, it stands to reason that a cardiac factor may be affecting the magnitude of CALM. Yet, to date no studies have directly measured the influence of cardiac mechanics on CALM.

The purpose of this study was to evaluate the role of both local arterial and central cardiac mechanics on the timing and magnitude of specific CALM events in young, healthy individuals and thereby advance the understanding of CCA longitudinal mechanics. We hypothesized that the timing of retrograde CALM would be primarily linked to LV mechanics, and the timing of anterograde CALM would be linked to local blood flow events at the carotid artery.

Methods

Participants and ethical approval

Ten young healthy individuals (6 males, 4 females) were recruited for this study. All participants were between the ages of 18–35 years, and free of known cardiovascular disease. Informed consent in writing was obtained prior to participation in the study. The study protocol was submitted to, and approved by, the Hamilton Integrated Research Ethics Board and conforms to the *Declaration of Helsinki* concerning the use of human subjects as research participants.

Experimental measures

All participants arrived at the lab between the hours of 0800–1000 in the fasted state, after refraining from exercise, alcohol and caffeine for >8 h. Participants then rested in the supine position for 10 min prior to any data collection. For data collection, participants were positioned in the left lateral decubitus position and equipped with three sets of single-lead ECG to provide heart rate signals to two ultrasound units and a data collection system used to align the simultaneous measures during analysis.

Carotid arterial longitudinal motion

Longitudinal motion was assessed on the far wall of the right CCA, 2–5 cm proximal to the carotid bifurcation in the lateral plane using a 12 MHz linear-array probe connected to a high-resolution ultrasound machine (Vivid q, GE Medical Systems, Horten, Norway). A single focal point was positioned at the far wall and scanning depth was standardized at 2.5 cm to maintain a consistent sampling rate of 102.5 fps. Immediately prior to image acquisition, participants were asked to briefly hold their breath, as breathing artifact has been demonstrated to superimpose movement over longitudinal motion measures (Cinthio et al. 2005). Three to six heart cycles were recorded. Following acquisition, images were stored offline in the Digital Imaging and Communications in

© 2016 The Authors. *Physiological Reports* published by Wiley Periodicals, Inc. on behalf of the American Physiological Society and The Physiological Society.

Medicine (DICOM) format, and separated into sequences of .jpg images for analysis. Carotid Arterial Longitudinal Motion (CALM) was measured using an in-house speckle tracking algorithm (SpecTAT; MatLab, The MathWorks, Natick, MA) (Tat et al. 2015). In brief, the program uses a multiblock matching scheme to track two-dimensional motion of the arterial wall. Gated to the R-spike on the ECG, the lower edge of a reference kernel block (5.52×0.414 mm^2) was manually placed over the media-adventitia interface of the far wall. To improve resolution, a surrounding region of interest was interpolated to increase the number of pixels by a factor of four. For each successive frame, a normalized cross correlation function identified the peak correlation value for all possible kernel matches, and a shift in pixel position was taken to represent tissue displacement. A value above a lower boundary of 0.7 was considered acceptable for tracking (Farron et al. 2009). The coefficient of variation for day-to-day measurements of CALM magnitude in our laboratory ($n = 10$) was 7.8%, which indicates a good reproducibility between measurements, and compares well to other reports (Zahnd et al. 2011; Yli-Ollila et al. 2013).

Echocardiography

In order to investigate contributions of LV contraction to events at the CCA, images were recorded from the parasternal and apical windows, simultaneously to CALM measurements. Echocardiographic image acquisition followed current guidelines for conventional variables (Lang et al. 2015) as well as for LV mechanics (Mor-Avi et al. 2011). In order to standardize rotation analysis across individuals, the basal level was defined as the highest plane at which the mitral leaflets were visible. The apical level was defined as the imaging plane closest to the apex with no visible papillary muscles, as previously described (Stöhr et al. 2011). In addition, apical four-chamber images were recorded. Images were taken with a 1.5–3.6 MHz phased-array probe connected to a second ultrasound machine (Vivid q, GE Medical Systems) at >60 fps. Following acquisition, images were stored off-line for further analysis using commercially available software (EchoPAC 110.0.2; GE Medical Systems, Horten, Norway). End-diastolic volume, stroke volume, and posterior wall thickness were estimated from LV short-axis images at the level of the base in M-mode. 2D speckle tracking with drift compensation was used to quantify left ventricular basal and apical rotation and rotation velocity from LV short-axis images, as well as basal septal displacement from the apical four-chamber view. These traces were exported to a custom data processing software (2DStrainAnalysis Tool, Stuttgart, Germany) for further processing, with the purpose of achieving a relative time alignment of cardiac and CALM events (Burns et al. 2008) as described in more detail below.

Carotid blood velocity

For an assessment of timing of events, carotid mean blood velocity (MBV) was recorded simultaneous to vascular and cardiac imaging using a nonimaging 4 MHz pulsed wave probe at an insonation angle of 40° placed immediately proximal to the vascular probe on the CCA. This nonimaging probe was directly attached to an external spectral analysis system (model Neurovision 500 M TCD; Multigon Industries, Yonkers, NY) to determine intensity weighted mean blood velocity traces through a fast-Fourier transform and these signals were subsequently sampled at 1000 Hz using commercially available hardware (PowerLab model ML 795; AD Instruments). To examine the relationship between the magnitude of carotid and cardiac events, MBV was also measured independent of other outcomes using a linear-array probe in Duplex mode at 4 MHz (Vivid q, GE Medical Systems) at an insonation angle of 60° at 2–3 cm proximal to the carotid bifurcation, and processed as above. CCA shear rate was estimated using the equation, shear rate ($1\ \text{sec}^{-1}$) = (8*Blood Velocity at the CCA)/(CCA End Diastolic Lumen Diameter) (Parker et al. 2009). End diastolic diameters were analyzed offline using a custom-designed semi-automated edge tracking software (Artery Measurement System Image and Data Analysis, Tomas Gustavsson; Sweden) (Liang et al. 2000).

Data analysis and definitions of CALM events

In order to account for different sampling rates and permit time alignment of parameters, all CALM and cardiac data were cubic-spline interpolated to 600 points per cardiac cycle, with the R-spike of the ECG denoting the first time point. Certain CALM events in the systolic period were consistently present in all individuals examined, as shown in Figure 1: (A) the onset of retrograde (negative) motion was determined as the first movement of the wall in retrograde direction; (B) the onset of anterograde (positive) motion was determined as the first movement in the anterograde direction, or the local positive peak of the 2nd derivative in the absence of a clear local minimum; (C) the peak anterograde (positive) displacement was determined as the maximal displacement in the anterograde direction away from the heart, or the local negative minimum of the 2nd derivative in the absence of a clear local maximum; and (D) the peak retrograde (negative) displacement was determined as the maximal displacement in the retrograde direction toward the heart.

© 2016 The Authors. *Physiological Reports* published by Wiley Periodicals, Inc. on behalf of the American Physiological Society and The Physiological Society.

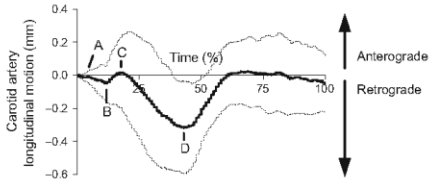

Figure 1. A typical CALM pattern expressed as percentage duration of a single cardiac cycle, gated to the R-spike of the concurrently recorded ECG. Positive deflections indicate movement in the anterograde direction (i.e., in the direction of blood flow), whereas negative deflections indicate movement in the retrograde direction (i.e., in the direction of the left ventricle). Point A represents the onset of the first deflection in the retrograde direction. Point B represents the onset of the first anterograde movement. Point C represents the peak anterograde displacement. Point D represents the peak retrograde displacement. Dashed lines represent interpolated ±1 SD.

Poor apical short-axis image quality for one participant resulted in only that apical data being removed from analysis. For all statistical comparisons, the raw individual traces were used to prevent the loss of motion information with a filtering process. The total magnitude of CALM was determined as the difference between peak anterograde and peak retrograde displacement of the arterial wall, with more negative values indicating a greater retrograde movement during late systole. The CALM pattern was also divided into anterograde (point C–point B) and retrograde (point D–point C) phases, both reported in absolute terms. An average of 3–5 cardiac cycles were used to compare simultaneous data.

In addition to apical and basal rotation, we investigated longitudinal displacement of the LV to assess the relationship of CALM events to cardiac motion in the longitudinal plane. Owing to its anatomical proximity to the CCA, the basal septal segment of the 2D strain analysis package was isolated using the custom-made 2DStrainAnalysis Tool (2DStrainAnalysis Tool, Stuttgart, Germany) and processed as above.

Statistical analyses

Statistical analyses were performed on the Statistical Package for the Social Sciences (version 20.0.0 for Mac; SPSS, Chicago, IL). Data were checked for normality using the Shapiro–Wilk test. Dependent Student's *t*-tests were used to assess differences in the timing between events at the same anatomical level (i.e., heart or carotid artery), expressed as a percentage of the cardiac cycle. For comparisons of local events at the CCA, where a time delay between events was not expected, nonsignificant *P*-values from the *t*-test and significant results from intraclass correlation coefficients (ICC) were interpreted as evidence for associations. Conversely, for comparisons between cardiac and CALM events, where a time delay between events was expected, only significant *P*-values from the *t*-test and significant results from intraclass correlation coefficients (ICC) were interpreted as evidence for associations. Because of the aforementioned expectation of a time delay between events at the heart and the carotid artery, relationships between the timing of CALM parameters with cardiac motion were determined from Consistency-type ICCs with a two-way random model.

To further explore associations revealed by the initial analyses, Pearson's correlations were applied to select variables that suggested associations between cardiac and CALM events. Analysis of data was performed on simultaneously collected heart cycles when possible, otherwise using an average of all available data for correlations. Statistical significance was set at $\alpha = 0.05$.

Results

The participant characteristics ($n = 10$; 6 males, 4 females; 22 ± 1 years) are presented in Table 1. The maximal excursion of retrograde CALM was significantly larger than the maximal excursion of anterograde CALM (0.42 ± 0.18 vs. 0.13 ± 0.12 mm; $P < 0.01$), and the total CALM displacement across one cardiac cycle was 0.50 ± 0.21 mm (Fig. 2).

Table 1. Participant characteristics ($n = 10$).

Variable	Mean ± SD
Sex (% Male)	60
Age (years)	22 ± 1
Height (m)	1.71 ± 0.08
Body mass (kg)	67.5 ± 9.9
SBP (mmHg)	116 ± 11
DBP (mmHg)	68 ± 6
MAP (mmHg)	87 ± 5
Heart rate (bpm)	61 ± 10
Cardiac parameters	
EDV (mL)	95 ± 15
Stroke volume (mL)	62 ± 10
PWT (mm)	0.88 ± 0.17
Peak apical rotation (°)	9.28 ± 5.30
Peak basal rotation (°)	−6.56 ± 3.03
Basal septal displacement (mm)	14.5 ± 2.0

SBP, systolic blood pressure; DBP, diastolic blood pressure; MAP, mean arterial pressure; CALM, carotid artery longitudinal motion; EDV, end-diastolic volume; PWT, posterior wall thickness.

© 2016 The Authors. *Physiological Reports* published by Wiley Periodicals, Inc. on behalf of the American Physiological Society and The Physiological Society.

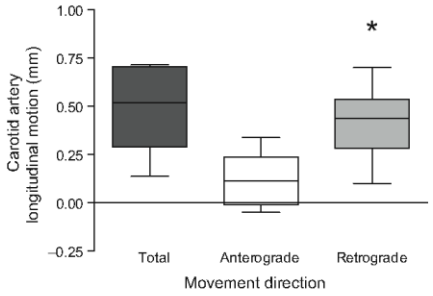

Figure 2. Total excursion, absolute anterograde, and absolute retrograde carotid artery longitudinal motion of the intima-media layer of the common carotid artery wall. The box represents the 25th, 50th (median), and 75th percentiles. The bars represent the minimum and maximum values. *$P < 0.01$ compared with anterograde motion.

Timing of CALM and cardiac events

Figure 3 represents the group averaged interpolated traces for simultaneous collection of: (A) longitudinal displacement of the basal septum; (B) apical rotation; and (C) basal rotation. The timings of events are presented in Table 2. According to our statistical requirements for temporal associations, we identified that peak CALM displacements were related to both local (i.e., MBV) and upstream (i.e., LV) events. The time the vascular wall was at peak anterograde displacement (CALM point C) was not different from the time of peak blood velocity (*t*-test $P = 0.94$), with the MBV wave consistently reaching peak velocity before peak anterograde displacement of the wall (ICC: 0.79, $P < 0.01$). The time at peak retrograde displacement (CALM point D) was different from the time of both peak apical (*t*-test $P < 0.01$) and basal (*t*-test $P < 0.01$) rotation, with peak cardiac displacements preceding peak retrograde wall displacements in both cases (apical ICC: 0.79, $P < 0.01$; basal ICC: 0.74, $P < 0.01$). This relationship was not found for peak basal septal displacement (*t*-test $P = 0.09$; ICC: 0.63, $P = 0.02$). Although we also investigated the relationship between early CALM events (points A and B) with local blood velocity and LV motion, these associations did not meet both a priori statistical criteria and were therefore not evaluated further.

Magnitude of cardiac and CALM events

Those variables that appeared to be temporally associated were further examined for associations between their magnitudes in order to gain greater insight into the strongest correlates between cardiac and CALM mechanics (Table 3 and Fig. 4). There was a moderate inverse correlation between retrograde CALM and participant height ($r = -0.48$; $P < 0.01$), with taller individuals exhibiting less motion. There was no correlation between the magnitudes of anterograde CALM and carotid shear rate ($r = -0.24$; $P = 0.20$). Retrograde CALM had a strong correlation with peak basal rotation ($r = -0.70$; $P = 0.02$) and shear rate ($r = 0.63$; $P = 0.05$), but no statistical correlation with basal septal longitudinal movement ($r = 0.11$; $P = 0.77$) or apical rotation ($r = 0.63$; $P = 0.09$).

Discussion

In this study, we show that longitudinal motion of the CCA (CALM) is associated with both local blood velocity and rotation of the LV base, but not with longitudinal septal displacement, thereby suggesting a physiological basis for the different phases of CALM previously observed. We propose that a complex relationship exists between the influences of local blood velocity and left ventricular rotation within the context of a structural ventricular-vascular coupling theory, as discussed in detail below.

Coupling theory

The role of cardiac contraction in CALM has been previously theorized in the literature but has never been reported (Cinthio et al. 2006; Ahlgren et al. 2012, 2015; Zahnd et al. 2012, 2014). In this study, we provide preliminary evidence for the influence of systolic cardiac events on the distinct longitudinal displacement of the arterial wall in the retrograde direction. Though the endocardium is not structurally continuous with the vascular wall of the CCA, the ventricular and vascular systems are anatomically directly linked by the aortic valve at the basal level of the LV, and indirectly by the ejection of blood from the LV. The present data suggest a previously unknown functional interdependence between the LV and CCA retrograde movement. These data are supported by Zahnd et al. (2014), who have demonstrated reductions in arterial wall motion along the length of the CCA, likely due to the distance from LV during systolic contraction. We, and others (Yli-Ollila et al. 2015), also report that taller individuals exhibit less longitudinal motion of the CCA intima-media complex, which is consistent with a reduction in CALM distal to the LV. Though this study shows a clear interaction between LV rotation and CALM, the exact determinants of interindividual variations in the CALM pattern and the potential

© 2016 The Authors. *Physiological Reports* published by Wiley Periodicals, Inc. on behalf of the American Physiological Society and The Physiological Society.

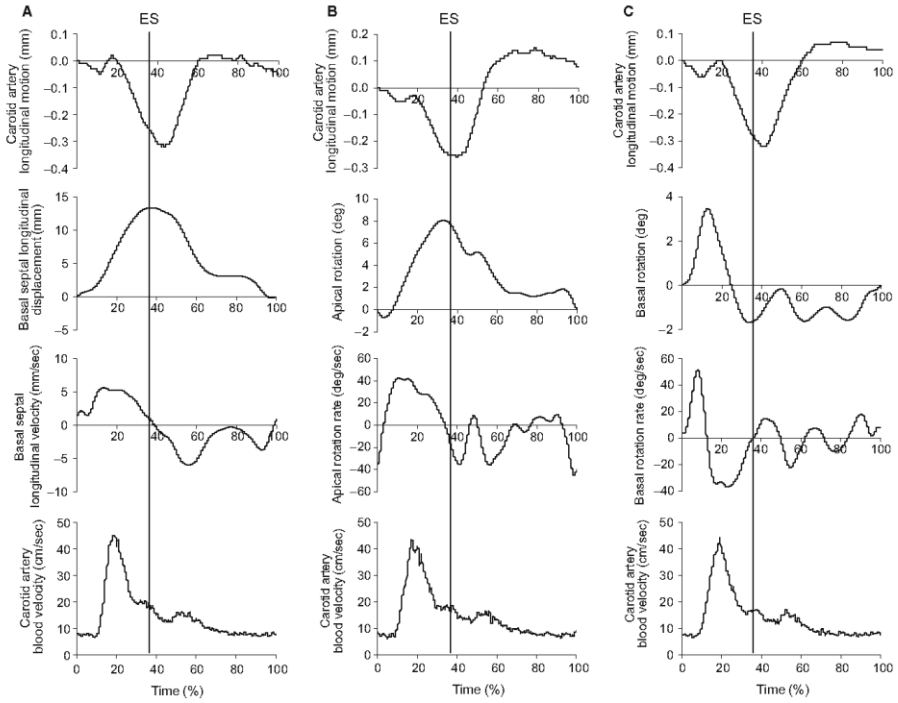

Figure 3. Group-averaged traces for the simultaneous assessment of cardiovascular parameters aligning with the carotid artery longitudinal motion (CALM) pattern. Panel A: Alignment of CALM with basal septal displacement (positive deflections indicating movement towards the apex), basal septal velocity, and carotid blood velocity. Panel B: Alignment of CALM with apical rotation (positive deflections indicating counter-clockwise rotation), rotation velocity and carotid blood velocity. Panel C: Alignment of CALM with basal rotation (positive deflections indicating counter-clockwise rotation), rotation velocity and carotid blood velocity. Standard deviation lines have been removed for clarity. ES, end-systole.

use of CALM analysis for indications of vascular health remain to be determined.

Timing of CALM events

Similar to previous reports, many CALM events were observed to be consistent across individuals (Golemati et al. 2003; Cinthio et al. 2006). Cardiac motion during systole appears to be related to motion of the retrograde segments of CALM, while the peak of the forward blood velocity wave is temporally linked with the peak anterograde segment of CALM. We found that the onset of retrograde CALM (point A in Fig. 1) occurred in concert with the onset of both basal septal longitudinal displacement and apical rotation, which is followed by a rapid increase in CCA blood velocity that coincides with the onset of anterograde wall motion (point B). However, we must note that these events did not meet both statistical requirements for association and we can only theorize their importance to the CALM pattern. As the blood velocity wave reaches peak magnitude, peak anterograde CALM displacement occurs (point C), and then retrograde motion resumes. We believe that during this period, the anterograde wall movement represents the interruption of the retrograde cardiac influence by the local mechanical blood velocity force (Nichols and O'Rourke 2005). When the anterograde blood velocity influence is waning, both LV longitudinal and rotational velocities reach peak instantaneous velocity. The now unopposed retrograde forces allow the arterial wall to

© 2016 The Authors. *Physiological Reports* published by Wiley Periodicals, Inc. on behalf of the American Physiological Society and The Physiological Society.

Table 2. Timing of events at the level of the left ventricle and the common carotid artery.

	Timing of events (% of heart cycle)						
Event pairing	CALM point		Comparison event	Mean difference 95% CI	*P*-value	ICC [95% CI]	*P*-value
CALM point A with							
Onset of septal movement	3.30 ± 2.31	vs.	5.10 ± 2.47	−4.58 to 0.98	0.18	−0.32 [−0.77 to −0.35]	0.83
Apical prerotation peak	4.57 ± 1.99	vs.	1.00 ± 5.16	−7.08 to 2.22	0.25	0.17 [−0.61 to 0.78]	0.34
Basal prerotation peak	2.70 ± 3.57	vs.	12.90 ± 3.57	−14.13 to −6.27	<0.01	−0.50 [−0.85 to 0.15]	0.94
CALM point B with							
Arrival of blood velocity wave	9.83 ± 3.03	vs.	10.73 ± 1.41	−2.19 to 0.39	0.17	−0.07 [−0.42 to 0.29]	0.65
Peak basal prerotation velocity	9.50 ± 3.31	vs.	7.60 ± 1.78	−0.83 to 4.63	0.15	−0.03 [−0.62 to 0.58]	0.54
CALM point C with							
Peak blood velocity	**18.57 ± 3.98**	**vs.**	**18.53 ± 2.81**	**−0.80 to 0.86**	**0.94**	**0.79 [0.61 to 0.90]**	**<0.01**
Peak basal rotation velocity	18.30 ± 4.85	vs.	20.30 ± 4.69	−5.66 to 1.66	0.25	0.43 [−0.24 to 0.82]	0.10
CALM point D with							
Peak septal displacement	42.60 ± 6.42	vs.	39.40 ± 5.72	−0.55 to 6.95	0.09	0.63 [0.04 to 0.89]	0.02
Peak apical rotation	**41.00 ± 7.81**	**vs.**	**35.33 ± 5.79**	**2.23 to 9.10**	**<0.01**	**0.79 [0.31 to 0.95]**	**<0.01**
Peak basal rotation	**41.80 ± 6.12**	**vs.**	**37.30 ± 5.66**	**1.44 to 7.56**	**<0.01**	**0.74 [0.24 to 0.93]**	**<0.01**

CALM, Carotid artery longitudinal motion; point A, onset of first deflection in the retrograde direction; point B, onset of first anterograde movement; point C, peak anterograde displacement; point D, peak retrograde displacement; 95% CI, 95% confidence interval. Bolded events are interpreted as occurring at a similar time. Values are means ± SD.
CALM points differ slightly in timing as analysis of data was performed on simultaneously collected heart cycles when possible.

Table 3. Correlations between CALM displacements with cardiac and blood flow stimuli.

event pairing	Pearson correlation coefficient	*P*-value
Anterograde CALM with		
Carotid shear rate	0.08	0.83
Retrograde CALM with		
Height	−0.48	<0.01
Carotid shear rate	0.63	0.05
Basal septal movement	0.11	0.77
Basal septal velocity	0.27	0.46
Apical rotation	0.60	0.09
Apical rotation velocity	0.58	0.12
Basal rotation	−0.70	0.02
Basal rotation velocity	0.51	0.13

CALM, Carotid artery longitudinal motion; Retrograde CALM and basal rotation are expressed as positive values.

reach peak retrograde displacement (point D) at end-systole. At this point, there were strong associations between the timing of peak retrograde displacement with peak apical (ICC: 0.79), and basal rotation (ICC: 0.74), where cardiac motion preceded motion at the CCA. As both of these left ventricular motion parameters inevitably peak at end-systole, we were unable to specify the greatest determinant of peak retrograde CALM displacement.

In summary, we hypothesize that motion at the LV initiates the movement pattern of CALM, which is interrupted during early-systole by the arrival of the forward blood velocity wave. Thus, the systolic CALM pattern may be conceived as two separate functions (i.e., a sustained retrograde cardiac-related wave that is briefly opposed by an anterograde blood velocity-related wave and a subsequent return to retrograde motion) that superimpose upon each other to create the observed summated function (Fig. 5). We hypothesize that interindividual variations in the CALM pattern during this time represent the individual force summation properties, with a larger cardiac stimulus reflecting a more retrograde summated function (see the −1 SD trace in Fig. 1), and a larger blood velocity stimulus reflecting a more anterograde function (see the +1 SD trace in Fig. 1). In this model, the timing of systolic phases remains consistent across individuals, albeit with much different motion magnitudes. Increased stiffness of the CCA is likely to influence this relationship, but the impact of arteriosclerosis on CALM is currently unknown.

Magnitude of CALM events

While our observations on the association between the timing of events yields insight into the factors associated with the pattern of CALM events during the systolic period, assessing the associations between the magnitude of events may offer further insight. In this regard, we observed no association between the magnitudes of the

© 2016 The Authors. *Physiological Reports* published by Wiley Periodicals, Inc. on behalf of the American Physiological Society and The Physiological Society.

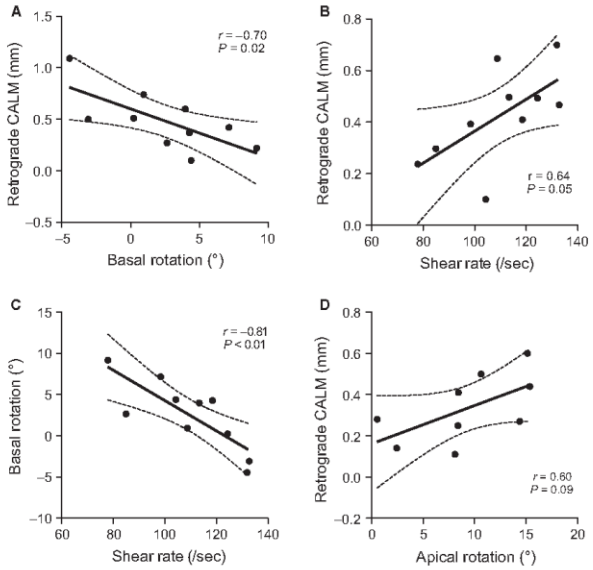

Figure 4. Correlations among the magnitude of events plotted with the 95% confidence intervals. (A) Basal rotation and retrograde CALM. (B) Carotid shear rate and retrograde CALM. (C) Carotid shear rate and basal rotation. (D) Apical rotation and retrograde CALM. Retrograde CALM and basal rotation are expressed as positive values.

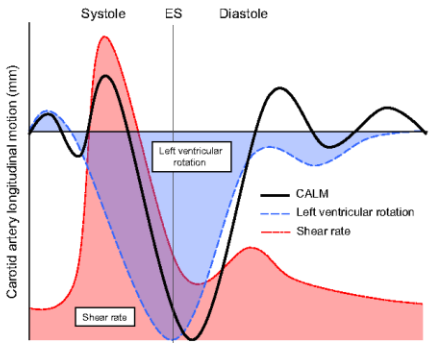

Figure 5. Schematicized theory of the influence of shear rate and left ventricular basal rotation on the CALM pattern as a summated function. Left ventricular rotation (blue) is theorized to begin at the first retrograde CALM displacement, which is briefly interrupted during early-systole by shear rate (red) at the carotid artery. ES, end systole.

anterograde CALM component and the local shear rate stimulus, similar to previous reports in a well-controlled model of the porcine carotid artery (Ahlgren et al. 2015). This lack of direct relationship may be due to the simultaneous competing influence of left ventricular rotation on the magnitude of movement of the carotid wall, as increases in both carotid shear rate and apical rotation occurred during the same period (see Fig. 5). Given that left ventricular contraction (whether displacement or rotation) approaches peak velocity during the same phase as peak carotid MBV (Fig. 3), it is not possible to isolate the contribution of the forward blood velocity wave to CALM event magnitudes from the confounding influence of ventricular motion in vivo. This has probably contributed to the lack of significant relationships between wall shear stress and CALM assessed by Ahlgren et al. (2015) through alpha- and beta-adrenergic stimulation, as adrenergic modulation would also act on left ventricular systolic function, impacting the early systolic influence of the heart on the CALM pattern.

With respect to retrograde motion of the arterial wall, we hypothesized that movement of the basal septum

© 2016 The Authors. *Physiological Reports* published by Wiley Periodicals, Inc. on behalf of the American Physiological Society and The Physiological Society.

would be the best candidate to predict the magnitude of retrograde CALM, as a pulling force would be applied to the vasculature directly through the aortic value in the same plane as the motion of the proximal aorta, and by extension the CCA. Contrary to our hypothesis, we did not observe any statistical relationship between the magnitudes of basal septal displacement and retrograde CALM. Instead, indices of LV rotation demonstrated relationships with the CALM pattern, suggesting that the natural twisting motion of the LV may have a stronger direct or indirect (through hemodynamics) effect on CALM than longitudinal LV displacement.

The consistency in which peak basal and apical rotation precede peak retrograde CALM displacement supports a direct relationship between LV rotation and arterial wall motion. Although the relationship between the LV base and CALM is supported by previous work suggesting that the kinetic energy of LV contraction appears to be greater at the LV base than the LV apex (Stöhr et al. 2014), the inverse linearity of the relationship between the magnitude of basal rotation and retrograde CALM seems to conflict with our coupling hypothesis. Instead of direct coupling, the LV base-CALM association may be indirectly mediated by carotid shear rate, which was also associated with both basal rotation and retrograde CALM (Fig. 4). For example, it is possible that a greater basal rotation may increase the hemodynamic vortices observed in the basal aspect of the LV, leading to a greater turbulence of flow than at lower basal rotation (Kilner et al. 2000). This in turn may lead to an altered angle of flow, which has been shown to impact on endothelial cell sensing (Wang et al. 2013). Purposeful examination of these concepts presents an exciting opportunity for future research.

Fully elucidating the competing roles of LV rotation and the local impact of shear rate is a difficult task as these elements appear to act in a coordinated system, impacting both each other, as well as the CALM pattern. Although we were not able to determine a causal relationship from our resting data, we believe our observational data has set a framework for the investigation into the roles of these competing stimuli to predict the magnitude of CALM displacements. Additional stimulus-response studies are required to further determine the factors that account of the magnitude of CALM events.

Perspectives: measurement of arterial stiffness

Recently, CALM has been investigated as a novel indicator of arterial health (Svedlund and Gan 2011; Zahnd et al. 2011, 2012; Taivainen et al. 2015; Tat et al. 2015). While these studies have identified clear differences in the CALM pattern between healthy and clinical populations, our findings indicate that caution must be used when interpreting these differences. While the majority of studies have reported peak displacements within the CALM pattern, the absolute magnitude of CALM may not be comparable between different individuals or groups without considering the influence from the heart. Indeed, our results indicate that other systemic factors such as afterload, contractility and heart rate have the potential to indirectly influence CALM via their effect on upstream LV rotation (Gibbons Kroeker et al. 1995; Weiner et al. 2012). Indices that are largely magnitude-independent such as the intramural shear strain index may be more appropriate indicators of arterial properties and have indeed shown sensitivity to detect differences in clinical populations (Cinthio et al. 2006; Tat et al. 2015). Zahnd et al. (2014) more recently theorized the use of an attenuation coefficient of motion along the CCA to enable tissue stiffness quantification, which may yield promising insights into a measure of arterial stiffness within the longitudinal plane (Zahnd et al. 2014). Finally, given the complex interaction between CALM, carotid shear rate and left ventricular rotation during systole, it may be of interest to examine 'passive' CALM events during diastole, as diastolic CALM would be largely unaffected from the influence of left ventricular rotation during the period when the aortic valve is closed. As new indices of arterial properties focused on the CALM pattern emerge, it is of utmost importance to consider the confounding contribution of cardiac motion when interpreting differences between healthy and clinical populations.

Limitations

While the simultaneous measurement of cardiac function and CALM controlled for the natural beat-to-beat variation in heart cycles, we were limited in the measurements that could be obtained concurrently. Other indices of left ventricular contraction were not investigated, such as longitudinal strain, circumferential strain, or tissue Doppler velocity of the mitral annulus. Our decision to focus on rotation as well as basal septal displacement was based on our objectives for examining the origin of retrograde CALM with respect to regional motion of the left ventricle. It was not possible to measure arterial Doppler blood velocity and CALM at the same segment of the CCA, although velocity measurements were taken immediately proximal to the high-resolution probe and should therefore not have caused a significant limitation to the present analyses. An in-house speckle tracking system was used to measure CALM. While this particular program has not been externally validated, there is currently no criterion standard for vascular speckle tracking. Even so,

© 2016 The Authors. *Physiological Reports* published by Wiley Periodicals, Inc. on behalf of the American Physiological Society and The Physiological Society.

CALM, as measured by our in-house program, showed good variability (CV = 7.8%) compared with other groups (Yli-Ollila et al. 2013). Finally, though this study may be underpowered in some specific comparisons, we were able to demonstrate strong correlations between outcome measures. The dual approach of examining associations between the timings as well as the magnitudes of cardiac and CALM events significantly increased our confidence in the determinants of CALM.

Conclusion

In summary, we observed a temporal relationship between the blood velocity wave and anterograde CALM, while retrograde CALM was associated in both timing and magnitude with left ventricular rotation, but not longitudinal septal displacement, as originally hypothesized. This relationship between carotid artery movement and left ventricular rotation may have important implications for the regulation of local vascular stiffness properties, and the complex interaction between left ventricular and vascular function.

Acknowledgments

We thank Hon Lam (Johnny) Choi for his assistance in data collection.

Conflict of Interest

None declared.

References

Ahlgren, A. R., M. Cinthio, H. W. Persson, and K. Lindström. 2012. Different patterns of longitudinal displacement of the common carotid artery wall in healthy humans are stable over a four-month period. Ultrasound Med. Biol. 38:916–925.

Ahlgren, A. R., S. Steen, S. Segstedt, T. Erlöv, K. Lindström, T. Sjöberg, et al. 2015. Profound increase in longitudinal displacements of the porcine carotid artery wall can take place independently of wall shear stress: a continuation report. Ultrasound Med. Biol. 41:1342–1353.

Burns, A. T., A. La Gerche, A. I. MacIsaac, and D. L. Prior. 2008. Augmentation of left ventricular torsion with exercise is attenuated with age. J. Am. Soc. Echocardiogr. 21:315–320.

Cinthio, M., and A. R. Ahlgren. 2010. Intra-observer variability of longitudinal displacement and intramural shear strain measurements of the arterial wall using ultrasound noninvasively in vivo. Ultrasound Med. Biol. 36:697–704.

Cinthio, M., A. R. Ahlgren, T. Jansson, A. Eriksson, H. W. Persson, and K. Lindström. 2005. Evaluation of an ultrasonic echo-tracking method for measurements of arterial wall movements in two dimensions. IEEE Trans. Ultrason. Ferroelectr. Freq. Control 52:1300–1311.

Cinthio, M., A. R. Ahlgren, J. Bergkvist, T. Jansson, H. W. Persson, and K. Lindström. 2006. Longitudinal movements and resulting shear strain of the arterial wall. Am. J. Physiol. Heart Circ. Physiol. 291:H394–H402.

Farron, J., T. Varghese, and D. G. Thelen. 2009. Measurement of tendon strain during muscle twitch contractions using ultrasound elastography. IEEE Trans. Ultrason. Ferroelectr. Freq. Control 56:27–35.

Gibbons Kroeker, C. A., J. V. Tyberg, and R. Beyar. 1995. Effects of load manipulations, heart rate, and contractility on left ventricular apical rotation. Circulation 92:130–141.

Golemati, S., A. Sassano, M. J. Lever, A. A. Bharath, S. Dhanjil, and A. N. Nicolaides. 2003. Carotid artery wall motion estimated from b-mode ultrasound using region tracking and block matching. Ultrasound Med. Biol. 29:387–399.

Kilner, P. J., G.-Z. Yang, A. J. Wilkes, R. H. Mohiaddin, D. N. Firmin, and M. H. Yacoub. 2000. Asymmetric redirection of flow through the heart. Nature 404:759–761.

Lang, R. M., L. P. Badano, V. Mor-Avi, J. Afilalo, A. Armstrong, L. Ernande, et al. 2015. Recommendations for Cardiac chamber quantification by echocardiography in adults: an update from the American Society of Echocardiography and the European Association of Cardiovascular Imaging. Eur. Heart J. Cardiovasc. Imaging 16:233–271.

Larsson, M., F. Kremer, P. Claus, T. Kuznetsova, L. Brodin, and J. D'hooge (2011). Ultrasound-based radial and longitudinal strain estimation of the carotid artery: a feasibility study. IEEE Trans. Ultrason. Ferroelectr. Freq. Control 58, 2244–2251.

Liang, Q., I. Wendelhag, J. Wikstrand, and T. Gustavsson. 2000. A multiscale dynamic programming procedure for boundary detection in ultrasonic artery images. IEEE Trans. Med. Imaging 19:127–142.

Mor-Avi, V., R. M. Lang, L. P. Badano, M. Belohlavek, N. M. Cardim, G. Derumeaux, et al. 2011. Current and evolving echocardiographic techniques for the quantitative evaluation of cardiac mechanics: ASE/EAE consensus statement on methodology and indications. J. Am. Soc. Echocardiogr. 24:277–313.

Nichols, W. W., and M. F. O'Rourke. 2005. McDonald's blood flow in arteries: theoretical, experimental and clinical principles. 5th ed. Hodder Arnold, London.

O'Donnell, M., A. R. Skovoroda, and B. M. Shapo. 1991. Measurement of arterial wall motion using fourier based speckle tracking algorithms. Proc. IEEE Ultrason. Symp. 1:1101–1104.

O'Donnell, M., A. R. Skovoroda, B. M. Shapo, and S. Y. Emelianov. 1994. Internal displacement and strain imaging using ultrasonic speckle tracking. IEEE Trans. Ultrason. Ferroelectr. Freq. Control 41:314–325.

© 2016 The Authors. *Physiological Reports* published by Wiley Periodicals, Inc. on behalf of the American Physiological Society and The Physiological Society.

Parker, B. A., T. L. Trehearn, and J. R. Meendering. 2009. Pick your Poiseuille: normalizing the shear stimulus in studies of flow-mediated dilation. J. Appl. Physiol. 107:1357–1359.

Persson, M., A. R. Ahlgren, T. Jansson, A. Eriksson, H. W. Persson, and K. Lindström. 2003. A new non-invasive ultrasonic method for simultaneous measurements of longitudinal and radial arterial wall movements: first in vivo trial. Clin. Physiol. Funct. Imaging 23:247–251.

Soleimani, E., M. M. Dizaji, and H. Saberi. 2011. Carotid artery wall motion estimation from consecutive ultrasonic images: comparison between block-matching and maximum-gradient algorithms. J. Tehran Heart Cent. 6:72–78.

Stöhr, E. J., J. González-Alonso, and R. Shave. 2011. Left ventricular mechanical limitations to stroke volume in healthy humans during incremental exercise. Am. J. Physiol. Heart Circ. Physiol. 301:H478–H487.

Stöhr, E. J., J. González-Alonso, I. N. Bezodis, and R. Shave. 2014. Left ventricular energetics: new insight into the plasticity of regional contributions at rest and during exercise. Am. J. Physiol. Heart Circ. Physiol. 306:H225–H232.

Svedlund, S., and L.-M. Gan. 2011. Longitudinal common carotid artery wall motion is associated with plaque burden in man and mouse. Atherosclerosis 217:120–124.

Taivainen, S. H., H. Yli-Ollila, M. Juonala, M. Kähönen, O. T. Raitakari, T. M. Laitinen, et al. 2015. Interrelationships between indices of longitudinal movement of the common carotid artery wall and the conventional measures of subclinical arteriosclerosis. Clin. Physiol. Funct. Imaging 1–9. doi: 10.1111/cpf.12305.

Tat, J., J. S. Au, P. J. Keir, and M. J. MacDonald. 2015. Reduced common carotid artery longitudinal wall motion and intramural shear strain in individuals with elevated cardiovascular disease risk using speckle tracking. Clin. Physiol. Funct. Imaging 1–11. doi: 10.1111/cpf.12270.

The Reference Values for Arterial Stiffness' Collaboration. 2010. Determinants of pulse wave velocity in healthy people and in the presence of cardiovascular risk factors: "establishing normal and reference values". Eur. Heart J. 31:2338–2350.

Townsend, R. R., I. B. Wilkinson, E. L. Schiffrin, A. P. Avolio, J. A. Chirinos, J. R. Cockcroft, et al. 2015. Recommendations for improving and standardizing vascular research on arterial stiffness. Hypertension 66:698–722.

Tozzi, P., D. Hayoz, C. Oedman, I. Mallabiabarrena, and L. K. von Segesser. 2001. Systolic axial artery length reduction: an overlooked phenomenon in vivo. Am. J. Physiol. Heart Circ. Physiol. 280:H2300–H2305.

Van Bortel, L. M., S. Laurent, P. Boutouyrie, P. Chowienczyk, J. K. Cruickshank, T. De Backer, et al. 2012. Expert consensus document on the measurement of aortic stiffness in daily practice using carotid-femoral pulse wave velocity. J. Hypertens. 30:445–448.

Wang, C., B. M. Baker, C. S. Chen, and M. A. Schwartz. 2013. Endothelial cell sensing of flow direction. Arterioscler. Thromb. Vasc. Biol. 33:2130–2136.

Weiner, R. B., A. E. Weyman, J. H. Kim, T. J. Wang, M. H. Picard, and A. L. Baggish. 2012. The impact of isometric handgrip testing on left ventricular twist mechanics. J. Physiol. 590:5141–5150.

Yli-Ollila, H., T. Laitinen, M. Weckström, and T. M. Laitinen. 2013. Axial and radial waveforms in common carotid artery: an advanced method for studying arterial elastic properties in ultrasound imaging. Ultrasound Med. Biol. 39:1168–1177.

Yli-Ollila, H., T. Laitinen, M. Weckström, and T. M. Laitinen. 2015. New indices of arterial stiffness measured from longitudinal motion of common carotid artery in relation to reference methods, a pilot study. Clin. Physiol. Funct. Imaging 1–13. doi: 10.1111/cpf.12240.

Zahnd, G., L. Boussel, A. Marion, M. Durand, P. Moulin, A. Sérusclat, et al. 2011. Measurement of two-dimensional movement parameters of the carotid artery wall for early detection of arteriosclerosis: a preliminary clinical study. Ultrasound Med. Biol. 37:1421–1429.

Zahnd, G., D. Vray, A. Sérusclat, D. Alibay, M. Bartold, A. Brown, et al. 2012. Longitudinal displacement of the carotid wall and cardiovascular risk factors: associations with aging, adiposity, blood pressure and periodontal disease independent of cross-sectional distensibility and intima-media thickness. Ultrasound Med. Biol. 38: 1705–1715.

Zahnd, G., S. Balocco, A. Sérusclat, P. Moulin, M. Orkisz, and D. Vray. 2014. Progressive attenuation of the longitudinal kinetics in the common carotid artery: preliminary in vivo assessment. Ultrasound Med. Biol. 41:339–345.

© 2016 The Authors. *Physiological Reports* published by Wiley Periodicals, Inc. on behalf of the American Physiological Society and The Physiological Society.

CHAPTER 3:

DIASTOLIC CAROTID ARTERY LONGITUDINAL WALL MOTION IS SENSITIVE TO BOTH AGING AND CORONARY ARTERY DISEASE STATUS INDEPENDENT OF ARTERIAL STIFFNESS

Published in *Ultrasound in Medicine and Biology*, [in press], 2017; doi: 10.1016/j.ultrasoundbio.2017.04.026.

Copyright © 2013 World Federation for Ultrasound in Medicine & Biology. Published by Elsevier Inc. All rights reserved. The authors retain the right to include the article in a thesis or dissertation whether in full or in part, subject to proper acknowledgement.

ARTICLE IN PRESS

Ultrasound in Med. & Biol., Vol. ■, No. ■, pp. 1–13, 2017
© 2017 World Federation for Ultrasound in Medicine & Biology
Printed in the USA. All rights reserved
0301-5629/$ - see front matter

ELSEVIER

http://dx.doi.org/10.1016/j.ultrasmedbio.2017.04.026

● *Original Contribution*

DIASTOLIC CAROTID ARTERY LONGITUDINAL WALL MOTION IS SENSITIVE TO BOTH AGING AND CORONARY ARTERY DISEASE STATUS INDEPENDENT OF ARTERIAL STIFFNESS

JASON S. AU,* SYDNEY E. VALENTINO,* PATRICK G. MCPHEE,† and MAUREEN J. MACDONALD*
*Department of Kinesiology, McMaster University, Hamilton, Canada; and †School of Rehabilitation Science, McMaster University, Hamilton, Canada

(*Received* 9 *December* 2016; *revised* 19 *April* 2017; *in final form* 24 *April* 2017)

Abstract—We investigated the ability of systolic and diastolic carotid artery longitudinal wall motion (CALM) to delineate expected differences in arterial health in individuals representing a range of both age and health status. We recruited 161 younger healthy adults (aged 24 ± 5 y), 51 older healthy adults (aged 70 ± 5 y) and 14 adults with coronary artery disease (aged 67 ± 8 y) for resting assessment of CALM and arterial stiffness. All CALM parameters were reduced in the old healthy adults and adults with coronary artery disease compared with the young healthy adults ($p < 0.01$), with diastolic velocity and maximum diastolic acceleration being further reduced in the adults with coronary artery disease than in the older healthy adults ($p < 0.01$). Diastolic CALM parameters were more strongly related to age (β range: −0.46 to −0.53) than systolic CALM parameters (β range: −0.24 to −0.44). In contrast to previous examinations of a variety of CALM parameters, diastolic CALM may provide superior promise in terms of characterizing arterial wall properties, with additional sensitivity to cardiovascular disease status. (E-mail: macdonmj@mcmaster.ca) **© 2017 World Federation for Ultrasound in Medicine & Biology.**

Key Words: **Arterial structure, Arterial compliance, Ultrasound, Aging, Coronary artery disease, Arterial wall motion, Speckle tracking.**

INTRODUCTION

Traditional measures of vascular structure and function have largely been studied in the radial plane, where more elastic arteries are characterized by slower pulse wave propagation and a high ratio of the cyclic change in cross-sectional area to pulse pressure (Nichols and O'Rourke 2005). Although only central arterial stiffness has been recommended as reflecting cardiovascular disease (CVD) risk (Reference Values for Arterial Stiffness' Collaboration 2010; Van Bortel et al. 2012), local common carotid artery (CCA) properties such as distensibility and intima–media thickness (IMT) have also been found to be sensitive to age and disease status (Engelen et al. 2015; Lorenz et al. 2007). Of particular clinical importance, measures of arterial stiffness in the radial plane have been suggested to increase throughout the life span in the absence of overt CVD (Mitchell et al. 2004), making them sensitive to CVD risk in otherwise healthy adults.

Recent advances in ultrasound image analysis have allowed measurement of arterial wall motion not only in the radial plane, but also in the longitudinal plane, along the length of an artery (Persson et al. 2003; Svedlund and Gan 2010). The study of carotid artery longitudinal wall motion (CALM) is an emerging field in vascular physiology, and some descriptive CALM parameters have been previously associated with local CCA distensibility, augmentation index and pulse wave velocity (PWV) (Taivainen et al. 2017; Yli-Ollila et al. 2015; Zahnd et al. 2012). The measurement of CALM has previously been reported to provide additional information beyond what is captured by traditional arterial stiffness assessment (Zahnd et al. 2012) and, therefore, has potential to be a vascular assessment tool that is complementary to traditionally measured arterial health indices. In addition, the measurement of CALM requires only the use of high-resolution ultrasound without the added complexity of local blood pressure measurements, making it distinct from

Address correspondence to: Maureen J. MacDonald, Department of Kinesiology, McMaster University, BSB 104, 1280 Main Street West, Hamilton, ON, L8S 4K1, Canada. E-mail: macdonmj@mcmaster.ca

pressure-dependent stiffness indexes acquired in the radial plane. Unfortunately, there currently exists only a small base of support for the clinical utility of CALM, and the relationship of CALM parameters to other stiffness measures has not yet been investigated across a large range of individuals with expected differences in arterial stiffness and CVD risk.

In this emerging field of CALM assessment, different research groups have represented longitudinal motion parameters in different ways, including the determination of simplified CALM displacements (Cinthio and Ahlgren 2010; Golemati et al. 2003; Svedlund and Gan 2011), displacement indices adjusted for relative motion between layers (Cinthio et al. 2006; Zahnd et al. 2012, 2014) and measurement of pattern length and complexity (Taivainen et al. 2017; Yli-Ollila et al. 2013, 2015). However, few of these parameters have a physiologic foundation on which to base their suggested associations with vascular structure. In agreement with early predictions that CALM would be influenced by the forces generated by both cardiac motion and arterial blood flow (Cinthio et al. 2006), our laboratory has recently reported a relationship between some CALM parameter magnitudes and both left ventricular rotation and local blood velocity during the systolic phase of the cardiac cycle (Au et al. 2016). We further suggest that differences in these influencing factors form the basis of the substantial inter-individual variability observed in systolic CALM parameters (Ahlgren et al. 2012; Yli-Ollila et al. 2013). In contrast, we hypothesize here that diastolic CALM will be relatively unaffected by variations in blood flow and ventricular motion, as active myocardial contraction is complete and the aortic valve is closed, limiting the complex physiologic interactions with CALM during systole. Therefore, diastolic measures may be more direct and sensitive indicators of the intrinsic properties of the arterial wall.

The aims of this study were: (i) to investigate the sensitivity of both systolic and diastolic CALM parameters to discriminate between groups of individuals with expected differences in arterial health status and (ii) to investigate the relationship between these parameters and arterial stiffness in a population of adults representing a broad range of age and CVD status. Furthermore, we wanted to explore which CALM parameters might provide unique arterial health information that is independent of traditional arterial stiffness. We hypothesized that diastolic CALM parameters would be related to local CCA arterial stiffness, and that these parameters would be more sensitive to differences in age and CVD health status compared with systolic CALM parameters.

METHODS

Participants and ethical approval

Two hundred and sixty-two participants were included in this analysis from previously collected data sets in our laboratory from 2012 to 2016. Healthy adults were grouped into younger healthy adults (YHA, <60 y old) and older healthy adults (OHA, ≥60 y old). Adults with documented coronary artery disease (CAD) met one of the following criteria: angiographically documented stenosis ≥50% in at least one major coronary artery; myocardial infarction, percutaneous coronary intervention or coronary artery bypass graft surgery; or positive exercise stress test determined by a positive nuclear scan or symptoms of chest discomfort accompanied by electrocardiogram (ECG) changes greater than 1 mm horizontal or downsloping ST-segment depression. Thirty-six participants were excluded because of poor image quality (primarily because of out-of-plane imaging and high echo backscatter; 17 YHA, 18 OHA, 1 CAD), resulting in a final analysis including 161 YHA (24 ± 5 y), 51 OHA (70 ± 5 y) and 14 adults with CAD (67 ± 8 y). All data collection was completed at the Vascular Dynamics Laboratory at McMaster University, Hamilton, Ontario, Canada. All participants gave verbal and written consent before participation in the study. The study protocols were approved by the Hamilton Integrated Research Ethics Board and conform to the Declaration of Helsinki concerning the use of human patients as research participants.

Experimental measures

All participants visited the laboratory between 0700 and 1100 hours in the fasted state, having refrained from exercise, alcohol and caffeine for >8 h. All measures were done in the supine position after a 10-min supine rest period. After the rest period, supine brachial blood pressure was measured in triplicate with a commercially available oscillometric device (Dinamap Pro 100, Critikon LCC, Tampa, FL, USA). All participants were continuously monitored for heart rate with single-lead ECGs (PowerLab Model ML 132, AD Instruments, Colorado Springs, CO, USA) and beat-to-beat finger blood pressures (Finometer MIDI, Finapres Medical Systems, Amsterdam, Netherlands).

Carotid artery longitudinal wall motion. Longitudinal motion was assessed as previously described (Au et al. 2016). In brief, brightness mode (B-mode), high-resolution ultrasound images were obtained at the right CCA, 1–3 cm proximal to the carotid bifurcation at 102.5 fps, using a 12-MHz linear-array probe connected to a commercial ultrasound unit (Vivid q, GE Medical Systems, Horten, Norway). Participants

were asked to briefly hold their breath during image acquisition, and three to six heart cycles were recorded. CALM was measured using an in-house speckle tracking algorithm (MATLAB, The MathWorks, Natick, MA, USA) (Tat et al. 2015). Gated to the R-spike on the ECG, two reference kernel blocks were manually placed on the far wall of the CCA to assess motion of two arterial wall layers. The first kernel was positioned so that the lower edge was placed on the media–adventitia interface (tracking the intima–media), while the second kernel was positioned immediately below, with the upper edge also placed on the media–adventitia interface (tracking the adventitia). All images in this study were analyzed by one of two observers (J.A. and S.V.). In a subset of 10 participants, values of the inter-rater reliability, ICC(2,2) absolute agreement, for anterograde, retrograde, and diastolic CALM were 0.92, 0.90, and 0.92 between these two observers, respectively.

Data analysis of CALM. We previously reported that certain CALM events are consistent within an individual and are related to physiologic events (Au et al. 2016). CALM traces were visualized for the detection of three primary phases of movement, which are found in all participants, regardless of inter-individual variations in the CALM pattern: systolic anterograde CALM (the first systolic anterograde movement to the peak systolic anterograde displacement), systolic retrograde CALM (the peak systolic anterograde displacement to the peak retrograde displacement) and diastolic CALM displacement (the peak retrograde displacement to the local diastolic anterograde plateau) (Fig. 1). Maximum longitudinal displacement is reported as maximum CALM. Mean diastolic velocity was calculated as the diastolic displacement over time. To obtain maximum instantaneous velocities and accelerations during the diastolic CALM phase, the displacement trace was digitally filtered (second-order, dual-pass Butterworth, Fc = 10 Hz) and subsequently differentiated into velocity and acceleration traces for peak detection. Shear strain was calculated between the intima–media and adventitia layers, as previous reported (Tat et al. 2015) (Fig. 1). Shearing angle was calculated using the equation (Cinthio et al. 2006)

$$\text{shear strain} = \arctan\left\{\frac{\left[\text{LPos}_{\text{IM}} - \text{LPos}_{\text{IM(ref)}}\right] - \left[\text{LPos}_{\text{Adv}} - \text{LPos}_{\text{Adv(ref)}}\right]}{\text{radial distance between ROI of IM and Adv}}\right\} \quad (1)$$

where LPos is longitudinal position, IM is intima–media, Adv is adventitia and ref is reference frame. The largest absolute shearing angle across the cardiac cycle is reported. For graphical representation only, and not for the purposes of generation of parameter values, the group-averaged longitudinal and radial plane displacement traces from three to six heart cycles per participant were linearly interpolated to 100 discrete points to account for variable heart cycle durations, which were then averaged within each population group.

Carotid artery distensibility. CCA distensibility was assessed using combined applanation tonometry (Model SPT-301, Millar Instruments, Houston, TX, USA) and B-mode ultrasound imaging. Local blood pressures were estimated from 10 high-quality pressure waveforms obtained at the CCA, where maximum, mean and minimum tonometer voltages were used to predict carotid blood pressure, calibrated to supine brachial blood pressure. Carotid maximum and minimum lumen diameters were assessed from images obtained with a 12-MHz linear-array ultrasound probe (Vivid q) positioned 2–5 cm proximal to the CCA bifurcation. Images were stored off-line in Digital Imaging and Communications in Medicine (DICOM) format for later analysis. Lumen diameters were measured using semi-automated edge-tracking software (Arterial Measurement System Image and Data Analysis, Tomas Gustavsson, Gothenburg, Sweden) (Liang et al. 2000). The equation for CCA distensibility was (Nichols and O'Rourke 2005)

$$\text{distensibility} = \frac{\text{LDmax} - \text{LDmin}}{\text{PP} \times \text{LDmin}} \quad (2)$$

where LDmax is the maximum lumen diameter, LDmin is the minimum lumen diameter, and PP is the pulse pressure.

Carotid–femoral pulse wave velocity. Carotid–femoral PWV was assessed according to the latest published guidelines (Van Bortel et al. 2012). High-quality pulse waves were recorded at the right common carotid and common femoral arteries using applanation tonometry (Model SPT-301) and sampled at 2000 Hz using commercially available hardware (PowerLab Model ML 795, AD Instruments). Pulse waves were bandpass filtered at 5–30 Hz to identify the time of the foot of

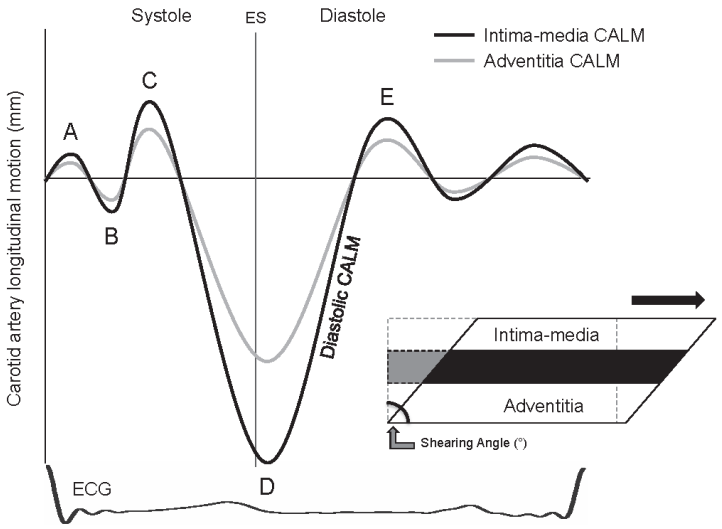

Fig. 1. Idealized CALM pattern of a single cardiac cycle, ECG-gated to the R–R interval. Points A–E represent consistent local maxima and minima between all participants. Systolic anterograde CALM is the difference in magnitude between C and B. Systolic retrograde CALM is the difference in magnitude between D and C. Diastolic CALM is the difference in magnitude between E and D. Shearing angle is calculated as the instantaneous angle between the intima–media (*black*) and adventitia (*grey*) wall layers. CALM = carotid artery longitudinal wave motion; ECG = electrocardiogram; ES = end-systole.

the waveform to calculate pulse transit time (Munakata et al. 2003). Carotid–femoral PWV was calculated as

$$\text{cfPWV} = \frac{80\%\ D}{\text{PTT}} \quad (3)$$

where 80% *D* is 80% of the distance between the carotid and femoral arteries measured using an anthropometric tape measure, and PTT is the foot-to-foot pulse transit time.

Intima–media thickness. Arterial wall thickness was assessed by B-mode ultrasound imaging of the right CCA, 2–5 cm proximal to the carotid bifurcation. A 30-s image was obtained in the lateral plane, with a single focus point positioned at the far wall. After acquisition, images were stored off-line in DICOM format. Images were analyzed using automated edge-tracking (EchoPac, GE Medical Systems), ECG-gated to end-diastole with a minimum of 100 discrete points used per frame to calculate an average far wall IMT. Because of the heterogeneity in some collected data, semi-automated edge-tracking was used instead of automated edge-tracking in 43 YHA (Arterial Measurement System Image and Data Analysis). Our laboratory has previously reported good agreement between the two methods (bias: 0.03 mm, 95% limits of agreement: −0.10 to 0.05 mm) (Shenouda et al. 2013), and therefore, these analysis methods were used interchangeably.

Statistical analysis

Statistical analyses were performed using IBM SPSS Statistics for Macintosh Version 20.0.0, (IBM, Armonk, NY, USA) and STATA Version 13 (STATA, College Station, TX, USA) for regressions. Data were checked for normality using the Shapiro–Wilk test and further examined *via* histogram plots, and were found to be highly non-normal; therefore non-parametric analyses were used. Group differences were assessed using the Kruskal–Wallis test with significant effects followed with the Mann–Whitney *U*-test with a Bonferroni correction. Relationships between CALM parameters and demographic characteristics (age, body mass index, heart rate, systolic blood pressure) were assessed with Spearman rank correlations (ρ). To test for predictors of CALM parameters, groups were combined and multiple regression analyses were performed using a backward regression model with each CALM parameter as a separate dependent variable. Models were adjusted for CALM confounders (*i.e.,* height, weight, heart rate, mean arterial

pressure and presence of CAD) based on previous findings (Svedlund et al. 2011; Zahnd et al. 2012). Models were further adjusted for the impact of arterial stiffness parameters (*i.e.,* cfPWV, CCA distensibility). IMT was found to be collinear with age, and was not included in any model. After the variables that could best predict the CALM parameter were determined, a series of cross-validation techniques (*i.e.,* bootstrapping) were performed to assess the generalizability of the model, with smaller shrinkage values indicating better generalizability. Data are reported as the median ± interquartile range, unless otherwise stated. For all analyses, the acceptable significance was set at $\alpha = 0.05$.

RESULTS

Group differences in arterial stiffness

Characteristics of participants are outlined in Table 1. Compared with YHA, OHA and CAD were older ($p < 0.01$), had greater body mass indexes ($p < 0.01$) and had higher supine blood pressures ($p < 0.01$). CAD also had lower heart rates compared with YHA and OHA ($p < 0.05$). OHA and CAD also had lower distensibility ($p < 0.01$), higher cfPWV ($p < 0.01$) and thicker IMT ($p < 0.01$) compared with YHA (Fig. 2).

Group differences in CALM

Group-averaged CALM traces are provided in Figure 3, and CALM parameters for the intima–media in Figure 4. Systolic anterograde, systolic retrograde and diastolic CALM displacements were quantifiable in all participants, regardless of inter-individual differences in CALM patterns. OHA and CAD exhibited less systolic anterograde (OHA: 0.12 ± 0.22 mm, CAD: 0.05 ± 0.14 mm vs. YHA: 0.24 ± 0.24 mm, $p < 0.01$), systolic retrograde (OHA: 0.26 ± 0.20 mm, CAD: 0.25 ± 0.23 mm vs. YHA: 0.46 ± 0.31 mm, $p < 0.01$) and maximum (OHA: 0.35 ± 0.33 mm, CAD: 0.34 ± 0.33 mm vs. YHA: 0.62 ± 0.31 mm, $p < 0.01$)

Table 1. Characteristics of participants (median ± interquartile range)

Variable	YHA (n = 161)	OHA (n = 51)	CAD (n = 14)
Sex (M/F)	117/44	30/21	14/0
Age (y)	23 ± 4	69 ± 6*	69 ± 12*
Height (m)	1.76 ± 0.13	1.70 ± 0.16*	1.75 ± 0.11
Body mass (kg)	72.8 ± 20.5	74.9 ± 16.7	83.1 ± 21.1
Body mass index (kg/m^2)	24.0 ± 4.8	26.1 ± 5.6*	28.0 ± 7.0*
Supine SBP (mm Hg)	116 ± 15	130 ± 20*	127 ± 37†
Supine DBP (mm Hg)	66 ± 6	73 ± 12*	74 ± 10*
Supine MAP (mm Hg)	85 ± 6	92 ± 16*	95 ± 24*
Supine heart rate (bpm)	61 ± 12	60 ± 14	51 ± 12*,‡

CAD = adults with coronary artery disease; DBP = diastolic blood pressure; MAP = mean arterial pressure; OHA = older healthy adults; SBP = systolic blood pressure; YHA = younger healthy adults.
* $p < 0.01$ different from YHA.
† $p < 0.05$ different from YHA.
‡ $p < 0.01$ different from OHA.

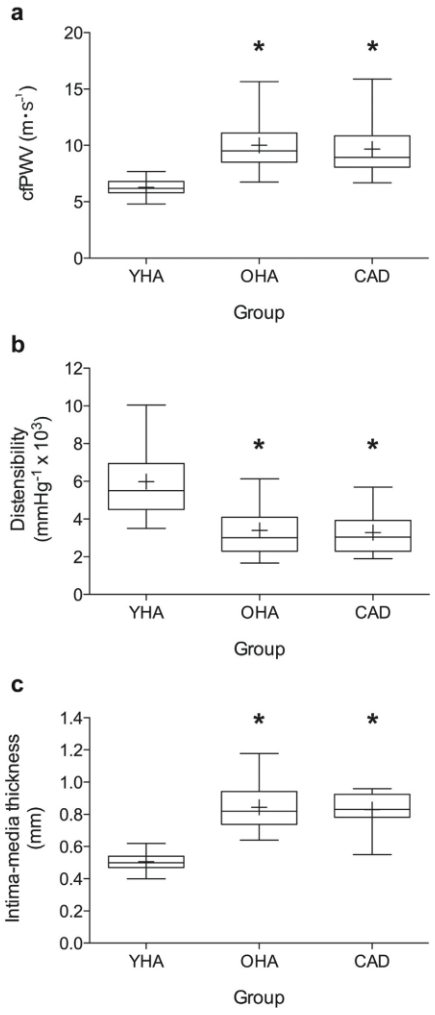

Fig. 2. Group differences in traditional measures of arterial health: (a) cfPWV; (b) common carotid artery distensibility; and (c) carotid intima–media thickness. The box represents the 25th, 50th (median) and 75th percentiles. The *cross* indicates the mean and the *bars* represent the 95% confidence interval. CAD = coronary artery disease; cfPWV = carotid–femoral pulse wave velocity; OHA = older healthy adults; YHA = younger healthy adults; *$p < 0.01$ different from YHA.

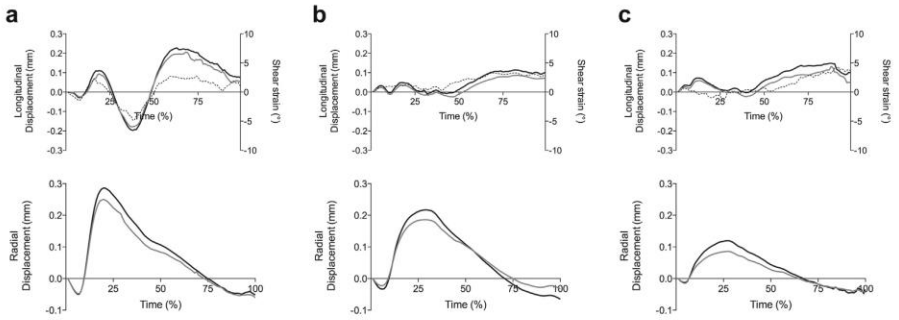

Fig. 3. Group-averaged traces of carotid artery longitudinal wall motion (top) and radial wall motion (bottom) of the intima–media (*black*) and adventitia (*gray*) with the accompanying shear strain (*dashed line*) for (a) younger healthy adults, (b) older healthy adults, and (c) adults with coronary artery disease. Traces are expressed as a percentage of a single cardiac cycle, ECG-gated to the R–R interval, with standard deviation lines removed for clarity.

CALM displacement compared with YHA. Similarly, OHA and CAD had smaller maximum shear strain angles compared with YHA (OHA: 9.14 ± 8.62°, CAD: 10.5 ± 5.80° vs. YHA: 16.3 ± 11.49°, $p < 0.01$). Diastolic CALM displacement (OHA: 0.21 ± 0.14 mm, CAD: 0.23 ± 0.12 mm vs. YHA: 0.53 ± 0.41 mm, $p < 0.01$) and maximum instantaneous diastolic velocity (OHA: 1.97 ± 1.78 m/s, CAD: 1.71 ± 1.12 m/s vs. YHA: 5.78 ± 4.80 m/s, $p < 0.01$) were also reduced in OHA and CAD compared with YHA. CAD exhibited slower mean diastolic velocity (CAD: 0.88 ± 0.39 m/s vs. OHA: 1.13 ± 0.72 m/s, $p = 0.01$, vs. YHA: 3.15 ± 2.21 m/s, $p < 0.01$) and slower maximum instantaneous diastolic acceleration (CAD: 52.79 ± 21.52 m/s^2 *vs* OHA: 64.82 ± 32.81 m/s^2, $p < 0.01$; *vs* YHA: 132.70 ± 86.12 m/s^2, $p < 0.01$) compared with both OHA and YHA. However, when diastolic velocity and maximum acceleration were controlled for maximal retrograde position, differences between OHA and CAD were no longer apparent ($p > 0.05$). All adventitial parameters had lower displacement, velocity and acceleration than intima–media parameters ($p < 0.05$, data not shown), with similar differences between groups, although diastolic CALM parameters were no longer different between OHA and CAD ($p > 0.05$; data not shown).

Correlations between CALM and arterial stiffness

Age was more highly correlated to all diastolic CALM parameters (ρ range: 0.42–0.54, $p < 0.01$) compared with systolic CALM parameters (ρ range: 0.20–0.33, $p < 0.01$), which was similar for relationships with both body mass index and mean arterial pressure (Table 2). All CALM parameters were correlated to cfPWV, CCA distensibility and IMT ($p < 0.01$), except for systolic anterograde CALM, which was correlated only with cfPWV ($\rho = -0.19$, $p < 0.01$) and IMT ($\rho = -0.15$, $p = 0.03$) (Figs. 5 and 6). Of note, the strongest correlate of cfPWV was mean diastolic CALM velocity ($\rho = -0.46$, $p < 0.01$), and the strongest correlate of distensibility was maximum instantaneous diastolic velocity ($\rho = 0.46$, $p < 0.01$).

Predictors of CALM

Multivariate regression was used to assess the predictors of CALM parameters (Table 3). Age was a significant predictor of all CALM parameters (except for shear strain), with older age being associated with a reduction in all CALM displacements and velocities. Of note, diastolic CALM parameters were the strongest models (R^2 range: 26.7%–33.1%) and had good generalizability (shrinkage range: 1.1%–12.5%). In contrast, systolic CALM parameters had lower model fits (R^2 range: 6.7%–20.5%) and a large range of generalizability (shrinkage range: 0.25%–74%), with systolic anterograde CALM performing the worst. When controlling for arterial stiffness parameters, diastolic CALM variables were more strongly related to age (β range: −0.46 to −0.53) than systolic CALM parameters (β range: −0.24 to −0.44), with no associations with either cfPWV or distensibility in any CALM parameter.

DISCUSSION

Our study is the first to provide evidence that diastolic, in comparison to systolic, CALM parameters have stronger relationships with intrinsic properties of arterial wall stiffness and provide added utility in discriminating between groups with expected differences in arterial health. We observed a reduced magnitude of

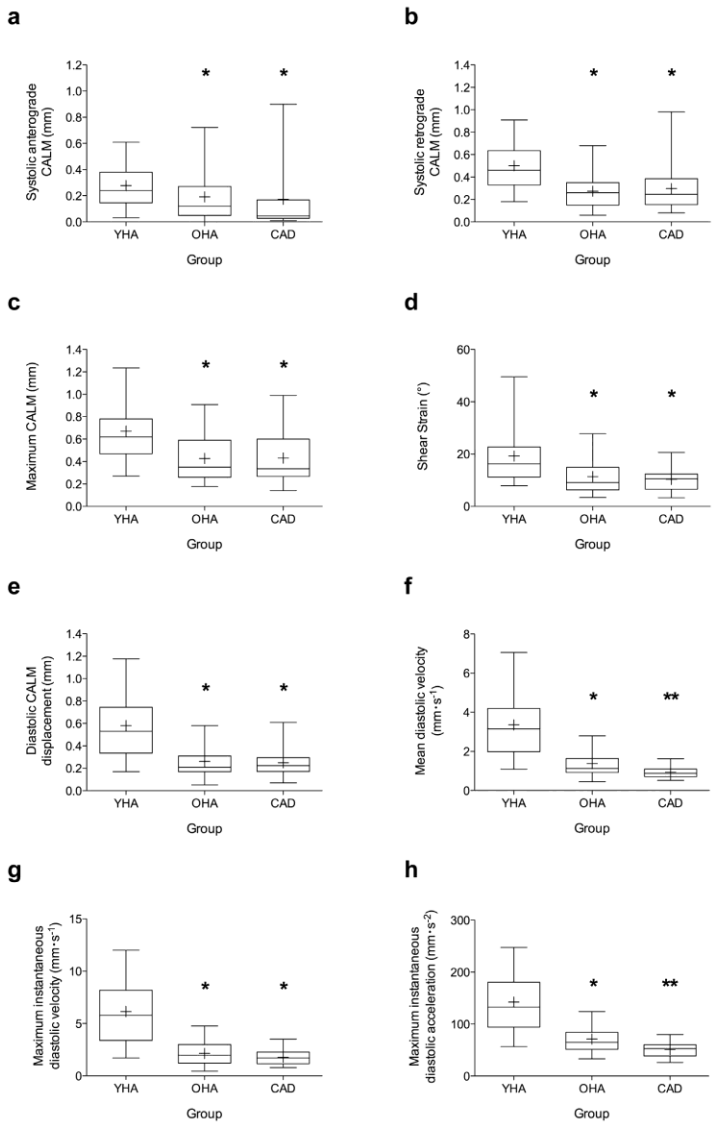

Fig. 4. Group differences in CALM parameters. (a–d) Systolic CALM parameters. (e–h) Diastolic CALM parameters. The box represents the 25th, 50th (median) and 75th percentiles. The *cross* indicates the mean, and the *bars* represent the 95% confidence interval. CAD = coronary artery disease, CALM = carotid artery longitudinal wave motion; OHA = older healthy adults; YHA = younger healthy adults. *$p < 0.01$ different from YHA. **$p < 0.01$ different from YHA and OHA.

Table 2. Spearman correlations between CALM and demographic characteristics

	Age		BMI		HR		MAP		IMT	
CALM parameter	ρ	*p*	ρ	*p*	ρ	*p*	ρ	*p*	ρ	*p*
Systolic CALM										
Anterograde	−0.20	<0.01	0.06	0.38	0.06	0.42	−0.01	0.96	−0.15	0.03
Retrograde	−0.30	<0.01	−0.24	<0.01	−0.10	0.13	−0.33	<0.01	−0.35	<0.01
Maximum	−0.27	<0.01	−0.28	<0.01	−0.14	0.05	−0.28	<0.01	−0.29	<0.01
Shear angle	−0.33	<0.01	−0.10	0.17	−0.07	0.31	−0.25	<0.01	−0.37	<0.01
Diastolic CALM										
Diastolic	−0.42	<0.01	−0.35	<0.01	−0.09	0.19	−0.39	<0.01	−0.38	<0.01
MDV	−0.51	<0.01	−0.34	<0.01	0.02	0.76	−0.39	<0.01	−0.46	<0.01
MIDV	−0.54	<0.01	−0.37	<0.01	0.01	0.93	−0.42	<0.01	−0.48	<0.01
MIDA	−0.47	<0.01	−0.32	<0.01	0.03	0.69	−0.37	<0.01	−0.45	<0.01

BMI = body mass index; HR = heart rate; IMT = intima–media thickness; MAP = mean arterial pressure; MDV = mean diastolic velocity; MIDA = maximum instantaneous diastolic acceleration; MIDV = maximum instantaneous diastolic velocity.

CALM across the different phases of the cardiac cycle with older age, while diastolic CALM parameters were further reduced in individuals with CAD. Although there were simple linear relationships between CALM and stiffness indices, diastolic CALM parameters were associated with age independent of cfPWV and CCA distensibility. Our findings indicate a relationship between CALM parameters and age independent of arterial stiffness in the radial plane. In particular, diastolic CALM parameters appear to more strongly reflect this association, which is likely the result of relative physiologic independence from the active systolic processes of the high-velocity phase of anterograde blood flow and active left ventricular motion caused by myocyte contraction.

Previous investigations have examined a wide range of CALM parameters (Cinthio et al. 2006; Zahnd et al. 2011) and have identified varying degrees of sensitivity of these parameters to health status; however, the physiologic determinants of CALM parameters remain to be determined. We previously reported that CALM displacements follow a predictable pattern that can be segmented into directional phases during the systolic and diastolic portions of the cardiac cycle. During systole, these phases correspond to physiologic events occurring both at the local CCA (*i.e.,* the blood velocity wave) and upstream at the heart (*i.e.,* left ventricular rotation parameters) (Au et al. 2016). These "active" systolic events may be confounders in interpreting inter-individual variation in CALM traces, as both CCA blood flow patterns and left ventricular rotation change with age and health status (Burns et al. 2008; Hirata et al. 2006; Takeuchi et al. 2007). Therefore, we were interested in the relationship between the relatively "passive" diastolic phase of CALM and its sensitivity to aging and arterial health status. We found that there is a consistent diastolic pattern in CALM, which we describe as a late, second anterograde displacement followed by a return to a reference position near the end of the cardiac cycle (Fig. 3). Although all CALM parameters were associated with age in a multivariate model, diastolic, versus systolic, CALM parameters had the best fit (R^2 values ranging from 26.7% to 33.1%) and best generalizability (shrinkage ranging from 1.1% to 12.5%), and were also better able to distinguish between healthy older adults and those with documented CAD in a group comparison (Fig. 4f–h).

Traditional measures of arterial stiffness in the radial plane increase with age across different ranges of blood pressures (Engelen et al. 2015; Reference Values for Arterial Stiffness' Collaboration 2010). We found similar structural changes in both the central elastic arteries (cfPWV) and local CCA (distensibility, IMT) in older adults, which was mirrored by reductions in both systolic and diastolic CALM displacements. Only two previous studies have compared CALM in older versus younger healthy adults (Golemati et al. 2003; Zahnd et al. 2011), similarly finding reduced total displacements in small cohorts. These reductions in motion magnitude may be due to structural remodeling of the vascular wall with age, including altered regulation of matrix metalloproteinases (Wang and Lakatta 2002), increases in vascular smooth muscle cell stiffness (Qiu et al. 2010), increases in inflammation (Mahmud and Feely 2005) and increased sympathetic tone (Giannattasio et al. 2005). Of particular note, one research group has recently reported that CALM displacements are reduced in response to increased sympathetic activity in a porcine model (Ahlgren et al. 2012, 2015), likely implicating the age-related increase in sympathetic activity as a regulatory factor in the reduction of longitudinal wall displacement. Our group has recently proposed an integrative model suggesting that local hemodynamics and upstream left ventricular function may account for inter-individual differences in CALM displacement magnitudes (Au et al. 2016), which is

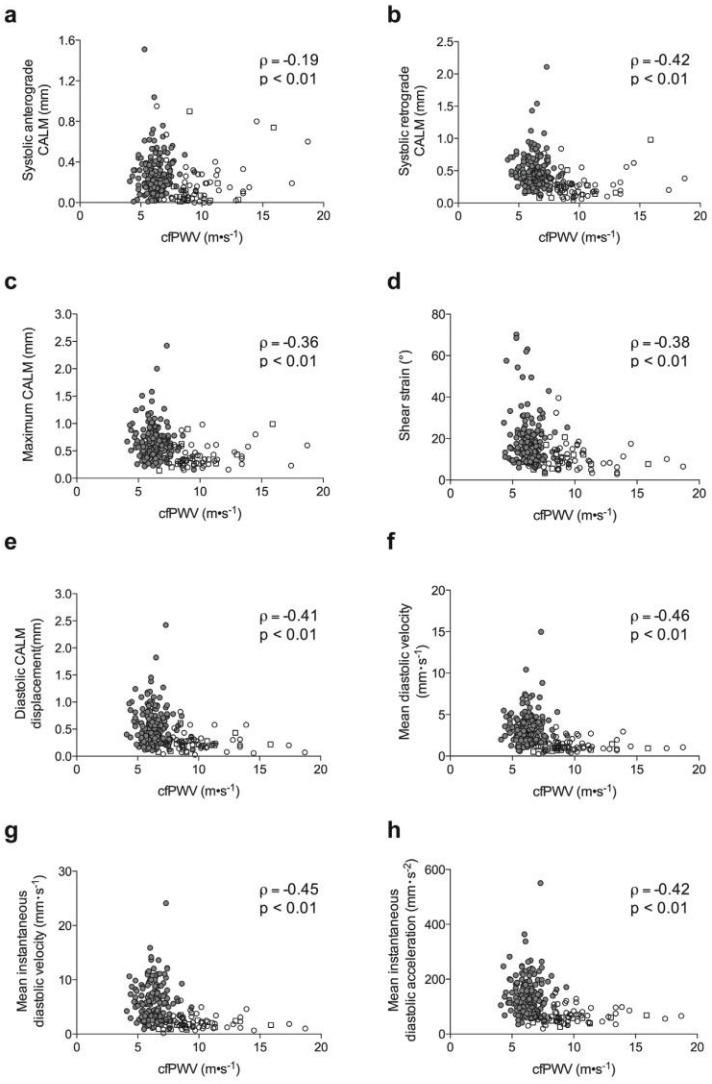

Fig. 5. Scatterplots of relationships between CALM parameters and cfPWV. (a–d) Systolic CALM parameters. (e–h) Diastolic CALM parameters. YHA are represented by *gray circles*, OHA by *white circles* and CAD by *white squares*. Scatterplots are labeled with Spearman rho (ρ) correlations. CAD = coronary artery disease; CALM = carotid artery longitudinal wave motion; cfPWV = carotid–femoral pulse wave velocity; OHA = older healthy adults; YHA = younger healthy adults.

partially supported by our cross-sectional observations with aging and CAD. In the context of this model, age- and/or disease-related changes in systemic regulatory factors may also affect the observed differences in diastolic CALM parameters. For example, the age-related increase in CCA diameter (Engelen et al. 2015;

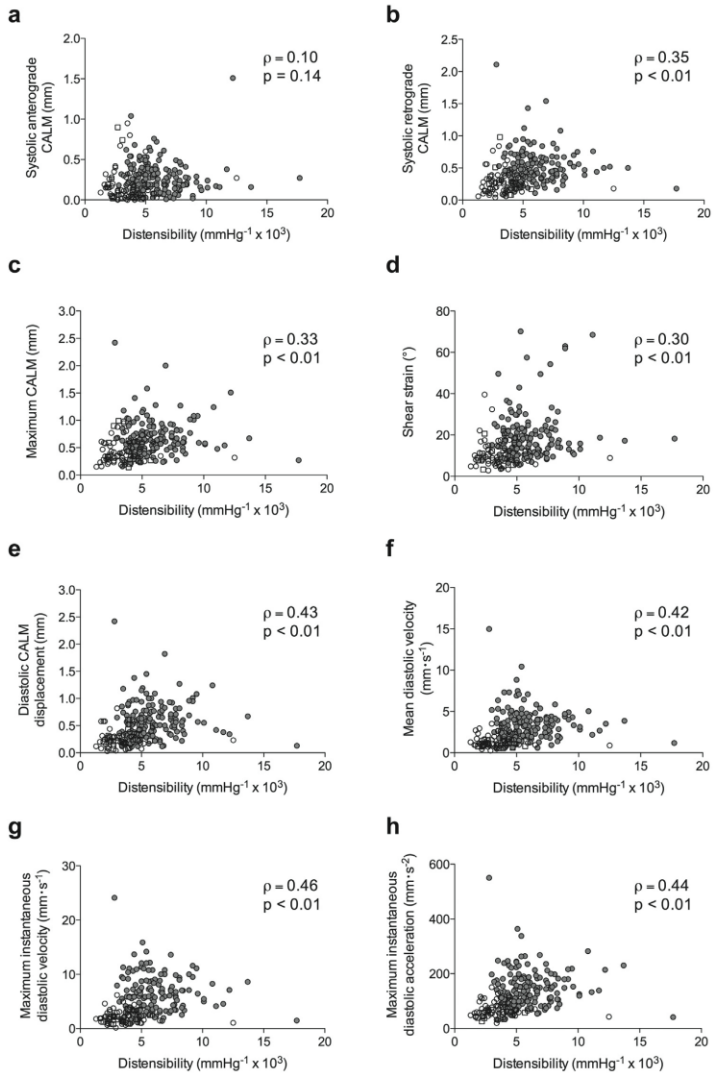

Fig. 6. Scatterplots of relationships between CALM parameters and distensibility. (a–d) Systolic CALM parameters. (e–h) Diastolic CALM parameters. YHA are represented by *gray circles*, OHA by *white circles*, and CAD by *white squares*. Scatterplots are labeled with Spearman rho (ρ) correlations.

Polak et al. 1996), increase in left ventricular torsion (Tavakoli and Sahba 2013) and decrease in left ventricular diastolic filling (Hollingsworth et al. 2012) may indirectly affect the anterograde, retrograde and diastolic phases of CALM, respectively. However, none of these mechanistic changes have yet been linked to reductions in CALM in controlled experimental studies, inviting an exciting new field of future research.

Table 3. Multiple regression analysis for significant predictors of CALM parameters

CALM parameter	Model information	*B*	*β*	*p*
Systolic CALM				
Anterograde CALM	Model R^2 = 6.7%, shrinkage = 74.0%			
	Age	−0.002	−0.24	<0.01
	Weight	0.002	0.13	0.05
Retrograde CALM	Model R^2 = 20.5%, shrinkage = 7.8%			
	Age	−0.004	−0.44	<0.01
	Heart rate	−0.003	−0.14	0.02
Maximum CALM	Model R^2 = 15.8%, shrinkage = 16.2%			
	Age	−0.004	−0.37	<0.01
	Heart rate	−0.005	−0.19	<0.01
Shearing angle	Model R^2 = 8.9%, shrinkage = 0.25%			
	Mean arterial pressure	−0.340	−0.30	<0.01
Diastolic CALM				
Diastolic CALM displacement	Model R^2 = 26.9%, shrinkage = 12.5%			
	Age	−0.006	−0.46	<0.01
	Weight	−0.003	−0.18	<0.01
	Heart rate	−0.005	−0.18	<0.01
MDV	Model R^2 = 27.2%, shrinkage = 1.1%			
	Age	−0.041	−0.52	<0.01
MIDV	Model R^2 = 33.1%, shrinkage = 2.02%			
	Age	−0.079	−0.53	<0.01
	Weight	−0.039	−0.19	0.01
MIDA	Model R^2 = 26.7%, shrinkage = 2.32%			
	Age	−1.49	−0.51	<0.01

MDV = mean diastolic velocity; MIDA = maximum instantaneous diastolic acceleration; MIDV = maximum instantaneous diastolic velocity.

Although it is tempting to liken the reductions in longitudinal displacement to the increases in arterial stiffness with age, our data indicate otherwise. We observed linear relationships among CALM parameters, arterial stiffness and age similar to previous reports (Taivainen et al. 2017; Zahnd et al. 2012), but when accounting for both anthropometrics and arterial stiffness, we found that CALM was uniquely related to age independent of arterial stiffness. Functionally, increases in radial plane arterial stiffness contribute to increases in blood pressure by reducing the pressure buffering capacity of the central elastic arteries, as well as shifting the reflected pressure wave earlier in the cardiac cycle and increasing pressure augmentation (Phan et al. 2016). It is unlikely that CALM parameters contribute to the same etiology of age-related increases in blood pressure similar to that of increasing pulse wave velocity, as CALM and radial distension occur in different planes. However, Yli-Ollila et al. (2016a, 2016b) recently reported a relationship between longitudinal motion and the distending pressure wave through principal component analysis, warranting further studies in more heterogeneous samples of adults. In theory, CALM may have a role in vascular aging and the etiology of atherosclerosis through its relationships to wall shear stress and endothelial health. The presence of multiphasic motion of the arterial wall both with and against the direction of blood flow is likely to alter wall shear stress and endothelium-mediated nitric oxide bioavailability in major conduit arteries, where CALM has previously been observed (Cinthio et al. 2006). In particular, wall shear stress during late systole may be severely underestimated because of the opposing directions of blood flow and the arterial wall, rather than standard assumption of a stationary wall. Although it is unknown exactly how alterations in the repetitive, cyclical action of longitudinal shear forces affect vascular wall health over the life span, this is certainly something that should be considered given high inter-individual variability in trace pattern in otherwise healthy adults (Yli-Ollila et al. 2013).

The measurement of arterial stiffness is an attractive measure of CVD risk for clinical use because of its ability to identify and reclassify risk for future cardiovascular events in otherwise healthy adults (Ben-Shlomo et al. 2014). However, arterial stiffness has not reached widespread clinical use, in part, because of the requirement of significant operator skill and the lack of integration of arterial stiffness measurement devices in clinical settings. These limitations are considerably reduced for CALM, which has the potential to offer information similar to that provided by arterial stiffness, while using non-invasive medical imaging equipment already in place in many clinical locations (*i.e.,* ultrasound). Our results support this idea, providing preliminary evidence that diastolic CALM parameters are more sensitive to the presence of CAD than traditional stiffness measures or systolic CALM parameters. Few studies have examined the relationship of CALM to overt CVD, though all report promising results. In particular, plaque burden has been

found to affect both the magnitude and pattern of CALM compared with younger, healthy adults (Svedlund and Gan 2011; Tat et al. 2016). Furthermore, Svedlund et al. (2011) reported that maximum CALM displacement was an independent predictor of major cardiovascular events in adults with suspect CAD (Svedlund et al. 2011). Although this is strong evidence to support the use of CALM parameters in CVD risk stratification, it should be noted that total CALM displacement is a systolic parameter, likely confounded by left ventricular systolic function (Au et al. 2016), which would explain the strong value in predicting future CVD events. It would be interesting to extend our findings on diastolic CALM parameters to event prediction, to study CALM independent of left ventricular function.

Limitations

Although we had a large sample of healthy adults, we did not include a cohort of middle-aged adults or women, which would be beneficial to improve the generalizability of our models between CALM parameters and age. However, we appeared to have adequate ranges of arterial stiffness and CALM magnitudes in which to study simple linear relationships. The sample size of our CAD group was small, and larger samples are needed to confirm reductions in diastolic CALM parameters in comparison to healthy age-matched controls. Furthermore, participants with CAD were medicated, with 79% on statins, 50% on beta-blockers and 43% on angiotensin-converting enzyme inhibitors. The use of beta-blockers likely accounts for the bradycardia in the CAD group, although it is unknown whether heart rate- or blood pressure-altering medication would have an impact on motion in the longitudinal direction. Although one group has suggested that longitudinal wall motion is related to the distending pressure wave (Yli-Ollila et al. 2016a, 2016b), there are no available experimental or paced studies that assess the dependence of CALM on heart rate or blood pressure. It should be noted that ~14% of recruited participants were not included in the analysis because of poor image quality, primarily because of out-of-plane imaging and high echo backscatter at the far wall of the CCA, highlighting that some degree of operator skill is needed for accurate recordings.

CONCLUSIONS

All CALM parameters are reduced with age, with diastolic CALM parameters being further reduced in individuals with CAD. CALM parameters were also related to age, independent of arterial stiffness, although CALM and stiffness themselves were linearly related in a simple model. Contrary to previously published reports on a variety of CALM parameters, diastolic, rather than systolic, CALM may offer unique arterial wall information that is independent of arterial stiffness, with additional sensitivity to CVD status. As the mechanisms underlying reduced diastolic CALM displacement and velocity with aging and disease are currently unknown, future work should evaluate whether these differences are linked to structural or functional changes within the vascular wall, as well as further investigate the relationship between radial and longitudinal arterial stiffness in humans.

Acknowledgments—We thank Johnny (Hon Lam) Choi, Ninette Shenouda, Stacey E. Priest, Ada Tang and Jem L. Cheng for their assistance in data collection. This study was supported by funding from the Natural Sciences and Engineering Research Council to MJM (DG No. 238819-13).

REFERENCES

Ahlgren AR, Cinthio M, Steen S, Nilsson T, Sjoberg T, Persson HW, Lindstrom K. Longitudinal displacement and intramural shear strain of the porcine carotid artery undergo profound changes in response to catecholamines. Am J Physiol Heart Circ Physiol 2012;302:H1102–H1115.

Ahlgren AR, Steen S, Segstedt S, Erlöv T, Lindström K, Sjöberg T, Persson HW, Ricci S, Tortoli P, Cinthio M. Profound increase in longitudinal displacements of the porcine carotid artery wall can take place independently of wall shear stress: A continuation report. Ultrasound Med Biol 2015;41:1342–1353.

Au JS, Ditor DS, MacDonald MJ, Stöhr EJ. Carotid artery longitudinal wall motion is associated with local blood velocity and left ventricular rotational, but not longitudinal, mechanics. Physiol Rep 2016;4:e12872.

Ben-Shlomo Y, Spears M, Boustred C, May M, Anderson SG, Benjamin EJ, Boutouyrie P, Cameron J, Chen CH, Cruickshank JK, Hwang SJ, Lakatta EG, Laurent S, Maldonado J, Mitchell GF, Najjar SS, Newman AB, Ohishi M, Pannier B, Pereira T, Vasan RS, Shokawa T, Sutton-Tyrell K, Verbeke F, Wang K-L, Webb DJ, Willum Hansen T, Zoungas S, McEniery CM, Cockcroft JR, Wilkinson IB. Aortic pulse wave velocity improves cardiovascular event prediction: An individual participant meta-analysis of prospective observational data from 17,635 subjects. J Am Coll Cardiol 2014;63:636–646.

Burns AT, La Gerche A, MacIsaac AI, Prior DL. Augmentation of left ventricular torsion with exercise is attenuated with age. J Am Soc Echocardiogr 2008;21:315–320.

Cinthio M, Ahlgren AR. Intra-observer variability of longitudinal displacement and intramural shear strain measurements of the arterial wall using ultrasound noninvasively *in vivo*. Ultrasound Med Biol 2010;36:697–704.

Cinthio M, Ahlgren AR, Bergkvist J, Jansson T, Persson HW, Lindström K. Longitudinal movements and resulting shear strain of the arterial wall. Am J Physiol Heart Circ Physiol 2006;291:H394–H402.

Engelen L, Bossuyt J, Ferreira I, Van Bortel LM, Reesink KD, Segers P, Stehouwer CD, Laurent S, Boutouyrie P. Reference values for local arterial stiffness: Part A. Carotid artery. J Hypertens 2015;33:1981–1996.

Giannattasio C, Failla M, Lucchina S, Zazzeron C, Scotti V, Capra A, Viscardi L, Bianchi F, Vitale G, Lanzetta M, Mancia G. Arterial stiffening influence of sympathetic nerve activity: Evidence from hand transplantation in humans. Hypertension 2005;45:608–611.

Golemati S, Sassano A, Lever MJ, Bharath AA, Dhanjil S, Nicolaides AN. Carotid artery wall motion estimated from B-mode ultrasound using region tracking and block matching. Ultrasound Med Biol 2003;29:387–399.

Hirata K, Yaginuma T, O'Rourke MF, Kawakami M. Age-related changes in carotid artery flow and pressure pulses: Possible

implications for cerebral microvascular disease. Stroke 2006;37: 2552–2556.
Hollingsworth KG, Blamire AM, Keavney BD, MacGowan GA. Left ventricular torsion, energetics, and diastolic function in normal human aging. Am J Physiol Heart Circ Physiol 2012;302:H885–H892.
Liang Q, Wendelhag I, Wikstrand J, Gustavsson T. A multiscale dynamic programming procedure for boundary detection in ultrasonic artery images. IEEE Trans Med Imaging 2000;19:127–142.
Lorenz MW, Markus HS, Bots ML, Rosvall M, Sitzer M. Prediction of clinical cardiovascular events with carotid intima–media thickness: A systematic review and meta-analysis. Circulation 2007;115: 459–467.
Mahmud A, Feely J. Arterial stiffness is related to systemic inflammation in essential hypertension. Hypertension 2005;46:1118–1122.
Mitchell GF, Parise H, Benjamin EJ, Larson MG, Keyes MJ, Vita JA, Vasan RS, Levy D. Changes in arterial stiffness and wave reflection with advancing age in healthy men and women: The Framingham Heart Study. Hypertension 2004;43:1239–1245.
Munakata M, Ito N, Nunokawa T, Yoshinaga K. Utility of automated brachial ankle pulse wave velocity measurements in hypertensive patients. Am J Hypertens 2003;16:653–657.
Nichols WW, O'Rourke MF. McDonald's blood flow in arteries: Theoretical, experimental and clinical principles. 5th edition. London: Hodder Arnold 2005. p. 54–57.
Persson M, Ahlgren AR, Jansson T, Eriksson A, Persson HW, Lindström K. A new non-invasive ultrasonic method for simultaneous measurements of longitudinal and radial arterial wall movements: First in vivo trial. Clin Physiol Funct Imaging 2003;23: 247–251.
Phan TS, Li JKJ, Segers P, Reddy Koppula M, Akers SR, Kuna ST, Gislason T, Pack AI, Chirinos JA. Aging is associated with an earlier arrival of reflected waves without a distal shift in reflection sites. J Am Heart Assoc 2016;5:e003733.
Polak JF, Kronmal RA, Tell GS, O'Leary DH, Savage PJ, Gardin JM, Rutan GH, Borhani NO. Compensatory increase in common carotid artery diameter: Relation to blood pressure and artery intima–media thickness in older adults. Stroke 1996;27:2012–2015.
Qiu H, Zhu Y, Sun Z, Trzeciakowski JP, Gansner M, Depre C, Resuello RRG, Natividad FF, Hunter WC, Genin GM, Elson EL, Vatner DE, Meininger GA, Vatner SF. Vascular smooth muscle cell stiffness as a mechanism for increased aortic stiffness with aging. Circ Res 2010;107:615–619.
Reference Values for Arterial Stiffness' Collaboration. Determinants of pulse wave velocity in healthy people and in the presence of cardiovascular risk factors: "Establishing normal and reference values.". Eur Heart J 2010;31:2338–2350.
Shenouda N, Proudfoot NA, MacDonald MJ, Timmons BW. A comparison between automated and semi-automated edge-tracking software for the analysis of carotid intima media thickness. Appl Physiol Nutr Metab 2013;38:1077.
Svedlund S, Gan LM. Longitudinal wall motion of the common carotid artery can be assessed by velocity vector imaging. Clin Physiol Funct Imaging 2010;31:32–38.
Svedlund S, Gan LM. Longitudinal common carotid artery wall motion is associated with plaque burden in man and mouse. Atherosclerosis 2011;217:120–124.
Svedlund S, Eklund C, Robertsson P, Lomsky M, Gan LM. Carotid artery longitudinal displacement predicts 1-year cardiovascular outcome in patients with suspected coronary artery disease. Arterioscler Thromb Vas Biol 2011;31:1668–1674.
Taivainen SH, Yli-Ollila H, Juonala M, Kahonen M, Raitakari OT, Laitinen TM, Laitinen TP. Interrelationships between indices of longitudinal movement of the common carotid artery wall and the conventional measures of subclinical arteriosclerosis. Clin Physiol Funct Imaging 2017;37:305–331.
Takeuchi M, Borden WB, Nakai H, Nishikage T, Kokumai M, Nagakura T, Otani S, Lang RM. Reduced and delayed untwisting of the left ventricle in patients with hypertension and left ventricular hypertrophy: A study using two-dimensional speckle tracking imaging. Eur Heart J 2007;28:2756–2762.
Tat J, Au JS, Keir PJ, MacDonald MJ. Reduced common carotid artery longitudinal wall motion and intramural shear strain in individuals with elevated cardiovascular disease risk using speckle tracking. Clin Physiol Funct Imaging 2015;37:106–116.
Tat J, Psaromiligkos IN, Daskalopoulou SS. Carotid atherosclerotic plaque alters the direction of longitudinal motion in the artery wall. Ultrasound Med Biol 2016;42:2114–2122.
Tavakoli V, Sahba N. Assessment of age-related changes in left ventricular twist by 3-dimensional speckle-tracking echocardiography. J Ultrasound Med 2013;32:1435–1441.
Van Bortel LM, Laurent S, Boutouyrie P, Chowienczyk P, Cruickshank JK, De Backer T, Filipovsky J, Huybrechts S, Mattace-Raso FUS, Protogerou AD, Schillaci G, Segers P, Vermeersch S, Weber T. Expert consensus document on the measurement of aortic stiffness in daily practice using carotid-femoral pulse wave velocity. J Hypertens 2012;30:445–448.
Wang M, Lakatta EG. Altered regulation of matrix metalloproteinase-2 in aortic remodeling during aging. Hypertension 2002;39:865–873.
Yli-Ollila H, Laitinen T, Weckström M, Laitinen TM. Axial and radial waveforms in common carotid artery: An advanced method for studying arterial elastic properties in ultrasound imaging. Ultrasound Med Biol 2013;39:1168–1177.
Yli-Ollila H, Laitinen T, Weckström M, Laitinen TM. New indices of arterial stiffness measured from longitudinal motion of common carotid artery in relation to reference methods, a pilot study. Clin Physiol Funct Imaging 2015;36:376–388.
Yli-Ollila H, Tarvainen MP, Laitinen TP, Laitinen TM. Principal component analysis of the longitudinal carotid wall motion in association with vascular stiffness: A pilot study. Ultrasound Med Biol 2016a; 42:2873–2886.
Yli-Ollila H, Tarvainen MP, Laitinen TP, Laitinen TM. Transfer function analysis of the longitudinal motion of the common carotid artery wall. Front Physiol 2016b;7:651.
Zahnd G, Boussel L, Marion A, Durand M, Moulin P, Sérusclat A, Vray D. Measurement of two-dimensional movement parameters of the carotid artery wall for early detection of arteriosclerosis: A preliminary clinical study. Ultrasound Med Biol 2011;37: 1421–1429.
Zahnd G, Vray D, Sérusclat A, Alibay D, Bartold M, Brown A, Durand M, Jamieson LM, Kapellas K, Maple-Brown LJ, O'Dea K, Moulin P, Celermajer DS, Skilton MR. Longitudinal displacement of the carotid wall and cardiovascular risk factors: Associations with aging, adiposity, blood pressure and periodontal disease independent of cross-sectional distensibility and intima–media thickness. Ultrasound Med Biol 2012;38:1705–1715.
Zahnd G, Balocco S, Sérusclat A, Moulin P, Orkisz M, Vray D. Progressive attenuation of the longitudinal kinetics in the common carotid artery: Preliminary in vivo assessment. Ultrasound Med Biol 2014;41:339–345.

CHAPTER 4:

CARDIAC AND HEMODYNAMIC DETERMINANTS OF CAROTID ARTERY LONGITUDINAL WALL MOTION

In preparation

Cardiac and hemodynamic determinants of carotid artery longitudinal wall motion

Jason S. Au[1], Paula A. Bochnak[1], Sydney E. Valentino[1], Jem L. Cheng[1], Eric J. Stöhr[2,3], Maureen J. MacDonald[1]

[1]*Department of Kinesiology, McMaster University, Hamilton, Canada*

[2]*Discipline of Physiology & Health, Cardiff School of Sport, Cardiff Metropolitan University, Cardiff, Wales*

[3]*Department of Medicine, Columbia University Irving Medical Centre, New York, USA*

RUNNING TITLE: Pulse pressure, LV rotation, carotid shear rate, and CALM

KEYWORDS: Arterial wall motion, echocardiography, speckle-tracking

Corresponding Author:
Maureen J. MacDonald, PhD
McMaster University
Department of Kinesiology
IWC E207, 1280 Main Street West
Hamilton, ON, Canada, L8S 4K1
Telephone: 905-525-9140 ext. 23580
Fax: 905-523-6011
Email: macdonmj@mcmaster.ca

ABSTRACT

Carotid artery longitudinal wall motion (CALM) has recently attracted interest as a potential indicator of arterial health; however, the regulation of CALM is poorly understood. We conducted a series of studies aimed at manipulating pulse pressure (PP), left ventricular (LV) motion, and carotid shear rate, which have been previously suggested to regulate various components of CALM pattern and magnitude. To determine the regulatory influences on CALM, fifteen healthy males (22±2 years) were exposed to three acute interventions: the Serial Subtraction Test (SST), the Cold Pressor Test (CPT), and exposure to sublingual nitroglycerin (NTG). The SST elicited increases in PP (P<0.01), apical LV rotation (P<0.01), and carotid shear rate (P<0.01), with no changes in CALM (P>0.05). Similarly, the CPT elicited increases in PP (P=0.01), basal LV rotation (P = 0.04) and carotid shear rate (P=0.01), with no changes in CALM (P>0.05). Conversely, exposure to NTG elicited no change in PP (P=0.22), basal (P=0.65) or apical LV rotation (P=0.45), but did decrease carotid shear rate (P<0.01), without altering CALM (P>0.05). When all three interventions were pooled, there was a proportional relationship between changes in LV basal rotation and changes in systolic retrograde CALM (r=-0.35, P=0.03; β=-0.025, P=0.03). These findings suggest that while the systolic, but not diastolic, CALM pattern is influenced by LV mechanics, discrete changes in LV rotation and shear rate do not generate detectable changes in CALM. Future investigations should focus on evaluations of diastolic-phase CALM components, which may provide additional value to characterizing arterial wall properties independent of LV rotation and pulse pressure.

INTRODUCTION

Distension of the central elastic arteries is primarily influenced by local pulse pressure (PP), vasomotor tone and the structural characteristics of the arterial wall. While much previous research has focused on vascular measures dependent upon radial distension (e.g., arterial distensibility, Young's modulus, pulse wave velocity) (37), there have been few studies that have acknowledged longitudinal displacement of the arterial wall. Carotid artery longitudinal wall motion (CALM) is biphasic (oscillating displacement with and against blood flow) (7), equal in magnitude to that of radial distension (26), and has recently been suggested to complement traditional stiffness measures in the prediction of cardiovascular disease risk (4, 46).

Much of the physiological regulation of CALM remains undetermined, despite arguments presented for the influence of PP (1, 42, 43), left ventricular (LV) rotation (3), and local wall shear stress (2, 3). While the above factors have been proposed and initially tested in a porcine model (1, 2), no study to date has experimentally altered local hemodynamics and LV mechanics in order to investigate the regulation of the CALM pattern in humans. Our lab has previously theorized a structural ventricular-vascular coupling model where systolic CALM is comprised of two components: anterograde motion, which represents the summation of anterograde-influencing shear forces caused by the local forward blood velocity wave and retrograde-influencing left ventricular (LV) rotation; and retrograde CALM, which is primarily induced by LV rotation (3). While our previous cross-sectional observational assessments provide some support for this theory, additional *in vivo* stimulus-response designs are necessary to verify causal links.

The purpose of this study was, therefore, to investigate the role of potential regulators of systolic CALM using an acute interventional model in humans. In order to examine the physiologic factors that influence the systolic CALM pattern, we performed a series of experiments intended to acutely alter PP and LV rotation through sympathetic activation (i.e., increases in blood pressure using either a serial subtraction test [SST], or a cold pressor test [CPT]) and local common carotid artery (CCA) shear rate through vascular smooth muscle relaxation (i.e., endothelial-independent vasodilation through sublingual nitroglycerin administration [NTG]). We hypothesized that increases in PP and LV rotation would be associated with increases in the systolic retrograde components of the CALM pattern, whereas increases in local CCA shear rate would be associated with increases in the systolic anterograde components of the CALM pattern, building upon our previously suggested model for structural ventricular-vascular coupling.

METHODS

Participants and ethical approval

Fifteen young healthy men (age: 22±2 years) were recruited for this study. All participants gave verbal and written consent prior to enrolment in the study. The study protocol was approved by the Hamilton Integrated Research Ethics Board and conforms to the *Declaration of Helsinki* concerning the use of human subjects as research participants.

Protocol Overview

All participants arrived at the lab between the hours of 0700 and 1000 in the fasted state, having refrained from caffeine, alcohol and vigorous physical activity for the past 12 hours. After 10 minutes of supine rest, the remainder of the protocol was completed with the participant in the left lateral decubitus position to facilitate acquisition of cardiac ultrasound images. In a single testing session, participants performed the three interventions (SST, CPT and NTG) in sequence with 10 minutes of rest in between each intervention. Two trained sonographers performed simultaneous ultrasound assessments to determine CALM and LV rotation before, during and after each intervention. Participants' heart rate and blood pressure were continuously monitored with single-lead ECG (PowerLab model ML 795; AD Instruments, Colorado Springs, CO, USA) and beat-to-beat finger blood pressure on the left hand (Finometer MIDI, Finapres Medical Systems; Amsterdam, The Netherlands), respectively.

Table 1. Participant characteristics and resting cardiovascular variables (n=15)

Variable	Mean ± SD
Age (yr)	22±2
Height (cm)	180±7
Body mass (kg)	81.9±11.0
Systolic blood pressure (mmHg)	114±8
Diastolic blood pressure (mmHg)	63±4
Mean blood pressure (mmHg)	82±5
Resting heart rate (bpm)	58±11
Resting CCA variables	
Intima-media thickness (mm)	0.57±0.09
Diastolic lumen diameter (mm)	5.9±0.5
Shear rate (1/s)	209±74
Resting LV variables	
Stroke volume (mL)	57±11
Cardiac output (L/min)	4.39±1.12
Relative wall thickness	0.37±0.06
LV mass (g)	188±40
LV mass index (g/m^2)	93.2±16.4

Values are means ± SD; CCA = common carotid artery; LV = left ventricular

Serial Subtraction Test: After baseline measurements were acquired, participants were given a standard set of instructions to complete the SST (20). During the test, 25 four-digit numbers were serially projected onto the ceiling for five seconds, allowing the participant to complete the test in the left lateral decubitus position. Participants were instructed to subtract the number '13' from each four-digit number, and then speak the answer in full within the five-second time limit. Study investigators provided immediate verbal feedback only when incorrect answers were given. Post-SST images were acquired within 10 seconds of test completion.

Cold Pressor Test: An ice bath with a temperature of 0.9±0.5 °C was prepared for the CPT. After the acquisition of baseline images, the participants were asked to immerse their right hand into the ice water up to wrist level until volitional cessation of the test (20). A maximum test duration of two minutes was established by the study investigators, but not revealed to participants. Images were obtained at 60 seconds of test duration and immediately within 10 seconds of hand removal.

Nitroglycerin: After baseline images were obtained, a sublingual spray of 0.4mg nitroglycerin was administered to participants. Vascular and cardiac images were assessed at six minutes post-administration, as previous studies have identified peak plasma NTG concentrations around this time, with a 2.5-minute half-life (23, 28).

Carotid artery longitudinal motion: CALM was assessed at the right CCA 2-5 cm proximal to the carotid bifurcation at an acquisition rate of 102.5 fps with a 12 MHz linear array probe connected to a high-resolution ultrasound machine (Vivid q, GE Medical Systems), as previously described (3, 4). Participants were asked to briefly hold their breath during image acquisition while images were recorded for three to six heart cycles, keeping the carotid bifurcation at the left side of the image. Images were stored offline for later analysis using an in-house speckle-tracking algorithm, gated to the R-spike of the ECG recording (MatLab, The MathWorks, Natick, MA) (36). A reference kernel block was positioned on the intima-media layer of the far CCA wall so that the lower edge of the kernel was placed on the media-adventitia interface. CALM displacement traces were then visualized for local maxima and minima point detection (MatLab, The MathWorks) as previously described (3, 4). In brief, CALM traces were segmented into three primary motion phases: systolic anterograde CALM (the first systolic anterograde movement to the peak systolic anterograde displacement), systolic retrograde CALM (the peak systolic anterograde displacement to the peak retrograde displacement), and diastolic CALM (the peak retrograde displacement to the local diastolic anterograde plateau). Displacements were digitally filtered (2^{nd} order, dual pass butterworth, Fc = 10Hz) and differentiated into velocity and acceleration traces for peak detection. For graphical representation of CALM, displacement traces were linearly interpolated to 100 discrete points to account for variable cardiac cycle length, and ensemble averaged between participants.

Carotid artery shear rate: Immediately after CALM image acquisition, mean blood velocity was acquired 2-5 cm proximal to the right carotid bifurcation using the same ultrasound unit (Vivid q; GE Medical Systems) in duplex mode with the pulse wave set at 4MHz. The audio signals from the pulsed wave blood velocity signals were processed using a spectral analyser (Neurovision 500M TCD; Multigon Instruments, Yonkers, NY, USA). During acquisition, velocities were sampled from across the entire lumen of the CCA at an angle of $\leq 60°$ and processed to determine a continuous intensity-weighted mean, which was acquired with an analogue-to-digital data acquisition system for further analysis (PowerLab; AD Instruments). Shear rate was calculated as 8 * mean blood velocity / end-diastolic lumen diameter (24).

Left ventricular measurements: A 1.5-3.6 MHz phased-array probe was connected to a second ultrasound unit (Vivid q; GE Medical Systems) and was used to collect images for determination of LV measurements following current guidelines for conventional variables (17) as well as for LV mechanics (33). The basal plane was defined as the highest plane in which the mitral leaflets were visible, while the apical plane was defined as the imaging plane closest to the apex with no visible papillary muscles, as previously described (32). Following acquisition, images were stored offline and analysed using commercially-available software (EchoPAC 110.0.2; GE Medical Systems, Horten, Norway). Due to the short time frame for data collection during the interventions, LV volumes were estimated from M-Mode analysis at the basal level of the LV from PLAX views. 2D speckle tracking was used to assess basal and apical rotation from short-axis

views, which were then exported to a custom data processing software (2DStrainAnalysis Tool, Stuttgart, Germany) for further processing. We were unable to calculate total LV twist due to different heart rates and blood pressures during basal and apical image acquisition after the SST and CPT, and therefore report LV basal and apical rotation separately.

Statistical Analysis: Statistical analyses were performed using IBM SPSS Statistics for Macintosh (version 20.0.0; IBM Corp., Armonk, N.Y., USA). *A priori* sample size was estimated based on Weiner *et al*. (2012) with an effect size of 0.89 to find blood pressure-mediated differences in LVT (two tailed, $\alpha = 0.05$, $\beta = 0.8$). Data were assessed for normality using the Kolmogorov-Smirnov test and were found to be normally distributed. Upon review of the heart rate and blood pressure data, the post-test time point for the CPT had significant interindividual variability and instead, we acquired and analysed data at the 60 sec time point for our primary objectives. Therefore, paired Student's t-tests were used to assess differences between time points within each test (SST: baseline *vs* post; CPT: baseline *vs* 60sec; NTG: baseline *vs* 6 minutes) on the outcome measures. Pearson's correlations were used to examine whether the magnitude of change in CALM variables were related to magnitude of change in potential regulatory control systems (i.e., PP, LV rotation, CCA shear rate), pooled across interventions. Since a limitation to these correlations is that participant data are represented in triplicate, a 'robust' regression was performed using the vcs(cluster) option in STATA (v14.2; College Station, TX) to

account for clustered data in the model. For all analyses, the acceptable level of significance was set at $\alpha = 0.05$.

RESULTS

Participant characteristics are presented in Table 1. All participants were normotensive at the time of study (< 140/90 mmHg). The changes in CCA and LV variables across each intervention are presented in Table 2.

Responses to the Serial Subtraction Test (SST)

All participants completed the SST, and had a range of incorrect responses to the test (5±5 errors, range 0 to 17). By the end of the SST, PP and heart rate were significantly elevated by +9±7 mmHg and +15±11 bpm, respectively ($P < 0.05$ vs baseline) (Figure 1A and 2A). Compared to baseline, basal rotation remained unchanged ($P = 0.10$) while apical rotation ($P < 0.01$), cardiac output ($P = 0.03$) and ejection fraction ($P < 0.01$) increased (Figure 4A and 4B; Table 2). There were no changes in end-diastolic volume ($P = 0.68$) or stroke volume ($P = 0.08$), but a significant decrease in end-systolic volume ($P = 0.05$). Mean blood velocity ($P < 0.01$) and CCA shear rate ($P < 0.01$) were also elevated at test completion. Conversely, all CALM displacements were unchanged during the post-test time point ($P > 0.05$) with heterogeneous changes in systolic anterograde (Δ range: -0.19 to 0.43 mm), systolic retrograde (Δ range: -0.29 to 0.30 mm) and diastolic (Δ range: -0.28 to 0.42 mm) CALM displacements (Figure 3A; Table 2).

Responses to the Cold Pressor Test (CPT)

One participant voluntarily ceased the test in the first 20 seconds due to discomfort, and was excluded from analysis, resulting in a total sample size of n=14. Similarly to the SST, at the end of the CPT, PP and heart rate were elevated by +12±12 mmHg and +4±13 bpm, respectively ($P < 0.05$) (Figure 1B and 2B). However, the changes in blood pressure and heart rate varied substantially at the end of the SST, resulting in a wide range of individual responses . Therefore, data at the 60sec time point was used for the primary analysis, with moderate increases in PP (+8±10 mmHg; $P < 0.01$) and heart rate (+11±10 bpm; $P < 0.01$). Compared to baseline, basal rotation increased ($P = 0.04$), while apical rotation ($P = 0.63$), cardiac output ($P = 0.09$) and ejection fraction ($P = 0.22$) remained unchanged (Figure 4C and 4D; Table 2). There were no changes in LV volumes or stroke volume ($P > 0.05$). CCA end-diastolic lumen diameter increased ($P = 0.03$), concomitant with an increase in CCA shear rate ($P = 0.01$) (Table 2). While the time-normalized CALM pattern was right-shifted due to the increase in heart rate (Figure 3B), there were no consistent changes in any CALM displacements at the 60sec time point ($P > 0.05$), which was attributable to the heterogeneous changes in systolic anterograde (Δ range: -0.31 to 0.15 mm), systolic retrograde (Δ range: -0.39 to 0.18 mm) and diastolic (Δ range: -0.35 to 0.16 mm) CALM displacements (Table 2).

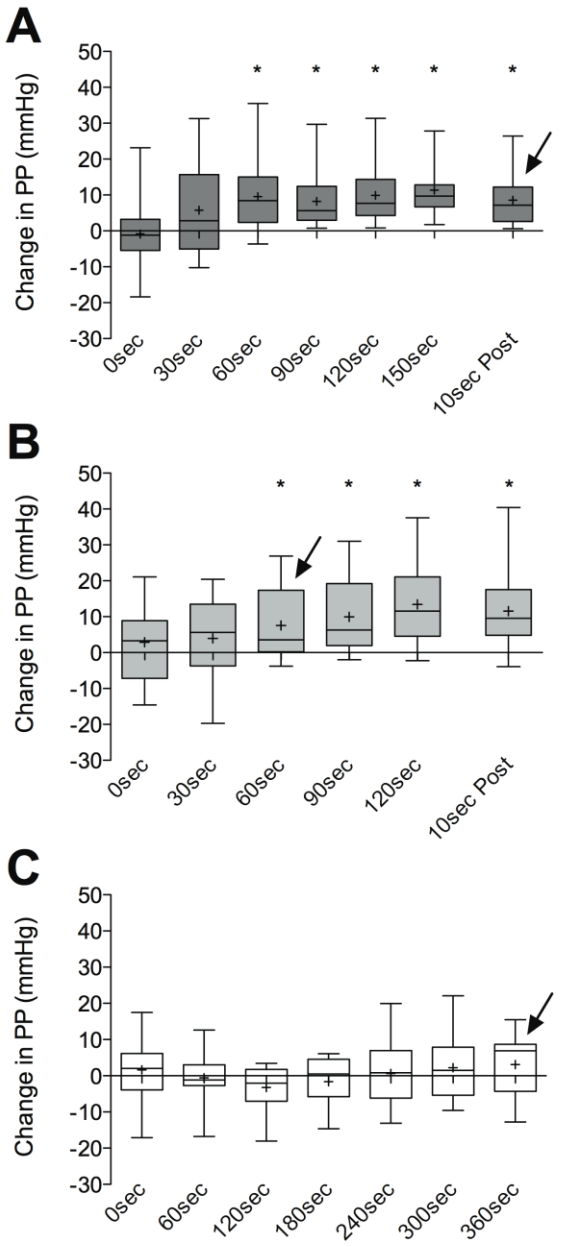

FIGURE 1: Changes in pulse pressure compared to baseline during: A) the Serial Subtraction Test; B) the Cold Pressor Test; and, C) the Nitroglycerin spray. Boxes represent the 25th, 50th (median), and 75th percentiles. The 10sec Post time point indicates the heart rate response immediately after the test. The cross indicates the mean and the bars represent the 95% confidence interval. The arrows represent the time point at which the main outcomes were measured. *$p<0.05$ different from baseline.

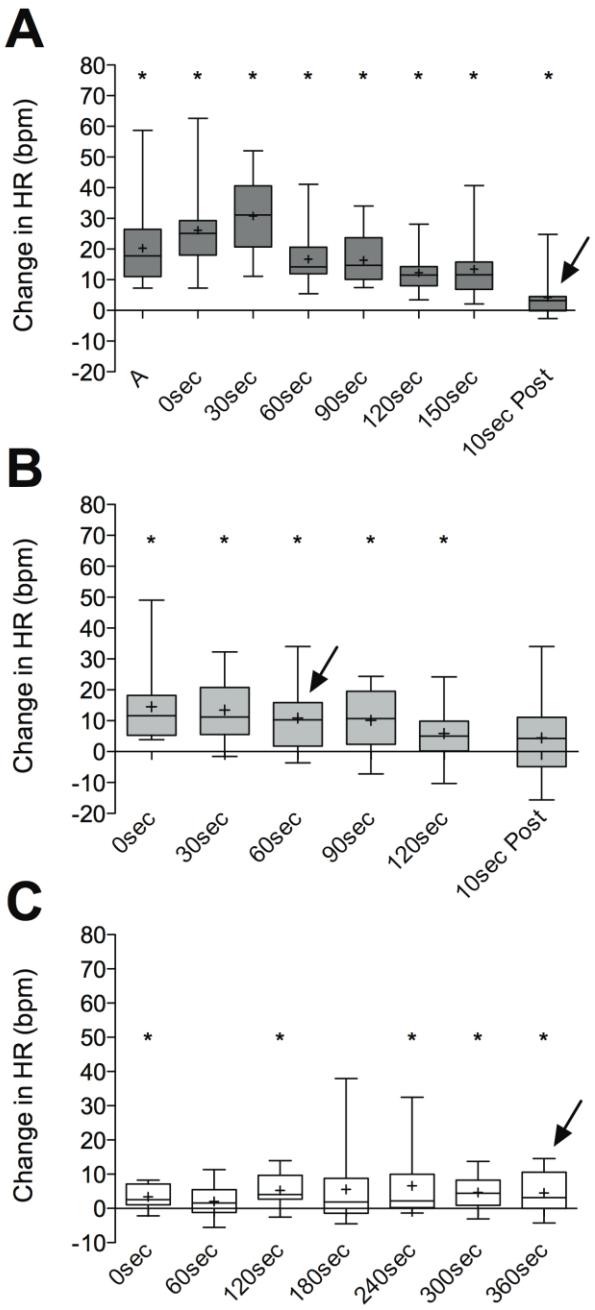

FIGURE 2: Changes in heart rate compared to baseline during: A) the Serial Subtraction Test; B) the Cold Pressor Test; and, C) the Nitroglycerin spray. The 10sec Post time point indicates the heart rate response immediately after the test. Boxes represent the 25th, 50th (median), and 75th percentiles. The cross indicates the mean and the bars represent the 95% confidence interval. The arrows represent the time point at which the main outcomes were measured. *$p<0.05$ different from baseline.

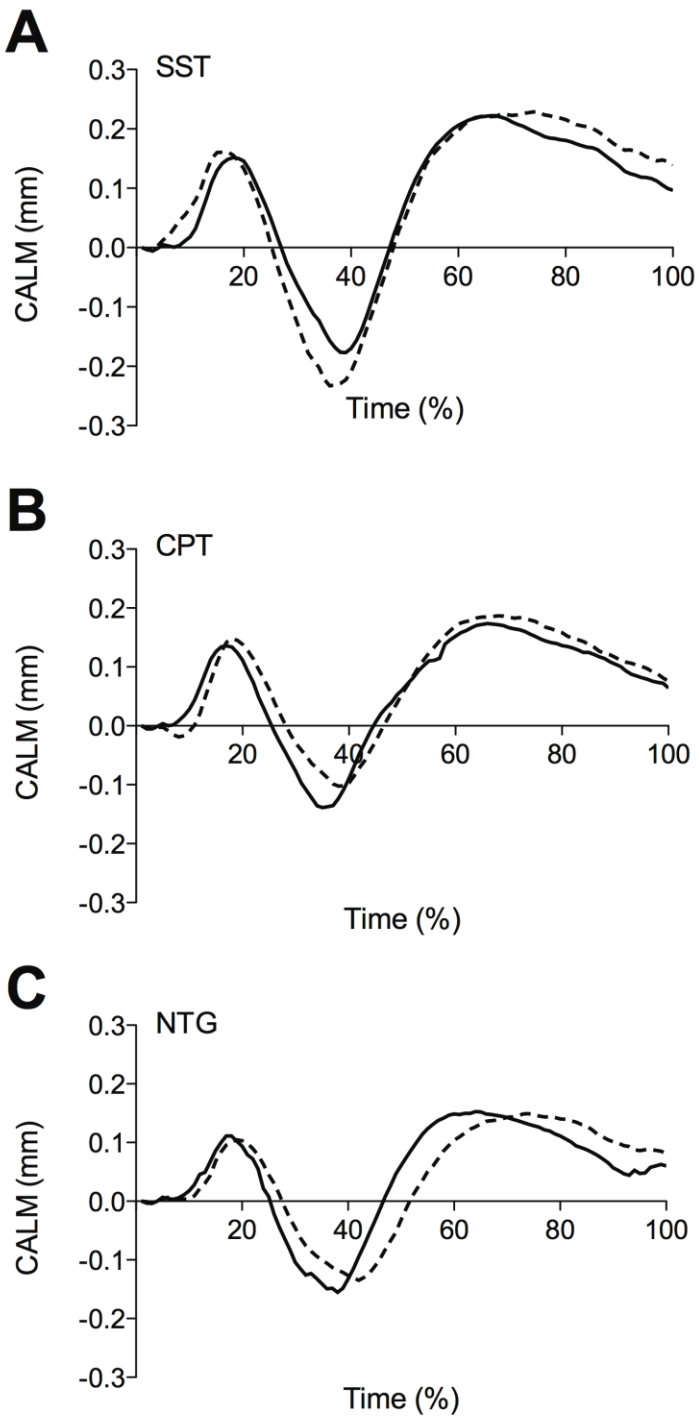

FIGURE 3: Group-averaged CALM traces at baseline (solid lines) and during (dashed lines): A) post SST; B) 60sec into the CPT; and, C) 6 minutes post-NTG. All traces are time-normalized to 100% of the cardiac cycle.

Responses to sublingual nitroglycerin (NTG)

Three participants did not perform the NTG intervention, and were excluded from analysis (n=12). PP remained unchanged at all time points ($P > 0.05$), while heart rate remained slightly elevated after 90 seconds post-spray until test completion at 6-minutes (+4±4 bpm; $P < 0.05$) (Figure 1C and 2C). At 6 minutes post-spray, there were no changes in either basal ($P = 0.65$) or apical ($P = 0.45$) rotation (Figure 4E and 4F), with no change in either cardiac output ($P = 0.90$) or ejection fraction ($P = 0.19$) (Table 2). However, end-diastolic ($P < 0.01$), end-systolic ($P < 0.01$), and stroke volumes ($P = 0.03$) were all reduced at the 6 minute time point. CCA end-diastolic lumen diameter increased ($P < 0.01$), with a concomitant decrease in CCA shear rate ($P < 0.01$). While there was a right-shift in the time-normalized CALM trace (Figure 3C), there were no differences in CALM displacements ($P > 0.05$) with heterogeneous changes in systolic anterograde (Δ range: -0.19 to 0.21 mm), systolic retrograde (Δ range: -0.34 to 0.29 mm) and diastolic (Δ range: -0.48 to 0.13 mm) CALM displacements (Table 2).

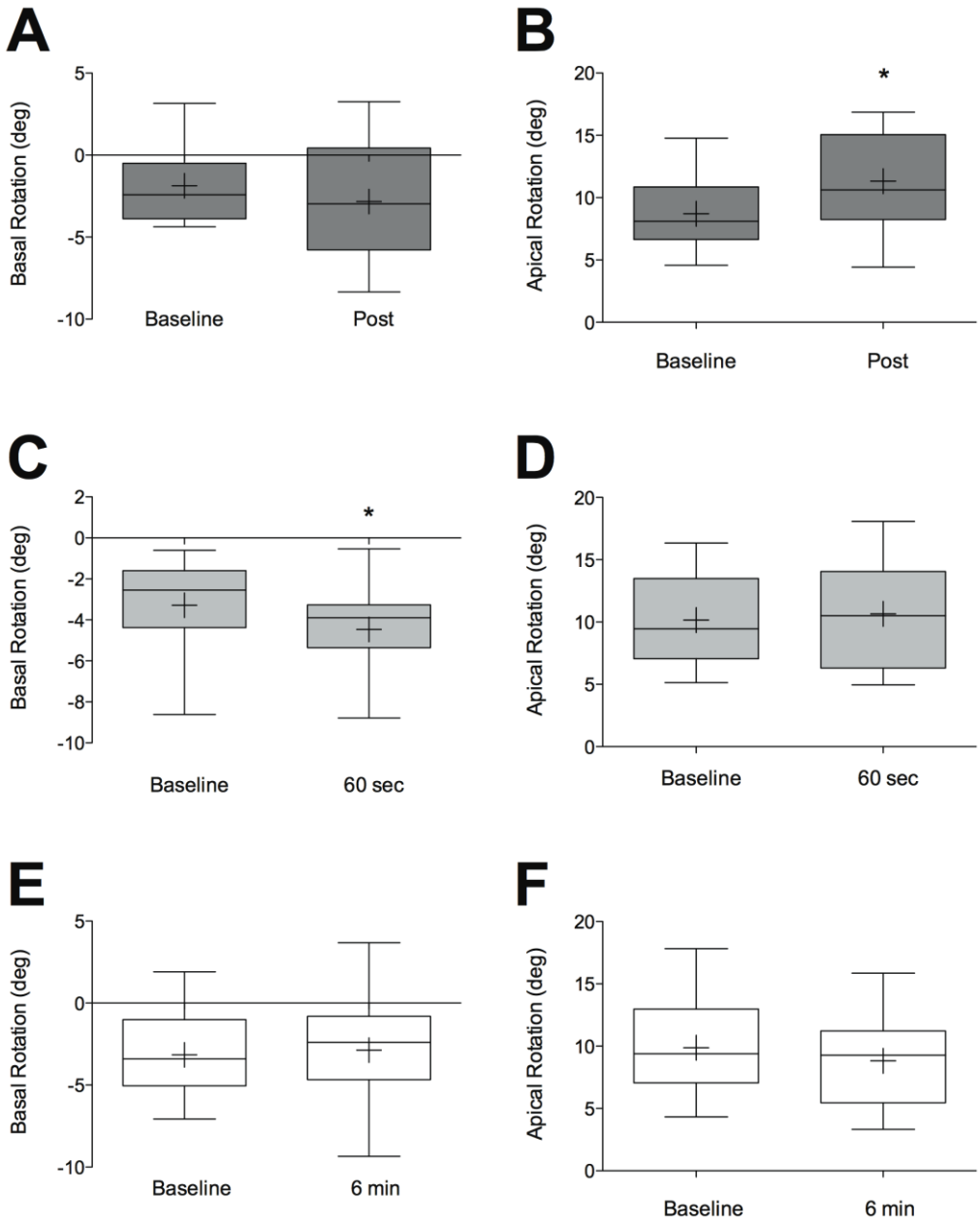

FIGURE 4: Left ventricular basal and apical rotation during the SST (A-B), CPT (C-D), and NTG (E-F). Boxes represent the 25th, 50th (median), and 75th percentiles. The cross indicates the mean and the bars represent the 95% confidence interval. Basal rotation is presented as negative values. *$p<0.05$ different from baseline.

Table 2. Carotid artery and left ventricular variables during experimental manipulation

Variable	SST (n=15)		CPT (n=14)		NTG (n=12)	
	Baseline	Post	Baseline	60 sec	Baseline	6 min
Carotid variables						
Ant CALM (mm)	0.27±0.16	0.30±0.19	0.24±0.15	0.25±0.13	0.23±0.13	0.21±0.14
Ret CALM (mm)	0.53±0.15	0.62±0.21	0.50±0.17	0.45±0.18	0.49±0.17	0.42±0.13
Dias CALM (mm)	0.56±0.18	0.62±0.22	0.52±0.18	0.45±0.23	0.50±0.26	0.39±0.16
Max CALM (mm)	0.62±0.15	0.71±0.22	0.59±0.13	0.53±0.19	0.57±0.22	0.48±0.13
MIDV (mm/s)	5.3± 1.7	6.0±2.2	5.1±2.0	4.4±2.0	4.6±2.6	3.7±1.7
MIDA (mm/s^2)	131± 33	148±52	127±39	113±42	119±50	97±38
LDd (mm)	5.9± 0.5	5.7±0.4	5.9±0.5	6.2±0.6*	5.9±0.6	6.4±0.6*
MBV (cm/s)	20.9±4.5	23.8±4.9*	18.5±4.3	23.3±6.0*	19.9±3.6	17.3±3.0*
Shear rate (1/s)	290±74	334±76*	253±69	305±81*	274±70	220±47*
LV variables						
Basal rotation (°)	-1.8±2.3	-3.0±3.3	-3.3±2.2	-4.5±2.4*	-3.2±2.6	-2.9±3.6
Apical rotation (°)	9.4±3.2	12.3±4.5*	10.2±3.7	10.7±4.1	9.9±4.1	8.8±3.7
CO (L/min)†	4.57±1.12	5.04±1.18*	4.07±0.96	4.73±1.50	4.58±1.06	4.61±0.88
EDV (mL)†	126±22	125±23	120±15	124±26	123±19	108±20*
ESV (mL)†	50±14	43±14*	50±9	52±12	48±11	42±11*
SV (mL)†	76±13	82±13	71±10	72±19	74±11	66±12*
EF (%)†	60±7	66±6*	59±5	58±6	61±5	62±6
E/e'	5.44±0.81	5.92±1.23	N / A	N / A	5.53±0.92	5.31±1.04

Values are means ± SD. Ant CALM = systolic anterograde CALM displacement; Ret CALM = systolic retrograde CALM displacement; Dias CALM = diastolic CALM displacement; Max CALM = maximum CALM displacement; MIDV = maximum instantaneous diastolic velocity; MIDA = maximum instantaneous diastolic acceleration; LDd = lumen diameter at end-diastole; MBV = mean blood velocity; PBV = peak blood velocity; CO = cardiac output; ESV = end-systolic volume; EDV = end-diastolic volume; SV = stoke volume; EF = ejection fraction. *p<0.05 different from baseline. †CPT n=8.

Pooled effects of interventions

To evaluate the intervention effects at an individual level, all interventions were pooled and correlations were assessed between CALM displacements and potential regulatory factors. An increase in systolic retrograde CALM was related to an increase in basal rotation (r = -0.35, P = 0.03; basal rotation is presented in negative degree units) (Figure 5). This relationship was also supported by the 'robust' regression to account for clustered data and conditions, where increases in rotation were associated with increases in systolic retrograde CALM (β = -0.025, P = 0.03). An increase in basal rotation was also related to increases in MAP (r = -0.35, P = 0.03; β = -1.654, P = 0.01). There was also a positive correlation between the change in shear rate and diastolic CALM displacement (r

= 0.32, *P* = 0.04; β = 0.0009, *P* = 0.01) but no association between the changes in either PP or heart rate with the changes in any CALM variable (*P* > 0.05).

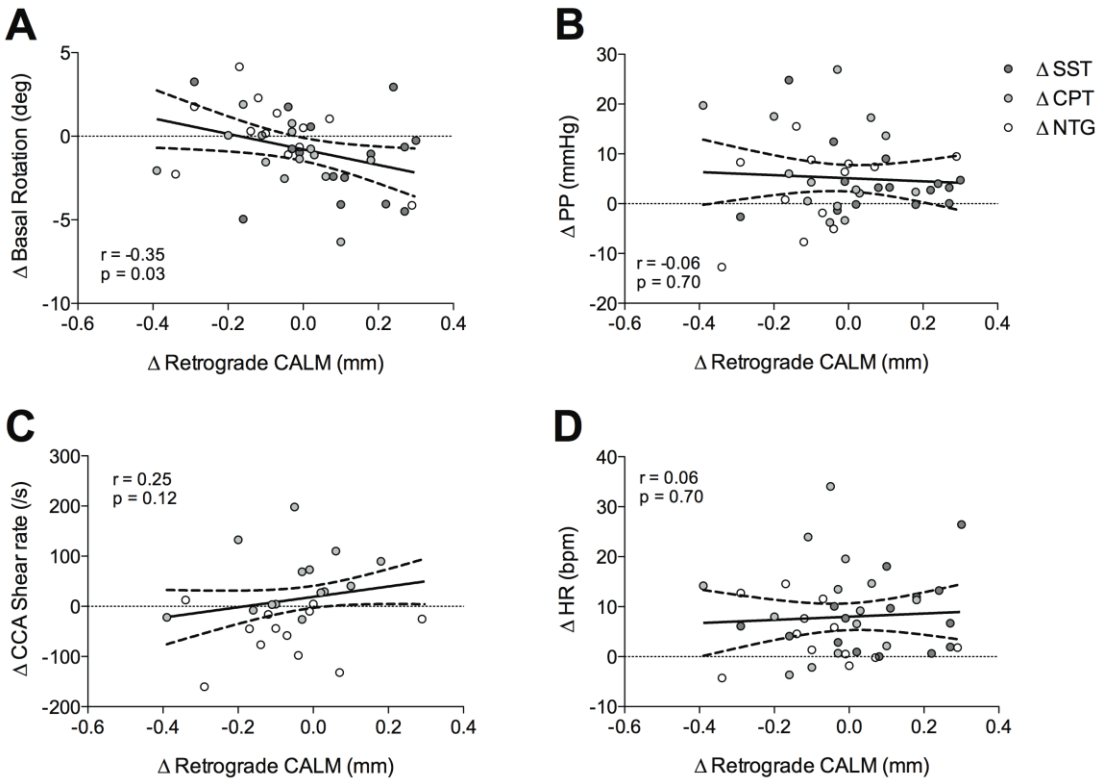

FIGURE 5: Scatterplots indicating the pooled relationship between the change in retrograde CALM and: A) the change in left ventricular basal rotation; B) the change in pulse pressure; C) the change in common carotid artery shear rate; and, D) the change in heart rate. Dark grey circles represent data from the SST, light grey circles represent data from the CPT, and open circles represent data from the NTG. Basal rotation is presented as negative values. Dashed lines represent the 95% confidence interval.

DISCUSSION

In this study, we successfully manipulated LV rotation and CCA shear rate in humans in a series of interventions through acute changes in sympathetic activity and vascular smooth muscle relaxation. There were no concomitant changes in PP, LV rotation, or CCA shear rate and systolic or diastolic CALM with any intervention,

however, when pooling the available data, we identified an effect of LV basal rotation on systolic retrograde CALM. These observations provide experimental evidence for a link between LV motion and systolic CALM consistent with our structural ventricular vascular coupling theory, although also suggest a moderating influence of LV rotation rather than a direct control mechanism. These findings help set a foundation for the determination of the physiological causes of CALM, and have important implications for the interpretation of changes in the CALM pattern with interventions and over time.

The regulation of CALM in healthy humans is poorly understood. The general CALM pattern has been well described over the last decade (7, 8, 26, 40), though only recently has data emerged to explain the origins of the biphasic motion commonly observed in healthy adults (2, 3, 42). We have recently proposed a model based on data related to the timing of CALM, LV, and local blood flow events whereby shear rate is a primary determinant of the systolic anterograde components of the CALM pattern, and LV rotation mechanics are the dominant influence of the systolic retrograde component (3). In the present study, we extended our previous observations to an experimental model where absolute changes in LV basal rotation were found to be related to absolute changes in systolic retrograde CALM displacement. Structurally, the right CCA branches from the brachiocephalic artery and the ascending aorta, and is connected to the LV at the ventriculo-aortic junction, which is a transition zone between the LV myocardium and fibrous annulus (9). The direct effect of LV motion on CALM would theoretically act at the ventriculo-aortic junction when the LV base descends towards the LV apex during systole (30), and may be estimated from left ventricular rotation mechanics (3). The role

of LV rotation on CALM is supported by findings that suggest a distal loss of centrally-generated kinetic energy, including cross-sectional correlations between participant height and CALM (3, 41), and observations of a progressive attenuation of the magnitude of total CALM along the length of the CCA (44). While our 'robust' regression analyses are novel, it is important to note we did not observe this effect discretely within each of the interventions, possibly due to underpowered effects. However, as we were sufficiently powered to detect changes in PP and LV rotation, it is possible the effect of LV rotation on CALM is not as strong as our theory would initially suggest, and may only moderate the influence of another factor.

Contrary to our hypothesis, in the current study, neither increases or decreases in CCA shear rate were related to changes in systolic anterograde CALM. We are not aware of any previous observations to support the theory that local arterial blood shear rate is a primary determinant of systolic anterograde CALM, although one previous study found no relationship between shear rate and CALM in pigs (2). Our timing data indicates there are simultaneous competing influences of the arrival of the forward blood velocity wave and initiation of LV rotation (3), which may complicate *in vivo* study of the regulation of anterograde CALM during the systolic phase, and may explain the absence of relationship between systolic anterograde CALM and shear rate. It would be of interest to investigate experimental models capable of eliciting independent changes in LV rotation and arterial shear rate in order to more accurately study the validity of our structural coupling theory.

In the current study, we sought to experimentally manipulate PP, LV rotational mechanics, and local arterial shear rate, to test their regulatory influence on CALM

displacements. While the SST and CPT both produce reliable pressor responses (15, 27) and increases in muscle sympathetic nerve activity (10), they have different underlying physiological control systems, which we hypothesized would allow us to probe differential regulation of CALM. The SST elicits a mental stress response through the HPA-axis, which primarily activates β_1-adrenoreceptors located in cardiac tissue, resulting in both cardiac chronotropic and inotropic effects (6, 29). We observed an increase in apical rotation, which may be due to greater β-receptor density in the LV apex compared to the base (21). Increases in rotation were observed with increased LV contractility (i.e., increased cardiac output and ejection fraction) without substantial increases in peripheral vascular resistance or metabolic demand, similar to previous observations in humans (29). Previously, acute increases in afterload have been associated with reduced apical rotation (5), however, the systolic blood pressure increase in our study was markedly lower (+25mmHg *vs* +35mmHg), which in combination with increased LV contractility, may explain the differences in LV rotational mechanics.

Similar to the SST, the CPT results in a well-documented neurogenic pressor response (14), primarily resulting in an increase in peripheral vascular resistance through α-adrenoreceptor mediated peripheral vasoconstriction (12), without increases in cardiac output due to increased afterload. We observed considerable inter-individual variability in the magnitude of heart rate and blood pressure responses, consistent with previous reports of 'vascular' versus 'myocardial' responders to the CPT (16). While increases in blood pressure have previously been associated with reduced LV rotation (5), we observed increased basal LV rotation in response to the CPT. Due to the time-sensitive nature of

data collection during the CPT, we were only able to measure LV functional outcomes in eight participants and may have been underpowered to detect changes in LV contractility. We also observed increased blood velocity at the CCA despite increased lumen diameter, which would suggest a change in LV outflow, and therefore contractility, which has a positive relationship with LV rotation (11). While both the SST and CPT were successful in eliciting acute changes in LV rotation and local CCA shear rate, we did not observe any changes in the magnitude of CALM displacements as a direct result of the interventions, contrary to our initial hypotheses. A more complex association may exist between LV rotation and retrograde CALM, and should be probed further with more isolated models of variable manipulation.

In comparison to the sympathetic-mediated tests, NTG is a known exogenous donor of nitric oxide, and is routinely used to assess endothelial-independent vasodilatory capacity. Sublingual NTG administration has also previously been shown to induce reductions in systemic vascular resistance, and increase cardiac output through elevations in heart rate in the supine position (34, 35). We observed reductions in end-systolic, end-diastolic and stroke volumes, consistent with previously described decreases in venous tone, which suggest reduced venous return and therefore reduced LV preload (18, 19, 22). However, reductions in end-diastolic volume were small (~15mL) and did not acutely modify LV rotation similar to previous work using *in vivo* unloading conditions (i.e., heating, saline infusion) (11, 31, 39). We did observe an increase in CCA lumen diameter and a reduction in CCA shear rate, indicative of an acute effect on the frictional forces acting on the local carotid wall. While we were able to modify local shear rate

independent of LV rotation, this reduced CCA shear rate did not change the systolic anterograde component of CALM, contrary to our hypothesis. These potential effects were likely further complicated by a direct effect of endothelium-independent smooth muscle relaxation, which may have opposed the hypothesized reduction in systolic anterograde CALM. As the CCA has a relatively low proportion of vascular smooth muscle compared to the peripheral vasculature, it would be interesting to study the effects of NTG on arterial longitudinal wall motion in the conduit arteries where vasodilatory effects may be more pronounced.

The current findings have important implications for analysis and interpretation of the CALM pattern in humans. Previous investigations of CALM outcome variables have largely focused on assessments of maximal wall displacements (13, 25, 45, 46), without considering the regulatory factors determining the timing and magnitude of the biphasic displacement. Our results indicate that it may be valuable to consider the phases of the CALM pattern rather than maximal displacement, as the systolic phase may be influenced by multiple upstream factors, and therefore, may not discretely and exclusively represent local vascular properties. In comparison, we did not find any changes to diastolic CALM displacement, velocity or acceleration with manipulation of PP, LV rotation or CCA shear rate during any intervention. We have previously provided support for the measurement of diastolic CALM variables as indices of arterial health in a large sample of healthy adults and individuals with coronary artery disease (4). The present findings support the validity of diastolic CALM as an indicator of vascular health, suggesting independence from blood pressure and LV motion in an acute model. Given the complex control

mechanisms that may regulate the systolic CALM pattern, we suggest that future studies should preferentially investigate the diastolic CALM kinetics to provide physiologically relevant information of arterial wall health.

Limitations: As the interventions were not randomized during the single visit, we did not control for cross-over effects for the CPT or NTG. However, as the purpose of this study was to study the direct relationship between potential regulatory factors and CALM, we were not interested in the effects of the interventions *per se*, but rather, the controlled degree of change in LV rotation or carotid artery shear rate, which we hypothesized would have a discrete structural coupling effect with CALM. We caution interpretation on the acute effects of the CPT and NTG administration, as our findings seem to differ from more tightly controlled models of afterload and preload dependence of left ventricular rotation (5, 38), and may be due to the delayed psychophysiological responses to the SST. In order to probe the influence of non-responders to the interventions in our analysis of variance, we repeated analyses with the top 50% of responders (n = 7), which yielded no differences in results compared to the full sample. While we did not investigate the influence of sex on these control mechanisms, we have previously found that the CALM pattern does not significantly differ between men and women (4); however, studies on sex-based differences are warranted in this novel field of research. Finally, the narrow age range in this study may not be generalizable to older populations; however, we aimed to minimize the confounding influence of increased

vascular stiffness in our hypothesis testing by studying a relatively homogenous group of young men.

CONCLUSION

In summary, we were able to successfully manipulate PP, LV rotation, and CCA shear rate with a series of acute physiological interventions in healthy men, which revealed an influence of LV basal rotation on the systolic retrograde CALM component. This evidence supports our structural ventricular-vascular coupling theory, though also suggests a moderating influence of LV rotation on CALM, rather than a direct role as originally hypothesized. Given the complex relationship between LV mechanics and the local CCA shear environment during systole, diastolic CALM variables may hold more promise in describing characteristics of the arterial wall independent of discrete manipulations of blood pressure and LV motion, and may provide benefit to quantify CALM and study its role in vascular health.

COMPETING INTERESTS

No competing interests, financial or otherwise, are declared by the authors.

AUTHOR CONTRIBUTIONS

All experiments were performed in the Vascular Dynamics Lab at McMaster University. J.A., P.B., S.V., E.S., and M.M. conceived and designed the work. J.A., J.C., P.B., S.V., acquired, analysed, or interpreted data for the work. J.A., P.B., S.V., J.C., E.S.,

and M.M. drafted the work and revised it critically for important intellectual content. All authors have approved the final version of the manuscript and agree to be accountable for all aspects of the work in ensuring that questions related to the accuracy or integrity of any part of the work are appropriately investigated and resolved. All persons designated as authors quality for authorship, and all those who quality for authorship are listed.

FUNDING

This study was supported by funding from the Natural Sciences and Engineering Research Council to Maureen MacDonald (DG # 238819-13, and RTI # 406308-11).

ACKNOWLEDGEMENTS

We would like to thank Daanish Mulla for his assistance with analysis, as well as the student volunteers who helped with data preparation for this study.

REFERENCES

1. **Ahlgren AR**, **Cinthio M**, **Steen S**, **Nilsson T**, **Sjoberg T**, **Persson HW**, **Lindstrom K**. Longitudinal displacement and intramural shear strain of the porcine carotid artery undergo profound changes in response to catecholamines. *Am J Physiol Heart Circ Physiol* 302: H1102–H1115, 2012.

2. **Ahlgren AR**, **Steen S**, **Segstedt S**, **Erlöv T**, **Lindström K**, **Sjöberg T**, **Persson HW**, **Ricci S**, **Tortoli P**, **Cinthio M**. Profound increase in longitudinal displacements of the porcine carotid artery wall can take place independently of wall shear stress: A continuation report. *Ultrasound Med Biol* 41: 1342–1353, 2015.

3. **Au JS**, **Ditor DS**, **MacDonald MJ**, **Stöhr EJ**. Carotid artery longitudinal wall motion is associated with local blood velocity and left ventricular rotational, but not longitudinal, mechanics. *Physiol Rep* 4: e12872, 2016.

4. **Au JS**, **Valentino SE**, **McPhee PG**, **MacDonald MJ**. Diastolic carotid artery longitudinal wall motion is sensitive to both aging and coronary artery disease status independent of arterial stiffness. *Ultrasound Med Biol* (April 20, 2017). doi: 10.1016/j.ultrasmedbio.2017.04.026.

5. **Balmain B**, **Stewart GM**, **Yamada A**, **Chan J**, **Haseler LJ**, **Sabapathy S**. The impact of an experimentally induced increase in arterial blood pressure on left ventricular twist mechanics. *Exp Physiol* 101: 124–134, 2015.

6. **Benschop RJ**, **Nieuwenhuis EES**, **Tromp EAM**, **Godaert GLR**, **Ballieux RE**, **van Doornen LJP**. Effects of β-adrenergic blockade on immunologic and cardiovascular changes induced by mental stress. *Circulation* 89: 762–769, 1994.

7. **Cinthio M**, **Ahlgren AR**, **Bergkvist J**, **Jansson T**, **Persson HW**, **Lindström K**. Longitudinal movements and resulting shear strain of the arterial wall. *Am J Physiol Heart Circ Physiol* 291: H394–H402, 2006.

8. **Cinthio M**, **Ahlgren AR**. Intra-observer variability of longitudinal displacement and intramural shear strain measurements of the arterial wall using ultrasound noninvasively *in vivo*. *Ultrasound Med Biol* 36: 697–704, 2010.

9. **de Kerchove L**, **Khoury El G**. Anatomy and pathophysiology of the ventriculo-aortic junction: implication in aortic valve repair surgery. *Ann Cardiothorac Surg* 2: 57–64, 2013.

10. **Dishman RK**, **Nakamura Y**, **Jackson EM**, **Ray CA**. Blood pressure and muscle sympathetic nerve activity during cold pressor stress: Fitness and gender. *Psychophysiol* 40: 370–380, 2003.

11. **Dong S-J**, **Hees PS**, **Huang W-M**, **Buffer SA Jr**, **Weiss JL**, **Shapiro EP**. Independent effects of preload, afterload, and contractility on left ventricular torsion. *Am J Physiol Heart Circ Physiol* 277: H1053–H1060, 1999.

12. **Frank SM**, **Raja SN**. Reflex cutaneous vasoconstriction during cold pressor test is mediated through α-adrenoceptors. *Clin Aut Res* 4: 257–261, 1994.

13. **Golemati S**, **Sassano A**, **Lever MJ**, **Bharath AA**, **Dhanjil S**, **Nicolaides AN**. Carotid artery wall motion estimated from b-mode ultrasound using region tracking and block matching. *Ultrasound Med Biol* 29: 387–399, 2003.

14. **Hines EA Jr**, **Brown GE**. The cold pressor test for measuring the reactibility of the blood pressure: Data concerning 571 normal and hypertensive subjects. *Am Heart J* 11: 1–9, 1936.

15. **Jern S**, **Pilhall M**, **Jern C**, **Carlsson SG**. Short-term reproducibility of a mental arithmetic stress test. *Clin Sci* 81: 593–601, 1991.

16. **Kline KA**, **Saab PG**, **Llabre MM**, **Spitzer SB**, **Evans JD**, **McDonald PAG**, **Schneiderman N**. Hemodynamic response patterns: Responder type differences in reactivity and recovery. *Psychophysiol* 39: 739–746, 2002.

17. **Lang RM**, **Badano LP**, **Mor-Avi V**, **Afilalo J**, **Armstrong A**, **Ernande L**, **Flachskampf FA**, **Foster E**, **Goldstein SA**, **Kuznetsova T**, **Lancellotti P**, **Muraru D**, **Picard MH**, **Rietzschel ER**, **Rudski L**, **Spencer KT**, **Tsang W**, **Voigt JU**. Recommendations for Cardiac Chamber Quantification by Echocardiography in Adults: An Update from the American Society of Echocardiography and the European Association of Cardiovascular Imaging. *Eur Heart J Cardiovasc Img* 16: 233–271, 2015.

18. **Mason DT**, **Braunwald E**. The effects of nitroglycerin and amyl nitrite on arteriolar and venous tone in the human forearm. *Circulation* 32: 755–767, 1965.

19. **Masuyama T**, **St Goar FG**, **Alderman EL**, **Popp RL**. Effects of nitroprusside on transmitral flow velocity patterns in extreme heart failure: A combined hemodynamic and doppler echocardiographic study of varying loading conditions. *J Am Coll Cardiol* 16: 1175–1185, 2003.

20. **Millar PJ**, **Bray SR**, **MacDonald MJ**, **McCartney N**. Cardiovascular reactivity to psychophysiological stressors: association with hypotensive effects of isometric handgrip training. *Blood Press Monit* 14: 190–195, 2009.

21. **Mori H**, **Ishikawa S**, **Kojima S**, **Hayashi J**, **Watanabe Y**, **Hoffman JIE**, **Okino H**. Increased responsiveness of left ventricular apical myocardium to adrenergic stimuli. *Cardiovasc Res* 27: 192–198, 1993.

22. **Niki K**, **Sugawara M**, **Chang D**, **Harada A**, **Okada T**, **Tanaka R**. Effects of sublingual nitroglycerin on working conditions of the heart and arterial system: analysis using wave intensity. *J Med Ultrasonics* 32: 145–152, 2005.

23. **Noonan PK**, **Benet LZ**. Incomplete and delayed bioavailability of sublingual nitroglycerin. *Am J Cardiol* 55: 184–187, 1985.

24. **Parker BA**, **Trehearn TL**, **Meendering JR**. Pick your Poiseuille: normalizing the shear stimulus in studies of flow-mediated dilation. *J Appl Physiol* 107: 1357–1359, 2009.

25. **Persson M**, **Ahlgren AR**, **Eriksson A**, **Jansson T**, **Persson HW**, **Lindström K**. Non-invasive measurement of arterial longitudinal movement. *Proc IEEE Ultrason Symp* 2: 1783–1786, 2002.

26. **Persson M**, **Ahlgren AR**, **Jansson T**, **Eriksson A**, **Persson HW**, **Lindström K**. A new non-invasive ultrasonic method for simultaneous measurements of longitudinal and radial arterial wall movements: first in vivo trial. *Clin Physiol Funct Imaging* 23: 247–251, 2003.

27. **Saab PG**, **Llabre MM**, **Hurwitz BE**, **Schneiderman N**, **Wohlgemuth W**, **Durel LA**, **Massie C**, **Nagel J**. The cold pressor test: Vascular and myocardial response patterns and their stability. *Psychophysiol* 30: 366–373, 1993.

28. **Sanders SW**, **Michaelis K**, **Maurette JM**, **Jaeger H**. Relative bioavailability of two spray formulations of nitroglycerin. *J Pharm Sci* 75: 244–246, 1986.

29. **Sherwood A**, **Allen MT**, **Obrist PA**, **Langer AW**. Evaluation of beta-adrenergic influences on cardiovascular and metabolic adjustments to physical and psychological stress. *Psychophysiol* 23: 89–104, 1986.

30. **Simonson JS**, **Schiller NB**. Descent of the base of the left ventricle: An echocardiographic index of left ventricular function. *J Am Soc Echocardiogr* 2: 25–35, 1989.

31. **Stöhr EJ**, **González-Alonso J**, **Pearson J**, **Low DA**, **Ali L**, **Barker H**, **Shave R**. Effects of graded heat stress on global left ventricular function and twist mechanics at rest and during exercise in healthy humans. *Exp Physiol* 96: 114–124, 2011.

32. **Stöhr EJ**, **González-Alonso J**, **Shave R**. Left ventricular mechanical limitations to stroke volume in healthy humans during incremental exercise. *Am J Physiol Heart Circ Physiol* 301: H478–H487, 2011.

33. **Stöhr EJ**, **Shave RE**, **Baggish AL**, **Weiner RB**. Left Ventricular Twist Mechanics in the Context of Normal Physiology and Cardiovascular Disease: A Review of

Studies using Speckle Tracking Echocardiography. *Am J Physiol Heart Circ Physiol* 311: H633–H644, 2016.

34. **Tahvanainen A**, **Leskinen M**, **Koskela J**, **Ilveskoski E**, **Alanko J**, **Kahonen M**, **Koobi T**, **Lehtimäki L**, **Moilanen E**, **Mustonen J**, **Pörsti I**. Non-invasive measurement of the haemodynamic effects of inhaled salbutamol, intravenous L-arginine and sublingual nitroglycerin. *Brit J Clin Pharmacol* 68: 23–33, 2009.

35. **Tahvanainen AM**, **Tikkakoski AJ**, **Leskinen MH**, **Nordhausen K**, **Kahonen M**, **Koobi T**, **Mustonen JT**, **Pörsti IH**. Supine and upright haemodynamic effects of sublingual nitroglycerin and inhaled salbutamol: a double-blind, placebo-controlled, randomized study. *J Hypertens* 30: 297–306, 2012.

36. **Tat J**, **Au JS**, **Keir PJ**, **MacDonald MJ**. Reduced common carotid artery longitudinal wall motion and intramural shear strain in individuals with elevated cardiovascular disease risk using speckle tracking. *Clin Physiol Funct Imaging* 37: 106–116, 2015.

37. **Townsend RR**, **Wilkinson IB**, **Schiffrin EL**, **Avolio AP**, **Chirinos JA**, **Cockcroft JR**, **Heffernan KS**, **Lakatta EG**, **McEniery CM**, **Mitchell GF**, **Naijar SS**, **Nichols WW**, **Urbina EM**, **Weber T**. Recommendations for improving and standardizing vascular research on arterial stiffness. *Hypertension* 66: 698–722, 2015.

38. **van Mil ACCM**, **Pearson J**, **Drane AL**, **Cockcroft JR**, **McDonnell BJ**, **Stöhr EJ**. Interaction between left ventricular twist mechanics and arterial haemodynamics during localised, non-metabolic hyperaemia with and without blood flow restriction. *Exp Physiol* 101: n/a–n/a, 2016.

39. **Weiner RB**, **Weyman AE**, **Khan AM**, **Reingold JS**, **Chen-Tournoux AA**, **Scherrer-Crosbie M**, **Picard MH**, **Wang TJ**, **Baggish AL**. Preload Dependency of Left Ventricular Torsion: The Impact of Normal Saline Infusion. *Circ Cardiovasc Img* 3: 672–678, 2010.

40. **Yli-Ollila H**, **Laitinen T**, **Weckström M**, **Laitinen TM**. Axial and radial waveforms in common carotid artery: An advanced method for studying arterial elastic properties in ultrasound imaging. *Ultrasound Med Biol* 39: 1168–1177, 2013.

41. **Yli-Ollila H**, **Laitinen T**, **Weckström M**, **Laitinen TM**. New indices of arterial stiffness measured from longitudinal motion of common carotid artery in relation to reference methods, a pilot study. *Clin Physiol Funct Imaging* 36: 376–388, 2015.

42. **Yli-Ollila H**, **Tarvainen MP**, **Laitinen TP**, **Laitinen TM**. Principal component

analysis of the longitudinal carotid wall motion in association with vascular stiffness: a pilot study. *Ultrasound Med Biol* 42: 2873–2886, 2016.

43. **Yli-Ollila H**, **Tarvainen MP**, **Laitinen TP**, **Laitinen TM**. Transfer function analysis of the longitudinal motion of the common carotid artery wall. *Front Physiol* 7, 2016.

44. **Zahnd G**, **Balocco S**, **Sérusclat A**, **Moulin P**, **Orkisz M**, **Vray D**. Progressive attenuation of the longitudinal kinetics in the common carotid artery: Preliminary in vivo assessment. *Ultrasound Med Biol* 41: 339–345, 2014.

45. **Zahnd G**, **Boussel L**, **Marion A**, **Durand M**, **Moulin P**, **Sérusclat A**, **Vray D**. Measurement of two-dimensional movement parameters of the carotid artery wall for early detection of arteriosclerosis: A preliminary clinical study. *Ultrasound Med Biol* 37: 1421–1429, 2011.

46. **Zahnd G**, **Vray D**, **Sérusclat A**, **Alibay D**, **Bartold M**, **Brown A**, **Durand M**, **Jamieson LM**, **Kapellas K**, **Maple-Brown LJ**, **O'Dea K**, **Moulin P**, **Celermajer DS**, **Skilton MR**. Longitudinal displacement of the carotid wall and cardiovascular risk factors: Associations with aging, adiposity, blood pressure and periodontal disease independent of cross-sectional distensibility and intima-media thickness. *Ultrasound Med Biol* 38: 1705–1715, 2012.

CHAPTER 5:

THE EFFECT OF EXERCISE TRAINING ON CAROTID ARTERY LONGITUDINAL WALL MOTION

In preparation

The effect of exercise training on carotid artery longitudinal wall motion

Jason S. Au[1], Ninette Shenouda[1], Sara Y. Oikawa[1], Jenna B. Gillen[1], Robert W. Morton[1], Martin J. Gibala[1], Stuart M. Phillips[1] and Maureen J. MacDonald[1]

[1]Department of Kinesiology, McMaster University, Hamilton, Canada

RUNNING HEAD: Exercise training and CALM

Corresponding Author:

Maureen J. MacDonald, PhD
McMaster University
Department of Kinesiology
IWC E207, 1280 Main Street West
Hamilton, ON, Canada, L8S 4K1
Telephone: 905-525-9140 ext. 23580
Fax: 905-523-6011
Email: macdonmj@mcmaster.ca

ABSTRACT

Purpose: Carotid artery longitudinal wall motion (CALM) is a novel indicator of arterial wall structure and is stable over time in healthy adults. Cross-sectional studies indicate differences in CALM between healthy versus individuals at elevated risk for cardiovascular disease; however, there have been no interventional studies examining changes in CALM with exercise training.

Methods: We examined the effect of 12 weeks of exercise training on CALM in data available from two studies. CALM was assessed before and after each intervention using high resolution ultrasound. Study 1 included moderate-intensity continuous training (45 minutes cycling at ~70% maximal heart rate; n=9), or sprint-interval training (3x20 second 'all-out' cycle sprints interspersed with 2 minutes of cycling at 50W; n=7) in sedentary men, compared to controls (n=4). Study 2 involved higher-repetition, lighter-load, resistance exercise training (3 sets of 20-25 repetitions; n=15), or lower-repetition, heavier-load, resistance exercise training (3 sets of 8-12 repetitions; n=15) in previously trained men, compared to activity-matched controls (n=16).

Results: At baseline, systolic retrograde CALM (P=0.05) and diastolic CALM acceleration (P=0.05) were elevated in men with a history of resistance exercise training compared to sedentary men. The general CALM pattern was unaltered after the training period for all conditions, with no differences in systolic or diastolic CALM magnitudes, velocities or accelerations (P>0.05).

Conclusion: We demonstrate no changes in the CALM pattern with 12 weeks of continuous, interval or resistance exercise training. However, physical activity status may

influence the systolic and diastolic components of the CALM pattern in healthy men. The normative responses established in this study lay the foundation for studies investigating training effects on CALM variables in individuals at elevated risk for cardiovascular disease.

INTRODUCTION

Carotid artery longitudinal wall motion (CALM) has recently emerged as a novel index of vascular structure (9, 37, 40). Importantly, CALM is less technically demanding to measure in comparison to, for example, arterial stiffness, and may be predictive of vascular risk (6, 27, 29, 41). High frame rate ultrasound imaging of the common carotid artery (CCA) reveals a biphasic movement pattern of the arterial wall, with longitudinal motion occurring in both the anterograde (i.e., in the direction of blood flow) and retrograde (i.e., against blood flow) directions (21). While the physiological determinants of this motion are poorly understood, a complex regulatory control model has been proposed that involves contributions from local shear stress, pulse pressure, and cardiac motion (3, 4, 38, 39).

CALM-derived indexes of vascular structure have been studied in both animal and cross-sectional human studies (2, 6, 28, 31, 32, 41), but there have been no interventional studies in humans, and in particular, no studies examining the impact of exercise interventions on CALM indices. Different exercise training modes have different positive effects on the vasculature, likely driven by differences in the hemodynamic stimulus generated during and after the exercise bouts. Bouts of moderate-intensity continuous training (MICT) elicit acute, sustained increases in cardiac output and mean arterial pressure, with increased conduit artery oscillatory shear stress contributing to training-induced changes in conduit artery endothelial function (7) and arterial structure (24). In comparison, bouts of resistance exercise training (RET) offer an intermittent challenge to the central vasculature, primarily though large increases in blood pressure (16), which, in

turn, affect left ventricular mechanics (35) and challenge the pressure-buffering capacity of the central elastic arteries (8). There is some debate as to whether RET adversely affects the central vasculature (5, 18), though the effects seem largely dependent on the volume and intensity of resistance exercise, as well as measurement method. These observations are relevant to the emergence of alternative 'higher-repetition, lighter-load' (HR-RET) protocols shown to provide similar musculoskeletal benefits to traditional 'lower-repetition, heavier-load' (LR-RET) protocols (20, 25), both of which we have recently shown to have beneficial effects on central arterial stiffness (5). Finally, low-volume sprint-interval training (SIT), involving brief bouts of intense intermittent exercise separated by recovery periods, occupies a sort of middle ground on the continuum between traditional endurance and resistance exercise training. In terms of the vascular stimulus, SIT is characterized by intermittent elevations in cardiac output and oscillatory shear stress against the vessel wall. However, there have been limited reports on the efficacy of SIT to promote vascular adaptations in healthy men (23, 26).

Given the varied acute hemodynamic stimuli conferred by MICT, RET and SIT, these diverse training models offer a method of assessing the impact of differing exercises on the vasculature, from which we might infer potential mechanisms underpinning changes. We have previously documented the metabolic and fitness-related improvements from a range of exercise training models, demonstrating some of the physiological changes occurring with each training type (11, 20). As CALM measurements have previously been established as a stable vascular variable (1), capable of providing unique vascular health information (6, 41), we aimed to determine whether CALM variables can

be similarly modified by exercise training. Therefore, we conducted a retrospective analysis of CALM data that was previously obtained from two exercise-training studies (Study 1: MICT *vs* SIT; Study 2: HR-RET *vs* LR-RET). We sought to describe the effects of 12-weeks of continuous, resistance, or interval exercise training on CALM variables compared to healthy, activity- and age-matched men, hypothesizing that exercise training would increase CALM magnitudes over the training period.

METHODS

Participants and ethical approval

A total of 75 men were recruited for two separate exercise training studies, the details of which have previously been reported (11, 20): Study 1) 12-weeks of MICT *vs* SIT in sedentary men (n=27); and Study 2) 12-weeks of HR-RET *vs* LR-RET in previously resistance-trained men (n=48). An activity-matched control group was included in each study. Two participants dropped out due to reasons unrelated to the studies. Due to poor image quality (poor backscatter or out-of-plane motion), seven participants were excluded from analysis, resulting in a final sample of n=20 (Study 1) and n=46 (Study 2). Both studies were approved by the local Hamilton Integrated Research Ethics Board and conformed to the *Declaration of Helsinki* regarding humans as research participants.

Table 1. Baseline participant characteristics

Variable	Study 1			Study 2		
	MICT (n=9)	SIT (n=7)	SED-CTL (n=4)	HR-RET (n=15)	LR-RET (n=15)	EX-CTL (n=16)
Age (yr)	27±8	24±5	23±3	23±3	23±2	24±2
Height (cm)	177±10	176±176	177±4	180±8	181±6	179±5
Body mass (kg)	80.7±18.7	82.1±82.1	73.1±15.1	86±18	84±11	81.1±9.2
BMI (kg/m^2)	25.7±4.9	26.2±4.9	23.3±3.9	26.3±3.9	25.8±3.0	25.3±2.3
SBP (mmHg)	112±8	117±117	109±10	123±7	122±13	116±7
DBP (mmHg)	67±7	68±68	65±6	65±9	70±11	62±4*
MAP (mmHg)	85±5	87±87	83±6	88±4	87±11	84±4
Resting HR (bpm)	64±12	65±65	64±11	64±8	58±8	60±8

SBP = systolic blood pressure; DBP = diastolic blood pressure; MAP = mean arterial pressure; HR = heart rate. Data are mean±SD; *p<0.05 different from LR-RET.

Experimental Methods

The experimental methods and time points of vascular assessment were identical for both studies. For all experimental testing sessions, participants arrived fasted at the lab, after refraining from food, alcohol and caffeine for >10 hours, and moderate-to-vigorous intensity activity for >24 hours. Participants rested in the supine position for 10 minutes prior to any data collection. Heart rate was continuously monitored with single-lead ECG (PowerLab model ML 132; AD Instruments, Colorado Springs, CO, USA), and supine blood pressures were assessed using an automated oscillometric cuff in triplicate at the right brachial artery (Dinamap Pro 100; Critikon LCC, Tampa, FL). All measures were taken at baseline and after 12 weeks of exercise training for both studies.

Carotid artery longitudinal wall motion: Longitudinal motion was assessed at the right common carotid artery (CCA) in the supine position, as previously described (4, 6). A 12 MHz linear-array probe connected to a high-resolution ultrasound machine (Vivid q, GE Medical Systems, Horten, Norway) was used to image the far wall of the CCA 1-2 cm proximal to the carotid bifurcation in the lateral plane. Participants were asked to briefly

hold their breath during image acquisition, and three to six heart cycles were recorded at 102.5 fps with a standard depth of 2.5 cm. CALM was measured using an in-house speckle tracking algorithm (MatLab, The MathWorks, Natick, MA) (31). Gated to the R-spike on the ECG, a reference kernel block was manually positioned so that the lower edge was placed on the media-adventitia interface of the far wall of the CCA to assess motion of the intima-media. Day-to-day measurements of CALM magnitude in our lab indicate good reproducibility (CV=7.8%; n=10) (4).

CALM Point Selection: Figure 1 demonstrates the pooled average CALM traces for Study 1 and Study 2, with points A-E identified as a guideline for the following descriptions. CALM traces were visualized for semi-automated point selection for the following events (4, 6): A) the onset of retrograde motion was determined as the first movement of the wall in retrograde direction; B) the anterograde shoulder was determined as the first movement in the anterograde direction, or the local positive peak of the 2nd derivative in the absence of a clear local minimum; C) the peak anterograde displacement was determined as the maximal displacement in the forward direction, or the local negative minimum of the 2nd derivative in the absence of a clear local maximum; D) the peak retrograde displacement was determined as the maximal displacement in the retrograde direction; and E) the diastolic anterograde displacement was determined as the first anterograde plateau during diastole. For data presentation, all traces were linearly interpolated to 100 discrete points to account for variable cardiac cycle length, and averaged between participants at each time point, though all traces were analysed using the raw displacement data.

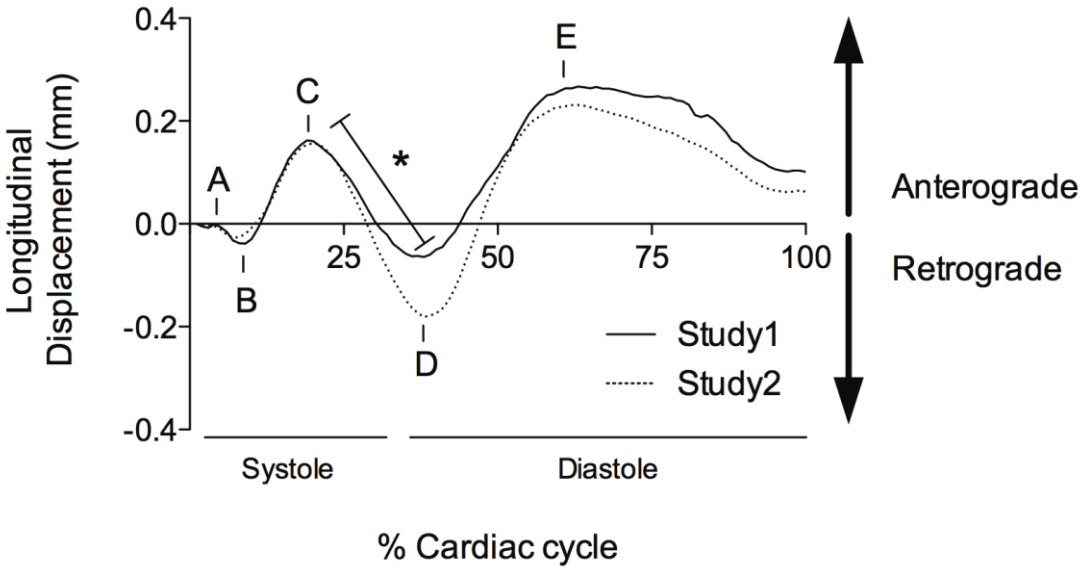

FIGURE 1: Baseline CALM pattern for Study 1 (solid) and Study 2 (dotted). Analysis points A-E correspond to local maxima and minima that remain consistent between individuals to allow for displacement calculations: systolic anterograde CALM (B-C), systolic retrograde CALM (C-D), and diastolic CALM (D-E). *p=0.05 systolic retrograde CALM different from Study 2.

CALM Phases: The absolute total CALM displacement (maximum CALM) was determined as the difference between peak anterograde and peak retrograde displacement of the arterial wall. The CALM pattern was also divided into systolic CALM (anterograde [point C – point B], retrograde [point D – point C]) and diastolic CALM (diastolic displacement [point E – point D]), all reported in absolute values. To calculate diastolic velocities and accelerations, displacements were digitally filtered (2^{nd} order, dual pass butterworth, Fc = 10Hz) and differentiated into first and second derivatives for peak detection.

Study 1: MICT and SIT

Participants completed 12-weeks of either MICT (n=9), SIT (n=7) or a non-training control period (SED-CTL; n=4) in a between-groups repeated-measures design, as previous described (11, 26). Training groups completed 30 supervised exercise sessions in a controlled environment, while the control group was asked to continue their current sedentary lifestyle over the 12 weeks. Participants were identified as sedentary based on an International Physical Activity Questionnaires (IPAQ) score of <600 MET minutes/week. As participants were sedentary at baseline, the training groups progressed from one exercise session in the first week, to two sessions the second week, and three sessions for the remaining weeks.

Maximal oxygen uptake (VO_2peak) was determined by an incremental ramp test to exhaustion on an electronically braked cycle ergometer (Lode Excalibur V 2.0, Groningen, The Netherlands) as previously described (11). All supervised exercise training sessions began with a two-minute warm-up and ended with a three-minute cool-down. MICT consisted of 45 minutes of continuous leg cycling (Ergo Race, Kettler, Ense-Parsit, Germany) at ~70% HR_{max} (~55% VO_2peak). Absolute workloads were increased as needed over the 12 weeks to maintain the desired relative heart rate. SIT consisted of three, 20-second 'all-out' sprints (Velotron, RacerMate, Seattle, WA, USA) against 5.0% body mass, interspersed with two minutes of active recovery at 50 watts.

Study 2: HR-RET and LR-RET

Participants completed 12-weeks of either HR-RET (n=15), LR-RET (n=15) or non-structured exercise control period (EX-CTL; n=16) in a between-groups repeated-measures design, as previous described (4, 20). Participants in RET and EX-CTL groups had a history of resistance training, which was defined as having engaged in RET more than two sessions per week, for at least the past two years. The EX-CTL group was asked to maintain current exercise habits in order to prevent deconditioning effects over the study period.

Participants randomized to the RET protocols performed whole-body exercise four times per week, separated as two workouts: 1) inclined leg press, seated row, bench press, cable hamstring curl and front planks; and 2) shoulder press, bicep curls, triceps extension, wide grip pull downs and knee extension. Three sets per exercise were performed until volitional failure. The HR-RET group performed 20-25 repetitions per set (~30%-50% of 1RM), while the LR-RET group performed 8-12 repetitions per set (~75%-90% of 1RM), with 1RM testing reassessed at 4, 7 and 10 weeks to ensure the progression of RET stimulus. In addition to the exercise training, both RET groups also consumed 30g of whey protein (BioPRO, Davisco Foods International, Le Seur, MN) twice per day.

Statistical Analysis: Statistical analyses were performed using IBM SPSS Statistics for Macintosh (version 20.0.0; IBM Comp., Armonk, N.Y., USA). Data were checked for normality using the Shapiro-Wilk test. To assess inter-study differences in participant

physical activity status, baseline data were pooled between groups within each study to compare baseline values using independent Student's t-tests. Group analysis revealed differences in CALM magnitudes between studies, and therefore, separate analyses for training effects were conducted for Study 1 and Study 2. We employed 3 x 2 (group x time) Mixed ANOVAs with Tukey's HSD post-hoc tests to assess changes in outcome variables over time between groups in Study 1 and Study 2. All data are reported as mean±SD. All analyses were two-tailed, with the level of statistical significance set at $\alpha = 0.05$.

RESULTS

Participant characteristics for both studies are presented in Table 1. The CALM patterns observed were consistent with previously published reports, with a biphasic anterograde-retrograde displacement in systole, followed by a return to the reference position by the end of the cardiac cycle (Figure 1). Local maxima and minima (CALM points A-E) were identified in all individuals, which allowed for standardized selection of systolic anterograde, systolic retrograde and diastolic CALM displacement. When groups were pooled within studies at baseline, there were inter-study differences in resting systolic blood pressure (Study 1 *vs* 2: 113±9 *vs* 120±10 mmHg; $P<0.01$), systolic retrograde CALM (Study 1 *vs* 2: 0.44±0.20 *vs* 0.55±0.21 mm; $P=0.05$), and CALM maximum instantaneous diastolic acceleration (Study 1 *vs* 2: 122±62 *vs* 155±60 mm/s^2; $P=0.05$). Due to these known differences in baseline CALM, analysis was performed separately on

Study 1 and Study 2 to avoid the confounding effect of differences in baseline arterial structure and prior history of physical activity.

Study 1: Effects of aerobic exercise training

When plotted on the same relative time scale, CALM retained the same general pattern within a group over the training period for MICT, SIT and SED-CTL (Figure 2A). No changes in systolic anterograde (group × time P=0.19), systolic retrograde (group × time P=0.59) or diastolic CALM displacement (group × time P=0.98) were observed over the training period for either MICT or SIT compared to SED-CTL (Table 2). Similarly, there were no changes in maximum instantaneous diastolic CALM velocities (group × time P=0.89) or accelerations (group × time P=0.13) across the training period.

Study 2: Effects of resistance exercise training

When plotted on the same relative time scale, CALM retained the same general pattern over the training period for HR-RET, LR-RET and EX-CTL (Figure 2B). No changes in systolic anterograde (group × time P=0.98), systolic retrograde (group × time P=0.67), or diastolic CALM displacement (group × time P=0.87) were observed over the training period for either HR-RET or LR-RET compared to EX-CTL (Table 3). There were no changes in maximum instantaneous diastolic CALM velocities (group × time P=0.87) or accelerations (group × time P=0.98) across the training period.

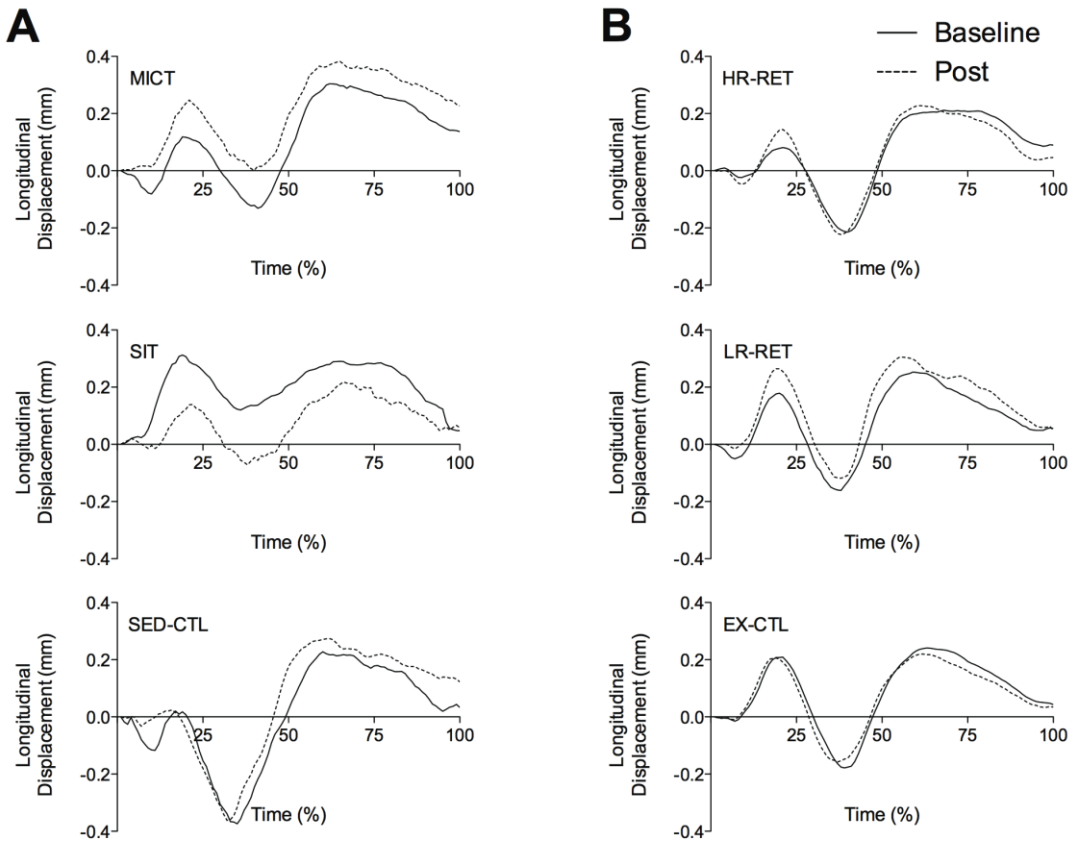

FIGURE 2: Group-averaged CALM traces for A) Study 1: moderate-intensity continuous training (MICT) *vs* sprint-interval training (SIT) *vs* sedentary control (SED-CTL), and B) Study 2: higher-repetition resistance exercise training (HR-RET) *vs* lower-repetition resistance exercise training (LR-RET) *vs* exercising control (EX-CTL), at baseline (solid) and post 12-weeks training (dashed) time points. All traces are expressed as a percentage of a single cardiac cycle, gated to the R-spike of the ECG-recording.

Pooled exercise training responses

As this is the first study to investigate potential changes to the CALM pattern over an intervention period, we were interested in the range of responses generated by the different exercise interventions. Figure 3 shows individual training responses in CALM displacements, velocities, and accelerations, coded by exercise training or control conditions. Dashed lines indicated the expected variability in measurement, presented as

±2*Typical Error of the change scores within the control conditions. The above noted absence of training responses is also reflected in these plots, with no discernible grouping of training conditions, with most falling within the expected limits of error for change scores.

Table 2. CALM variables in Study 1: Endurance and sprint-interval exercise training

Variable	MICT		SIT		SED-CTL	
	Baseline	12-wks	Baseline	12-wks	Baseline	12-wks
Systolic Anterograde CALM (mm)	0.27±0.12	0.31±0.21	0.39±0.19	0.31±0.14	0.22±0.12	0.21±0.18
Systolic Retrograde CALM (mm)	0.37±0.14	0.38±0.15	0.43±0.24	0.34±0.18	0.60±0.19	0.58±0.21
Diastolic CALM (mm)	0.51±0.27	0.50±0.40	0.39±0.29	0.36±0.30	0.78±0.31	0.74±0.32
Max CALM (mm)	0.56±0.22	0.62±0.34	0.53±0.22	0.49±0.22	0.81±0.25	0.74±0.31
MDV (mm/s)	3.73± 2.79	3.36±2.05	2.27±1.33	1.92±1.12	4.62±1.52	4.08±1.29
MIDV (mm/s)	5.86±414	5.10±2.88	3.70±2.47	3.37±2.29	8.31±3.09	7.07±2.81
MIDA (mm/s^2)	128±72	144±67	89±42	89±40	168±38	126±50

CALM = carotid artery longitudinal wall motion; MDV = mean diastolic velocity; MIDV = maximum instantaneous diastolic velocity; MIDA = maximum instantaneous diastolic acceleration. Data are mean±SD; no significant group x time interactions or main effects.

Table 3. CALM variables in Study 2: Higher-repetition and lower-repetition resistance exercise training

Variable	HR-RET		LR-RET		EX-CTL	
	Baseline	12-wks	Baseline	12-wks	Baseline	12-wks
Systolic Anterograde CALM (mm)	0.28±0.11	0.31±0.21	0.39±0.27	0.40±0.25	0.31±0.17	0.33±0.20
Systolic Retrograde CALM (mm)	0.52±0.18	0.54±0.21	0.60±0.26	0.58±0.19	0.53±0.18	0.56±0.15
Diastolic CALM (mm)	0.62±0.25	0.62±0.26	0.63±0.34	0.61±0.22	0.57±0.22	0.58±0.26
Max CALM (mm)	0.67±0.21	0.67±0.23	0.76±0.27	0.72±0.22	0.64±0.18	0.68±0.18
MDV (mm/s)	4.02± 1.60	3.76±1.50	3.73±1.96	3.63±1.44	3.37±1.31	3.20±1.06
MIDV (mm/s)	6.61±2.74	6.77±2.84	6.52±3.98	6.45±2.65	6.11±2.36	5.85±2.40
MIDA (mm/s^2)	161±55	157±48	162±75	162±51	142±48	140±40

CALM = carotid artery longitudinal wall motion; MDV = mean diastolic velocity; MIDV = maximum instantaneous diastolic velocity; MIDA = maximum instantaneous diastolic acceleration. Data are mean±SD; no significant group x time interactions or main effects.

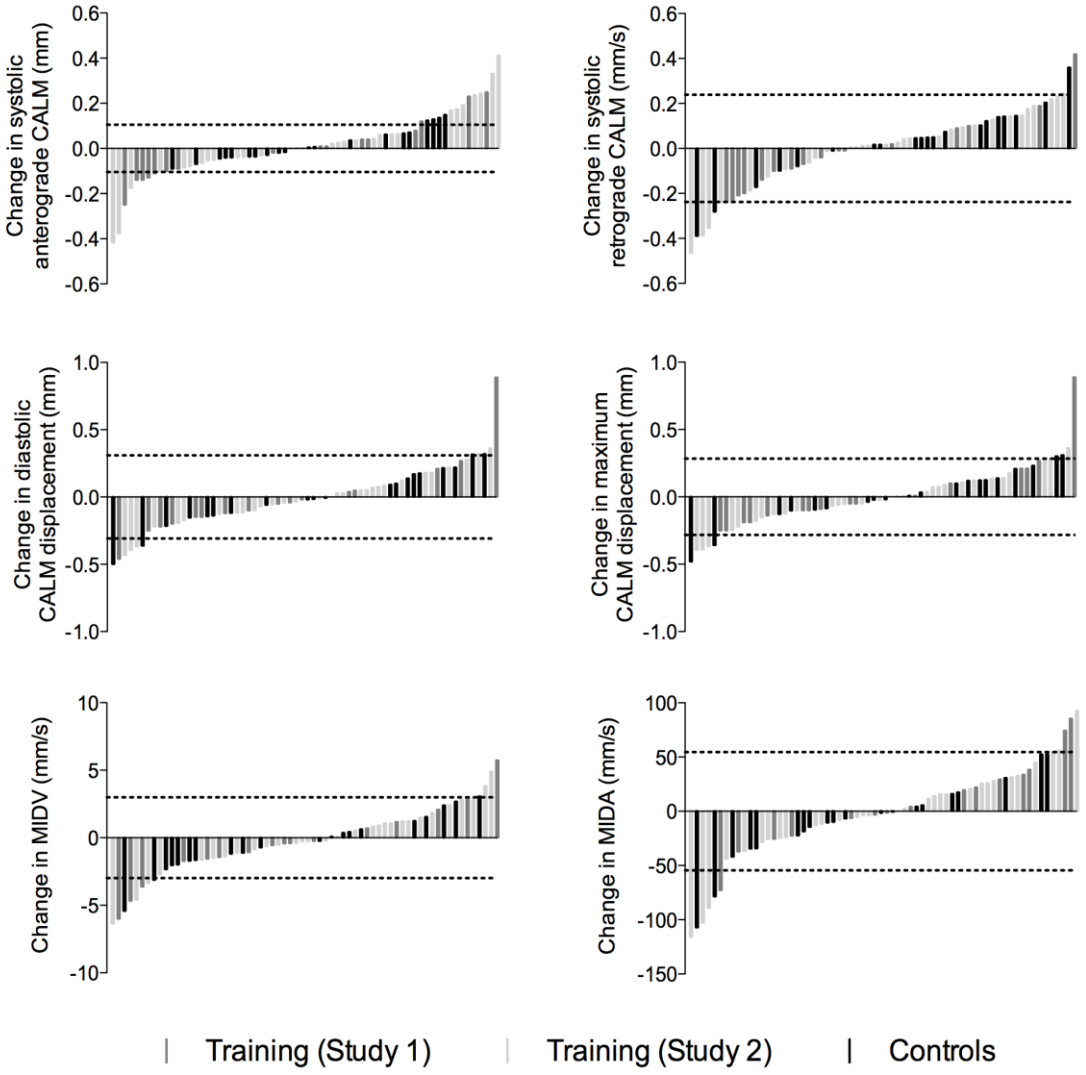

FIGURE 3. Individual training responses in CALM variables over the training period for training groups in Study 1 (dark grey) and Study 2 (light grey), and control groups (black). Dashed lines represent ± 2*Typical Error change scores of the control groups over the training period.

DISCUSSION

This is the first study to examine CALM in response to various exercise training interventions in humans. We report baseline differences in systolic retrograde CALM and diastolic CALM acceleration in men with different physical activity histories; however, there were no changes in the CALM pattern over the 12-week interventions. This general conclusion was the same regardless of training or control conditions, with no changes in the magnitude of systolic or diastolic CALM variables. While it is not clear whether changes in other regulatory processes, such as local blood flow or left ventricular adaptations, impacted our ability to observe changes in CALM magnitude, we demonstrate no changes in CALM variables in response to exercise training in healthy men.

Recent work from multiple groups has shown that CALM variables change with age and health status in a wide range of populations (6, 28, 29, 31, 41). However, these cross-sectional studies have observed groups with wide discrepancies in health and/or age status, typically comparing older individuals and clinical populations to idealized younger healthy adults. Only one study has performed a longitudinal follow-up of CALM patterns in humans, finding that motion displacements were stable over a 4-month period in free-living adults (1). Previous studies suggest that CALM yields reproducible information of arterial physiology that could indicate differences in health status among humans. As such, the measurement of CALM may hold promise as a feasible non-invasive monitoring tool for changes in arterial health. Nonetheless, no studies have previously investigated how CALM changes with lifestyle interventions in humans. In the present study, we

investigated the effects of four types of exercise training modes in a large sample of healthy men. Concomitant with the retention of the general shape of the CALM pattern, we did not observe any differences in the magnitude of motion displacement or velocity over the 12-week training period. Our data indicate that it may be difficult to change the CALM pattern in healthy men, even with highly structured exercise programs of varying intensities with documented cardiometabolic benefits (5, 11, 20, 26). Stability in arterial health is similarly observed in the measurement of carotid intima-media thickness, which is resistant to changes with exercise training over similar time frames (33). Given that cross-sectional carotid intima-media thickness is a stable indicator of arterial wall structure and is highly predictive of cardiovascular events (15), it may be of interest to measure CALM variables for long-term risk prediction, in addition to monitoring transient changes in arterial wall health.

Currently, there is no consensus of what comprises a ‘favourable’ CALM pattern, although some studies suggest retrograde-dominant patterns (32) and greater absolute displacement magnitudes (6, 29) may be associated with superior vascular function. In the present study, it may be that these men were at near-optimal health when entering the training program, possibly limiting the chronic central vascular adaptations to structured exercise, especially within the time frame of the interventions. Individuals at greater risk for cardiovascular disease may have a greater capacity for change and do appear to undergo structural arterial remodelling with exercise training (13, 19). Previous exercise training studies in healthy adults have demonstrated a tendency for improvements in central, rather than peripheral, stiffness (12, 30), although conflicting reports also exist

(22, 34). Future studies should assess the impact of exercise interventions on CALM in populations with known central vascular dysfunction in order to probe the possible implications for vascular health, similar to traditional indicators of arterial structure and function (13).

We have previously demonstrated that the CALM pattern may be closely linked to the local shear pattern at the CCA and the rotation of the left ventricle (4), in addition to being related to local arterial stiffness (6). Other groups have suggested that the general CALM pattern may be explained by the distending blood pressure wave (3, 38, 39), although these hypotheses may be equally confounded by left ventricular contraction kinetics (14) and/or arterial stiffness (17), respectively. Changes in left ventricular motion and arterial stiffness, in addition to local changes in the intrinsic stiffness properties of the CCA, make it difficult to interpret differences in CALM between individuals, and within an individual over time. In this group of healthy men, we have shown through other publications that local CCA distensibility was not altered over the training period (5, 26), possibly explaining the absence of change in CALM magnitudes with exercise training. We propose that future exercise training studies adopt an integrative measurement approach when examining longitudinal changes in CALM to aid trace interpretation.

We observed baseline differences in CALM between study cohorts, possibly indicating an effect of long term exercise training history on resting CALM magnitudes, which could reflect the different training statuses of the participants from each study. The participants in Study 2 had a history of RET, and we have previously reported baseline CCA distensibility acquired from both study cohorts (5, 26), which was greater in men

with a history of RET compared to their sedentary counterparts (5.5±1.5 *vs* 4.9±1.0 $mmHg^{-1}\times10^{-3}$; *P*=0.04). Local CCA distensibility has previously been correlated with indices of systolic and diastolic CALM (6, 29), which may account for some of this difference. Future studies may benefit from incorporating both local blood flow and left ventricular measurements into the design of chronic intervention studies in order to comprehensively assess the potential regulatory factors controlling the CALM pattern in humans (4).

Limitations: Owing to the relatively small sample size of the MICT and SIT training conditions, and the moderate range of published coefficients of variation for CALM variables (10, 36), Study 1 was likely underpowered to detect small changes in CALM over the training period. Generally, the inclusion of a non-training control group mitigates some of the variability in detecting changes over time, however, within this study, data dropout within the control group was high, which could falsely increase variability in control responses. To ensure an underpowered control group did not mask any potential training effects, all analyses were repeated excluding the control group, which did not alter our results. Whey protein was supplied to participants in Study 2, though supplementation during training would not affect baseline differences between studies. Lastly, as this sample was restricted to healthy men, our findings may not be generalizable to women, or individuals at greater cardiovascular risk.

CONCLUSION

In a novel assessment of the responses of CALM to four different exercise training programs in healthy men, we demonstrate baseline differences in systolic retrograde CALM and diastolic CALM acceleration between men with different chronic physical activity status. Systolic and diastolic CALM variables were unchanged, however, after 12 weeks of supervised endurance, resistance and sprint interval training. The responses established in this study are important for several reasons and lay the foundation for studies investigating training effects on CALM variables in individuals with, for example, elevated cardiovascular disease risk. As blood flow, blood pressure and left ventricular information may be key to interpreting possible shifts in CALM magnitude over time, we propose that future studies use an integrative measurement approach to study the regulatory factors impacting the stability and/or propensity for change in this novel arterial motion variable.

ACKNOWLEDGEMENTS

This study was supported by funding from the Natural Sciences and Engineering Research Council of Canada to S.M.P. (RGPIN-2015-04613) M.J.G. (RGPIN-2015-04632) and M.J.M. (DG 238819-13). SMP thanks the Canada Research Chairs Program for their support.

CONFLICT OF INTEREST

The authors have no conflicts of interest to declare. The results of this study are presented clearly, honestly, and without fabrication, falsification, or inappropriate data manipulation.

REFERENCES

1. **Ahlgren AR**, **Cinthio M**, **Persson HW**, **Lindström K**. Different patterns of longitudinal displacement of the common carotid artery wall in healthy humans are stable over a four-month period. *Ultrasound Med Biol* 38: 916–925, 2012.

2. **Ahlgren AR**, **Cinthio M**, **Steen S**, **Nilsson T**, **Sjoberg T**, **Persson HW**, **Lindstrom K**. Longitudinal displacement and intramural shear strain of the porcine carotid artery undergo profound changes in response to catecholamines. *Am J Physiol Heart Circ Physiol* 302: H1102–H1115, 2012.

3. **Ahlgren AR**, **Steen S**, **Segstedt S**, **Erlöv T**, **Lindström K**, **Sjöberg T**, **Persson HW**, **Ricci S**, **Tortoli P**, **Cinthio M**. Profound increase in longitudinal displacements of the porcine carotid artery wall can take place independently of wall shear stress: A continuation report. *Ultrasound Med Biol* 41: 1342–1353, 2015.

4. **Au JS**, **Ditor DS**, **MacDonald MJ**, **Stöhr EJ**. Carotid artery longitudinal wall motion is associated with local blood velocity and left ventricular rotational, but not longitudinal, mechanics. *Physiol Rep* 4: e12872, 2016.

5. **Au JS**, **Oikawa SY**, **Morton RW**, **MacDonald MJ**, **Phillips SM**. Arterial Stiffness Is Reduced Regardless of Resistance Training Load in Young Men. *Med Sci Sports Exerc* 49: 342–348, 2016.

6. **Au JS**, **Valentino SE**, **McPhee PG**, **MacDonald MJ**. Diastolic carotid artery longitudinal wall motion is sensitive to both aging and coronary artery disease status independent of arterial stiffness. *Ultrasound Med Biol* (April 20, 2017). doi: 10.1016/j.ultrasmedbio.2017.04.026.

7. **Birk GK**, **Dawson EA**, **Atkinson C**, **Haynes A**, **Cable NT**, **Thijssen DHJ**, **Green DJ**. Brachial artery adaptation to lower limb exercise training: role of shear stress. *J Appl Physiol* 112: 1653–1658, 2012.

8. **Black JM**, **Stöhr EJ**, **Stone K**, **Pugh CJA**, **Stembridge M**, **Shave R**, **Esformes**

JI. The effect of an acute bout of resistance exercise on carotid artery strain and strain rate. *Physiol Rep* 4: e12959, 2016.

9. **Cinthio M**, **Ahlgren AR**, **Bergkvist J**, **Jansson T**, **Persson HW**, **Lindström K**. Longitudinal movements and resulting shear strain of the arterial wall. *Am J Physiol Heart Circ Physiol* 291: H394–H402, 2006.

10. **Cinthio M**, **Ahlgren AR**. Intra-observer variability of longitudinal displacement and intramural shear strain measurements of the arterial wall using ultrasound noninvasively *in vivo*. *Ultrasound Med Biol* 36: 697–704, 2010.

11. **Gillen JB**, **Martin BJ**, **MacInnis MJ**, **Skelly LE**, **Tarnopolsky MA**, **Gibala MJ**. Twelve Weeks of Sprint Interval Training Improves Indices of Cardiometabolic Health Similar to Traditional Endurance Training despite a Five-Fold Lower Exercise Volume and Time Commitment. *PLoS ONE* 11: e0154075, 2016.

12. **Hayashi K**, **Sugawara J**, **Komine H**, **Maeda S**, **Yokoi T**. Effects of aerobic exercise training on the stiffness of central and peripheral arteries in middle-aged sedentary men. *Jpn J Physiol* 55: 235–239, 2005.

13. **Huang C**, **Wang J**, **Deng S**, **She Q**, **Wu L**. The effects of aerobic endurance exercise on pulse wave velocity and intima media thickness in adults: A systematic review and meta-analysis. *Scand J Med Sci Sports* 26: 478–487, 2016.

14. **Kilner PJ**, **Yang G-Z**, **Wilkes AJ**, **Mohiaddin RH**, **Firmin DN**, **Yacoub MH**. Asymmetric redirection of flow through the heart. *Nature* 404: 759–761, 2000.

15. **Lorenz MW**, **Markus HS**, **Bots ML**, **Rosvall M**, **Sitzer M**. Prediction of Clinical Cardiovascular Events With Carotid Intima-Media Thickness: A Systematic Review and Meta-Analysis. *Circulation* 115: 459–467, 2007.

16. **MacDougall JD**, **Tuxen D**, **Sale DG**, **Moroz JR**, **R SJ**. Arterial blood pressure response to heavy resistance exercise. *J Appl Physiol* 58: 785–790, 1985.

17. **Mitchell GF**, **Parise H**, **Benjamin EJ**, **Larson MG**, **Keyes MJ**, **Vita JA**, **Vasan RS**, **Levy D**. Changes in Arterial Stiffness and Wave Reflection With Advancing Age in Healthy Men and Women: The Framingham Heart Study. *Hypertension* 43: 1239–1245, 2004.

18. **Miyachi M**, **Kawano H**, **Sugawara J**, **Takahashi K**, **Hayashi K**, **Yamazaki K**, **Tabata I**, **Tanaka H**. Unfavorable Effects of Resistance Training on Central Arterial Compliance: A Randomized Intervention Study. *Circulation* 110: 2858–2863, 2004.

19. **Miyachi M**. Effects of resistance training on arterial stiffness: a meta-analysis. *Brit*

J Sport Med 47: 393–396, 2013.

20. **Morton RW**, **Oikawa SY**, **Wavell CG**, **Mazara N**, **McGlory C**, **Quadrilatero J**, **Baechler BL**, **Baker SK**, **Phillips SM**. Neither load nor systemic hormones determine resistance training-mediated hypertrophy or strength gains in resistance-trained young men. *J Appl Physiol* 121: 129–138, 2016.

21. **Persson M**, **Ahlgren AR**, **Jansson T**, **Eriksson A**, **Persson HW**, **Lindström K**. A new non-invasive ultrasonic method for simultaneous measurements of longitudinal and radial arterial wall movements: first in vivo trial. *Clin Physiol Funct Imaging* 23: 247–251, 2003.

22. **Rakobowchuk M**, **Stuckey MI**, **Millar PJ**, **Gurr L**, **MacDonald MJ**. Effect of acute sprint interval exercise on central and peripheral artery distensibility in young healthy males. *Eur J Appl Physiol* 105: 787–795, 2009.

23. **Rakobowchuk M**, **Tanguay S**, **Burgomaster KA**, **Howarth KR**, **Gibala MJ**, **MacDonald MJ**. Sprint interval and traditional endurance training induce similar improvements in peripheral arterial stiffness and flow-mediated dilation in healthy humans. *Am J Physiol Regul Integr Comp Physiol* 295: R236–R242, 2008.

24. **Rowley NJ**, **Dawson EA**, **Birk GK**, **Cable NT**, **George KP**, **Whyte G**, **Thijssen DHJ**, **Green DJ**. Exercise and Arterial Adaptation in Humans: Uncoupling Localised and Systemic Effects. *J Appl Physiol* 110: 1190–1195, 2011.

25. **Schoenfeld BJ**, **Peterson MD**, **Ogborn D**, **Contreras B**, **Sonmez GT**. Effects of Low- Versus High-Load Resistance Training on Muscle Strength and Hypertrophy in Well-Trained Men. *J Strength Cond Res* 29: 2954–2963, 2015.

26. **Shenouda N**, **Gillen JB**, **Gibala MJ**, **MacDonald MJ**. Changes in brachial artery endothelial function and resting diameter with moderate-intensity continuous but not sprint interval training in sedentary men. *J Appl Physiol* (May 25, 2017). doi: 10.1152/japplphysiol.00058.2017.

27. **Svedlund S**, **Eklund C**, **Robertsson P**, **Lomsky M**, **Gan LM**. Carotid Artery Longitudinal Displacement Predicts 1-Year Cardiovascular Outcome in Patients With Suspected Coronary Artery Disease. *Arterioscler Throm Vas Biol* 31: 1668–1674, 2011.

28. **Svedlund S**, **Gan L-M**. Longitudinal common carotid artery wall motion is associated with plaque burden in man and mouse. *Atherosclerosis* 217: 120–124, 2011.

29. **Taivainen SH**, **Yli-Ollila H**, **Juonala M**, **Kähönen M**, **Raitakari OT**, **Laitinen TM**, **Laitinen TP**. Interrelationships between indices of longitudinal movement of

the common carotid artery wall and the conventional measures of subclinical arteriosclerosis. *Clin Physiol Funct Imaging* 37: 305–313, 2017.

30. **Tanaka H**, **Dinenno FA**, **Monahan KD**, **Clevenger CM**, **DeSouza CA**, **Seals DR**. Aging, Habitual Exercise, and Dynamic Arterial Compliance. *Circulation* 102: 1270–1275, 2000.

31. **Tat J**, **Au JS**, **Keir PJ**, **MacDonald MJ**. Reduced common carotid artery longitudinal wall motion and intramural shear strain in individuals with elevated cardiovascular disease risk using speckle tracking. *Clin Physiol Funct Imaging* 37: 106–116, 2017.

32. **Tat J**, **Psaromiligkos IN**, **Daskalopoulou SS**. Carotid atherosclerotic plaque alters the direction of longitudinal motion in the artery wall. *Ultrasound Med Biol* 42: 2114–2122, 2016.

33. **Thijssen DHJ**, **Cable NT**, **Green DJ**. Impact of exercise training on arterial wall thickness in humans. *Clin Sci* 122: 311–322, 2012.

34. **Tomoto T**, **Sugawara J**, **Hirasawa A**, **Imai T**, **Maeda S**, **Ogoh S**. Impact of short-term training camp on arterial stiffness in endurance runners. *J Physiol Sci* 65: 445–449, 2015.

35. **Weiner RB**, **DeLuca JR**, **Wang F**, **Lin J**, **Wasfy MM**, **Berkstresser B**, **Stöhr E**, **Shave R**, **Lewis GD**, **Hutter AM Jr**, **Picard MH**, **Baggish AL**. Exercise induced left ventricular remodeling among competitive athletes: A phasic phenomenon. *Circ Cardiovasc Imaging* 8: e003651, 2015.

36. **Yli-Ollila H**, **Laitinen T**, **Weckström M**, **Laitinen TM**. Axial and radial waveforms in common carotid artery: An advanced method for studying arterial elastic properties in ultrasound imaging. *Ultrasound Med Biol* 39: 1168–1177, 2013.

37. **Yli-Ollila H**, **Laitinen T**, **Weckström M**, **Laitinen TM**. New indices of arterial stiffness measured from longitudinal motion of common carotid artery in relation to reference methods, a pilot study. *Clin Physiol Funct Imaging* 36: 376–388, 2015.

38. **Yli-Ollila H**, **Tarvainen MP**, **Laitinen TP**, **Laitinen TM**. Principal component analysis of the longitudinal carotid wall motion in association with vascular stiffness: a pilot study. *Ultrasound Med Biol* 42: 2873–2886, 2016.

39. **Yli-Ollila H**, **Tarvainen MP**, **Laitinen TP**, **Laitinen TM**. Transfer function analysis of the longitudinal motion of the common carotid artery wall. *Front Physiol* 7, 2016.

40. **Zahnd G**, **Balocco S**, **Sérusclat A**, **Moulin P**, **Orkisz M**, **Vray D**. Progressive attenuation of the longitudinal kinetics in the common carotid artery: Preliminary in vivo assessment. *Ultrasound Med Biol* 41: 339–345, 2014.

41. **Zahnd G**, **Vray D**, **Sérusclat A**, **Alibay D**, **Bartold M**, **Brown A**, **Durand M**, **Jamieson LM**, **Kapellas K**, **Maple-Brown LJ**, **O'Dea K**, **Moulin P**, **Celermajer DS**, **Skilton MR**. Longitudinal displacement of the carotid wall and cardiovascular risk factors: Associations with aging, adiposity, blood pressure and periodontal disease independent of cross-sectional distensibility and intima-media thickness. *Ultrasound Med Biol* 38: 1705–1715, 2012.

CHAPTER 6:

GENERAL DISCUSSION

6.1 Discussion Overview

The study of carotid artery longitudinal wall motion (CALM) is a topic of growing interest in vascular physiology with many unanswered questions. While the biphasic motion trace has been well described (12, 48), there have been few studies to probe potential health applications for the non-invasive measurement of CALM. Two main limitations of the previous investigations have been the lack of experimental data from human models to study the regulation of wall motion, and the lack of comprehensive examinations of potential confounders that may impede interpretation of CALM information for cardiovascular disease (CVD) risk prediction and assessment. These factors must be explored before meaningful conclusions can be drawn from longitudinal wall motion data obtained from individuals across a wide range of vascular health.

Therefore, the broad aims of this thesis were to examine the regulatory control of CALM in humans, to evaluate the relationship between CALM and established measures of arterial stiffness, and to assess the use of CALM as a novel vascular variable to monitor changes in arterial health. Through a series of studies, we have provided preliminary experimental support for a structural ventricular-vascular coupling theory (Chapters 2 and 4), which informed the use of diastolic CALM variables to infer vascular health information in both cross-sectional (Chapter 3) and prospective intervention (Chapter 5) studies in humans. This broad discussion will focus on the major contributions of this work by addressing the challenges in studying CALM, the limitations to the measurement and interpretation of 2D arterial wall motion traces, as

well as the necessary future directions this field must take to further advance the study of CALM as a novel indicator of arterial health.

6.2 Individual variability in CALM patterns: Segmentation method

The fundamental limitation to interpreting the CALM pattern in humans has been the large inter-individual variability in healthy adults. These observations were best described by Yli-Ollila *et al*. (2013), who reported three basic patterns in a small sample of healthy adults. The three basic patterns originally identified were: primarily anterograde displacement, primarily retrograde displacement, and oscillating anterograde-retrograde displacement (48). Our findings in Chapter 3 largely support these original observations, yet extended the work by characterizing modest variability in systolic anterograde and systolic retrograde CALM displacements within an otherwise homogenous group of 161 healthy younger adults. The identified inter-individual variability in wall displacement makes it difficult to characterize and interpret differences in CALM patterns between individuals. Furthermore, the standard peaks and inflection points in the traditional radial plane distension trace do not correlate to events in any of the three typical CALM patterns. While some research groups have simplified CALM variables into maximal displacement over a cardiac cycle (16, 28, 53, 54), this method disregards important features such as the nuanced information available through more detailed assessments of the pattern and direction of the CALM trace.

To address individual variability, we (5, 38) and others (1, 12, 13, 25, 26) have attempted to segment the complex CALM trace into basic elements based on the

assessment of timing and magnitude of local maxima and minima in the systolic and diastolic phases of the trace. In Chapter 2, we present physiological data to support the segmentation process and suggest that discrete physiological events may be regulatory determinants of the CALM pattern, which we described through a structural ventricular-vascular coupling theory (5). Specifically, the timing of CALM event data provides correlational evidence that the timing of the systolic anterograde component is related to the forward blood velocity wave, the timing of the systolic retrograde component is related to left ventricular (LV) rotation, and that some variables representing the diastolic component may be more representative of intrinsic wall stiffness due to the fact that it has less overlap with the active systolic events. These relationships between local blood velocity and LV events have previously been theorized to explain some CALM pattern observations (12, 48), although the study in Chapter 2 was the first to support the theory with human data. While the cross-sectional correlative nature of our study limited our ability to make conclusions related to a direct coupling effect, the timing data did support the segmentation of the CALM pattern into a dual-function system, where anterograde and retrograde components can be interpreted based on physiological events (Chapter 2, Figure 5). This method is similar to the one employed in arterial pulse wave analysis where forward and backward propagating waves summate to form the central pressure waveform, which explains inter-individual variability across different ages and health statuses (20). We were able to apply this segmentation process to a large sample of adults in Chapter 3, and our findings indicated this method generated an assessment approach that has sensitivity to older age independent of traditional measures of arterial stiffness.

While the aforementioned segmentation method has foundations in physiological events and informs understanding of regulatory control of CALM, there are still limitations to its use. CALM has been demonstrated to attenuate along the length of the common carotid artery (CCA) even within a 3 cm ultrasound window (52), and has been observed to be smaller in magnitude in taller individuals when imaging is standardized to the carotid bifurcation (5, 49). Therefore, while CALM segmentation provides an approach that can be used to standardize measurements within different movement patterns, the anatomical location of image acquisition is a potential confounder for interpretation of any variables representing the magnitude of CALM events. Recently, other methods have been proposed to account for image location and displacement attenuation including an attenuation coefficient (52), radial-axial excursion (36, 49) and polynomial curve fitting (36, 49). However, these methods have limited physiological rationale and will require careful consideration of regulatory control of the CALM pattern before describing any characteristics of vascular health.

6.3 Regulation of CALM and systolic confounders

Previous studies have postulated that CALM may be influenced by the forward blood velocity wave, blood pressure, arterial stiffness and LV motion (12, 48), although few studies have investigated these factors through experimental design. In the only published experimental reports, Ahlgren *et al*. used a porcine model in a series of studies to examine the effects of catecholamines on CALM (2-4). These authors observed β_2-adrenoreceptor activation reduced CALM magnitude, while α-adrenoreceptor activation increased

CALM magnitude (2), both independent of arterial wall shear stress (4). While intriguing, subtle differences between pig and human cardiovascular anatomy raise the need for replication of these investigations in human models (15, 40).

We addressed these issues in Chapter 4 through a series of human model acute interventional studies aimed at examining the regulation of CALM in the context of our structural ventricular-vascular coupling theory outlined in Chapter 2. We found a modest relationship between pressure-related changes in LV basal rotation and systolic retrograde CALM, without relationships between arterial wall shear stress and systolic anterograde CALM. In contrast to the studies conducted by Ahgren *et al*. (2), we were unable to elicit discrete mean changes in CALM with a pressor stimulus. One factor determining these differences might be that we were only able to increase pulse pressure 20-30% with non-invasive methods, whereas Ahlgren *et al*. were able to elicit a 60% increase in pulse pressure with catecholamine infusion. Consideration should also be given to other systemic factors that are affected by a 60% increase in pulse pressure, such as the direct effect of sympathetic activation on vascular smooth muscle constriction (11), and afterload-related changes in LV mechanics (34). Given that arterial distension is highly regulated by pulse pressure (9), it is somewhat surprising that CALM is not similarly affected by the modest increase in pulse pressure we achieved. It may be that with increases in pulse pressure and radial distension, the orientation of elastin and collagen fibres in the vascular wall, which are aligned circumferentially to accommodate vessel distention with high intraluminal pressures (29, 47) do not translate to changes in CALM. The arterial wall is highly resistant to tearing along the axial plane (29), suggesting there

are few longitudinally-oriented fibres that would naturally slide along the length of the wall during arterial distension; though this theory has not previously been tested. The blood pressure-dependency of CALM should be further investigated, as traditional measures of radial-plane arterial stiffness are all dependent upon blood pressure, to some degree (22).

In our structural ventricular-vascular coupling theory, we hypothesized that the LV was a primary regulator of retrograde CALM in humans. This idea stemmed from observations of motion attenuation along the length of the CCA (52) and reports that CALM decreased with increasing participant height (49), indicating a loss of kinetic energy distal to the heart. Given that the aortic root descends towards the apex in the same plane as CALM during systole (32), we postulated that LV motion would be a variable of interest in controlling the CALM pattern in the proximal vasculature. While the model we proposed in Chapter 2 (Figure 5) places emphasis on the role of LV rotation in retrograde CALM, our experimental data do not fully support a direct influence of LV motion on CALM. In Chapter 4, we were able to simulate isolated increases in LV apical rotation and basal rotation, but were unable to detect companion changes in systolic retrograde CALM using our within-subjects design. However, when pooling all responses together, we observed an effect of LV basal rotation on systolic retrograde CALM, consistent with our coupling theory. Rather than a direct control mechanism, LV rotation may have a moderating effect on systolic retrograde CALM, which may be driven by another variable. Pulse pressure has been suggested to account for some variability in the CALM pattern (2, 4, 50, 51), although elevations in pressure are inherently linked to other

systemic changes, including that of LV contractility, compression of the intima-media complex, and vascular smooth muscle constriction through sympathetic activation. Furthermore, we did not observe any correlations between pulse pressure and any CALM variable in our acute intervention studies. The exact role of LV motion in the regulation of CALM needs to be further developed through tightly controlled experimental designs.

We theorized the direct role of shear stress on the vascular wall in Chapter 2 through observations of event timing; however, this relationship is not supported by experimental data. In both Chapter 2 and Chapter 4, we were unable to observe correlations between carotid shear rate and systolic anterograde CALM, similar to other groups (4), even when CCA shear rate was reduced through nitroglycerin administration. This lack of experimental support for links between shear stress and CALM may be explained by the dual-system model proposed in Chapter 2, where there are competing influences from both the forward blood velocity wave and the onset of LV rotation on CALM during the early systolic period. With observational designs, it may be difficult to separate these opposing factors, and therefore describe the independent effects of shear rate on systolic anterograde CALM in humans. This issue, as well as the issues in interpreting the direct impact of LV rotation, necessitates the use of more tightly controlled models to isolate the local shear environment from a structural coupling effect. It may be possible to investigate this in humans with abnormal cardiovascular physiology, such as in cases of premature ventricular contractions (LV contraction before complete filling) (27) or patients with LV assist devices (continuous blood flow without LV

contraction) (19), although the prevalence of comorbidities in these populations would be a major limitation to these human models.

6.4 Does CALM reflect arterial stiffness properties?

The measurement of CALM may offer a feasible tool to study arterial properties and cardiovascular health in clinical settings, as it only requires non-invasive ultrasound with minimal acquisition time, minimal operator skill, and relatively automated analyses. In fact, the driving interest behind CALM has been the potential for a technically feasible novel index of arterial health that provides unique information for arterial stiffness and CVD risk prediction. This goal has been met with mild success in previous reports. Most notably, small maximum CALM displacements predicted the 1-year occurrence of a major adverse cardiovascular event, controlled for intima-media thickness (IMT) and radial strain, in patients with suspect coronary artery disease (35). Maximum CALM displacement has also been related to age and pulse pressure independent of local CCA distensibility in adults with periodontal disease (54). However, as mentioned above, maximum CALM displacement disregards the pattern and direction of motion, and may not be physiologically relevant to arterial stiffness information. Currently, there is only one large cross-sectional report of systolic anterograde and retrograde CALM, of which retrograde CALM was weakly correlated to cfPWV and CCA distensibility in a sample of middle-aged healthy adults (36). However, given our findings from Chapter 2 and Chapter 4, systolic CALM variables may be confounded to some degree by other factors, and may not be optimal indices of arterial properties.

To address ambiguity in which CALM variables hold promise as indicators of vascular health, we designed the study in Chapter 3 to measure both systolic and diastolic CALM in a large sample of healthy adults. While there were independent associations between systolic CALM and age when controlling for cfPWV and CCA distensibility, there were clear advantages to using diastolic CALM displacement, velocity and acceleration in comparison to systolic CALM variables. In addition, both simple correlations and multivariate regression models for the associations between diastolic CALM variables and age were superior in strength compared to previous reports (36, 54). These findings are in line with our ventricular-vascular coupling theory in Chapter 2, where we hypothesized that diastolic CALM would be relatively free of systemic confounders, and may better represent intrinsic wall properties than systolic CALM. It is likely that the anterograde CALM displacement commonly observed during early diastole is partly attributable to a passive return to resting wall tension and sometimes results in an overshoot of the reference position, indicating a passive elastic component in the longitudinal plane of the arterial wall. Compared to traditional measures of arterial stiffness (e.g., cfPWV and CCA distensibility), which are based on indexes related to systolic distension, diastolic indices of passive elements might contribute additional value to describe arterial wall health without confounding adjustments for distending pressure.

While the results of the study described in Chapter 3 demonstrate that several diastolic CALM variables are sensitive indices of aging and coronary artery disease status, these outcomes are still limited in part by systolic CALM displacement. Discrete assessment of diastolic displacement of the arterial wall is not completely independent

from the preceding retrograde ‘stretch’ that occurs during systole, and therefore may be a poor method of standardizing motion among vessels of different stiffness properties. The measurement of diastolic velocity and acceleration may better describe the passive return to resting longitudinal tension and may be less dependent on the preceding magnitude of systolic motion. Despite these limitations, there may still be value in assessing diastolic displacement, as the arterial wall overshoots the reference position in late diastole, resulting in unique displacement and velocity information compared to the systolic phase. This assertion is likely expressed in the greater model strength of diastolic CALM displacement compared to systolic retrograde CALM displacement for predicting age in Chapter 3.

6.5 Sensitivity of CALM to change with exercise training interventions

With the data to support the use of diastolic CALM variables as potential indicators of arterial health status, we were then interested in whether these variables could be impacted by a health intervention in humans. Chronic exercise training is known to improve vascular stiffness not only in individuals with poor vascular health (18), but also in otherwise healthy adults (6, 14, 30, 31), thereby supporting our hypothesis that CALM may by similarly affected by exercise training. In Chapter 5 we investigated whether diastolic CALM variables would be similarly improved by four types of exercise training in healthy men. Given that CALM displacement magnitudes are smaller with older age and disease status, we hypothesized that CALM magnitudes would increase with exercise training as an indicator of vascular health improvement. While these interventions were

conducted with high quality methods, including age- and activity-matched control groups, we did not observe any changes in systolic or diastolic CALM variables over the 12 week training period for any training program examined.

The potential reasons for the absence of observations of any exercise effects are discussed in Chapter 5, including potential ceiling effects, lack of parallel changes in local CCA distensibility (6, 31), and variability in measurement; however, the most interesting aspect of these studies was the baseline difference in systolic retrograde CALM and diastolic CALM acceleration between resistance-trained men and their sedentary counterparts. Exercise is a potent stimulus for physiological changes driven by pressure-, metabolic-, and energy-dependent perturbations during a bout of exercise. When performed repeatedly over time, these perturbations often result in positive changes to vascular health (17, 18). Even so, not all health indices improve with exercise training. For example, carotid IMT is difficult to change with exercise training in healthy populations (37, 41), and is better able to delineate differences in cardiovascular risk when examined discretely (42) rather than with repeated measurements over time (23). The stability of carotid IMT with exercise training is likely related to the structural mechanisms that change wall thickness over time, such as collagen:elastin ratio and vascular smooth muscle cell hypertrophy. A similar response may exist for CALM variables, though the structural and regulatory determinants of longitudinal wall motion are yet unknown. While short-term (e.g., 12-weeks) exercise training may not have been sufficient to impact CALM, there may be an effect of long-term (e.g., 2-years) exercise training, as seen through baseline differences between men with and without history of

resistance exercise training. Resistance exercise is a potent cardiovascular stimulus characterized by cyclic elevations in blood pressure (24) which challenge LV output (45) and arterial tissue mechanics (10). The CALM pattern in resistance-trained men may have been chronically influenced by altered local wall structural properties or LV morphology as a result of training history, although we were unable to compare these factors between participant groups. In future studies, it would be interesting to extend these incidental findings to a full observational design to examine the impact of long-term cardiac and hemodynamic changes with resistance exercise training on the CALM pattern in healthy adults.

6.6 Future Directions: Keep CALM and Carry On

The studies presented in this dissertation represent the first experimental investigations of several CALM variables and regulatory factors in humans. As such, there are numerous basic physiological studies that should be conducted in the future to further probe the regulation and control of the CALM pattern across the lifespan as well as with the development of atherosclerosis and arteriosclerosis. These future study designs should use the scientific framework set by research in the measurement of arterial stiffness as an investigation model, carefully studying the role of neural, hormonal, mechanical and anatomical factors in the regulation of CALM in both human and animal models.

For example, while there are reports on the relationship between pulse pressure and CALM (2, 50, 51), a mechanical link between the pressure waveform and CALM has not been proposed. The relationship between blood pressure and radial-plane stiffness has

been extensively studied, with an established two-phase stress-strain relationship involving offloading tension from elastin to collagen elements (44), as well as support for pressure- *vs*. structural-dependent changes in arterial stiffness through vasoactive drug experimentation (33). It is currently unknown whether longitudinal displacement of the arterial wall is similarly affected by a two-phase stress-strain relationship, or if it is pressure-dependent. Our results from Chapter 4 challenge the notion of any dependence, although more tightly controlled studies using advanced methodology (e.g., vasoactive drugs, lower-body negative/positive pressure, saline-loading) and greater magnitude changes in pulse pressure are needed the provide further evidence.

Although orientations of extracellular matrix proteins have been investigated in other contexts, there have been no focused studies of the effect of fibre orientation on longitudinal wall displacement. Our observations indicate CALM is controlled by factors beyond that of fibre orientation during vessel distension, though this has been neither confirmed nor refuted in *ex vivo* models. A methodological limitation to *ex vivo* investigation is longitudinal retraction of excised arteries (46), which makes it difficult to simulate *in vivo* longitudinal wall displacements.

The focus of this thesis was on displacement of the intima-media complex, but it is also possible to measure adventitial motion as well as intramural shear strain between vascular wall layers. While we did not report any relationships between intramural shear strain and traditional measures of arterial stiffness in Chapter 3, previous studies indicate that shear strain may be a valuable measure of arterial wall structure (2, 12). However, methodological and theoretical concerns limit the utility of a single shear strain value for

use in clinical comparisons. It is well reported that CALM patterns can be either anterograde-oriented or retrograde-oriented, which would result in either positive or negative shear strain values, respectively. Given that the direction of CALM may be controlled by different physiological processes, it may not be possible to compare positive and negative shear strain values. Nonetheless, a measure of intramural forces could be a valuable indicator of wall stress, and has not been thoroughly investigated in tissue mechanics models. Future studies should continue to evaluate the physiological relevance of intramural shear strain and how it might relate to long-term remodelling of the vascular wall with age and atherosclerosis.

Of clinical relevance, there are no data indicating when changes in CALM magnitude occur in the development of atherosclerosis and arteriosclerosis in natural aging. It is generally accepted that changes in arterial stiffness precede development of cardiovascular disease by enabling conditions where vascular disease can flourish (21). It would be of interest to include measures of CALM in large prospective population studies to investigate the time course of changes in CALM direction and magnitude previously observed in cross-sectional studies (7, 36, 39). CALM can be easily assessed from ultrasound cineloops at the CCA bifurcation, and therefore may be a candidate for retrospective analysis of population databases, given the appropriate resources.

Finally, the role of exercise training in modifying the pattern and magnitude of CALM is left undetermined from our studies. Building upon our findings in Chapter 5, it would be of value to examine the effects of exercise training on CALM in a population with elevated arterial stiffness. Our findings were likely limited by a ceiling-effect for

improvements in vascular health, as the study participants began exercise training with high levels of baseline health with normal vascular function. Assessing the sensitivity of CALM to exercise training or other lifestyle interventions in populations at risk for CVD would provide stronger support for the measurement of diastolic CALM alongside traditional measures of arterial stiffness.

6.7 Conclusions

Throughout this dissertation, there have been numerous instances where we state that CALM is a 'novel' variable of arterial health, a phrase that is increasingly being used in scientific literature to exaggerate results in research articles (8, 43). However, given the dearth of literature on CALM and the increasing interest in developing sensitive and feasible prediction tools to identify individuals at risk for CVD, our results make important contributions to the field of vascular research and have the potential to re-shape how we study mechanical behaviour of the arterial wall. We have provided standardized methods and recommendations to study CALM in humans, as well as evidence to support the physiological determinants of CALM as part of a structural ventricular-vascular coupling effect. We identified diastolic CALM variables as outcomes of interest due to their independent relationship with age and theoretical separation from the forward blood velocity wave and LV rotation, and suggest the inclusion of assessment of diastolic CALM variables in future studies as a measure of vascular health. Finally, in the first intervention study to test the sensitivity of CALM to lifestyle changes, we did not find any changes in diastolic CALM after 12 weeks of four different modes of exercise

training in healthy men, but did observe increases in systolic retrograde CALM displacement and diastolic CALM acceleration in men with a history of resistance exercise training. The normative values we establish both for the measurement CALM across the lifespan as well as for the expected variability in exercise training responses will be valuable for future studies investigating changes in CALM with health interventions in populations at risk for CVD. Through this series of studies, our novel findings suggest that CALM represents a complicated regulatory system related to both arterial wall structure and ventricular-vascular coupling, which has clinical value to complement traditional measures of arterial stiffness in humans.

6.8 REFERENCES

1. **Ahlgren AR**, **Cinthio M**, **Persson HW**, **Lindström K**. Different patterns of longitudinal displacement of the common carotid artery wall in healthy humans are stable over a four-month period. *Ultrasound Med Biol* 38: 916–925, 2012.

2. **Ahlgren AR**, **Cinthio M**, **Steen S**, **Nilsson T**, **Sjoberg T**, **Persson HW**, **Lindstrom K**. Longitudinal displacement and intramural shear strain of the porcine carotid artery undergo profound changes in response to catecholamines. *Am J Physiol Heart Circ Physiol* 302: H1102–H1115, 2012.

3. **Ahlgren AR**, **Cinthio M**, **Steen S**, **Persson HW**, **Sjöberg T**, **Lindström K**. Effects of adrenaline on longitudinal arterial wall movements and resulting intramural shear strain: a first report. *Clin Physiol Funct Imaging* 29: 353–359, 2009.

4. **Ahlgren AR**, **Steen S**, **Segstedt S**, **Erlöv T**, **Lindström K**, **Sjöberg T**, **Persson HW**, **Ricci S**, **Tortoli P**, **Cinthio M**. Profound increase in longitudinal displacements of the porcine carotid artery wall can take place independently of wall shear stress: A continuation report. *Ultrasound Med Biol* 41: 1342–1353, 2015.

5. **Au JS**, **Ditor DS**, **MacDonald MJ**, **Stöhr EJ**. Carotid artery longitudinal wall motion is associated with local blood velocity and left ventricular rotational, but not longitudinal, mechanics. *Physiol Rep* 4: e12872, 2016.

6. **Au JS**, **Oikawa SY**, **Morton RW**, **MacDonald MJ**, **Phillips SM**. Arterial Stiffness Is Reduced Regardless of Resistance Training Load in Young Men. *Med Sci Sports Exerc* 49: 342–348, 2016.

7. **Au JS**, **Valentino SE**, **McPhee PG**, **MacDonald MJ**. Diastolic carotid artery longitudinal wall motion is sensitive to both aging and coronary artery disease status independent of arterial stiffness. *Ultrasound Med Biol* (April 20, 2017). doi: 10.1016/j.ultrasmedbio.2017.04.026.

8. **Ball P**. "Novel, amazing, innovative": positive words on the rise in science papers. *Nature*: 2015.

9. **Benetos A**, **Laurent S**, **Hoeks AP**, **Boutouyrie PH**, **Safar ME**. Arterial Alterations With Agingand High Blood Pressure: A noninvasive study of carotid and femoral arteries. *Arteriosclerosis and Thrombosis* 13: 90–97, 1993.

10. **Black JM**, **Stöhr EJ**, **Stone K**, **Pugh CJA**, **Stembridge M**, **Shave R**, **Esformes JI**. The effect of an acute bout of resistance exercise on carotid artery strain and strain rate. *Physiol Rep* 4: e12959, 2016.

11. **Boutouyrie P**, **Lacolley P**, **Girerd X**, **Beck L**, **Safar M**, **Laurent S**. Sympathetic activation decreases medium-sized arterial compliance in humans. *Am J Physiol Heart Circ Physiol* 267: H1368–H1376, 1994.

12. **Cinthio M**, **Ahlgren AR**, **Bergkvist J**, **Jansson T**, **Persson HW**, **Lindström K**. Longitudinal movements and resulting shear strain of the arterial wall. *Am J Physiol Heart Circ Physiol* 291: H394–H402, 2006.

13. **Cinthio M**, **Ahlgren AR**. Intra-observer variability of longitudinal displacement and intramural shear strain measurements of the arterial wall using ultrasound noninvasively *in vivo*. *Ultrasound Med Biol* 36: 697–704, 2010.

14. **Ciolac EG**, **Bocchi EA**, **Bortolotto LA**, **Carvalho VO**, **Greve JM**, **Guimarães GV**. Effects of high-intensity aerobic interval training vs. moderate exercise on hemodynamic, metabolic and neuro-humoral abnormalities of young normotensive women at high familial risk for hypertension. *Hypertens Res* 33: 836–843, 2010.

15. **Crick SJ**, **Sheppard MN**, **Ho SY**, **Lior G**, **Anderson RH**. Anatomy of the pig heart: comparisons with normal human cardiac structure. *J Anat* 193: 105–119, 1998.

16. **Golemati S**, **Sassano A**, **Lever MJ**, **Bharath AA**, **Dhanjil S**, **Nicolaides AN**. Carotid artery wall motion estimated from b-mode ultrasound using region tracking and block matching. *Ultrasound Med Biol* 29: 387–399, 2003.

17. **Green DJ**. Exercise training as vascular medicine: Direct impacts on the vasculature in humans. *Exerc Sport Sci Rev* 37: 196–202, 2009.

18. **Huang C**, **Wang J**, **Deng S**, **She Q**, **Wu L**. The effects of aerobic endurance exercise on pulse wave velocity and intima media thickness in adults: A systematic review and meta-analysis. *Scand J Med Sci Sports* 26: 478–487, 2016.

19. **Kakino T**, **Saku K**, **Sakamoto T**, **Sakamoto K**, **Akashi T**, **Ikeda M**, **Ide T**, **Kishi T**, **Tsutsui H**, **Sunagawa K**. Prediction of Hemodynamics under Left Ventricular Assist Device. *Am J Physiol Heart Circ Physiol* 312: ajpheart.00617.2016, 2016.

20. **Kelly R**, **Hayward C**, **Avolio A**, **O'Rourke M**. Noninvasive determination of age-related changes in the human arterial pulse. *Circulation* 80: 1652–1659, 1989.

21. **Lakatta EG**, **Levy D**. Arterial and Cardiac Aging: Major Shareholders in Cardiovascular Disease Enterprises: Part I: Aging Arteries: A "Set Up" for Vascular Disease. *Circulation* 107: 139–146, 2003.

22. **Lim J**, **Pearman M**, **Park W**, **Alkatan M**, **Machin DR**, **Tanaka H**. Impact of Blood Pressure Perturbations on Arterial Stiffness. *Am J Physiol Regul Integr*

Comp Physiol 309: 1540-1545, 2015.

23. **Lorenz MW**, **Polak JF**, **Kavousi M**, **Mathiesen EB**, **Völzke H**, **Tuomainen T-P**, **Sander D**, **Plichart M**, **Catapano AL**, **Robertson CM**, **Kiechl S**, **Rundek T**, **Desvarieux M**, **Lind L**, **Schmid C**, **DasMahapatra P**, **Gao L**, **Ziegelbauer K**, **Bots ML**, **Thompson SG**, **Group OBOTP-IS**. Carotid intima-media thickness progression to predict cardiovascular events in the general population (the PROG-IMT collaborative project): a meta-analysis of individual participant data. *Lancet* 379: 2053–2062, 2012.

24. **MacDougall JD**, **Tuxen D**, **Sale DG**, **Moroz JR**, **R SJ**. Arterial blood pressure response to heavy resistance exercise. *J Appl Physiol* 58: 785–790, 1985.

25. **Nilsson T**, **Ahlgren AR**, **Jansson T**, **Persson HW**, **Nilsson J**, **Lindström K**, **Cinthio M**. A method to measure shear strain with high spatial resolution in the arterial wall non-invasively *in vivo* by tracking zero-crossings of B-mode intensity gradients. *Proc IEEE Ultrason Symp* 1: 481-494, 2010.

26. **Nilsson T**, **Ricci S**, **Ahlgren AR**, **Jansson T**, **Lindström K**, **Tortoli P**, **Persson HW**, **Cinthio M**. Methods for measurements of the longitudinal movement and the shear-induced longitudinal elastic modulus of the arterial wall. *Proc IEEE Ultrason Symp* 1: 317-320, 2009.

27. **Niwano S**, **Wakisaka Y**, **Niwano H**, **Fukaya H**, **Kurokawa S**, **Kiryu M**, **Hatakeyama Y**, **Izumi T**. Prognostic significance of frequent premature ventricular contractions originating from the ventricular outflow tract in patients with normal left ventricular function. *Heart* 95: 1230–1237, 2009.

28. **Persson M**, **Ahlgren AR**, **Eriksson A**, **Jansson T**, **Persson HW**, **Lindström K**. Non-invasive measurement of arterial longitudinal movement. *Proc IEEE Ultrason Symp* 2: 1783–1786, 2002.

29. **Purslow PP**. Positional variations in fracture toughness, stiffness and strength of descending thoracic pig aorta. *J Biomechanics* 16: 947–953, 1983.

30. **Rakobowchuk M**, **Tanguay S**, **Burgomaster KA**, **Howarth KR**, **Gibala MJ**, **MacDonald MJ**. Sprint interval and traditional endurance training induce similar improvements in peripheral arterial stiffness and flow-mediated dilation in healthy humans. *Am J Physiol Regul Integr Comp Physiol* 295: R236–R242, 2008.

31. **Shenouda N**, **Gillen JB**, **Gibala MJ**, **MacDonald MJ**. Changes in brachial artery endothelial function and resting diameter with moderate-intensity continuous but not sprint interval training in sedentary men. *J Appl Physiol* (May 25, 2017). doi: 10.1152/japplphysiol.00058.2017.

32. **Simonson JS**, **Schiller NB**. Descent of the base of the left ventricle: An echocardiographic index of left ventricular function. *J Am Soc Echocardiogr* 2: 25–35, 1989.

33. **Stewart AD**, **Jiang B**, **Millasseau SC**, **Ritter JM**, **Chowienczyk PJ**. Acute reduction of blood pressure by nitroglycerin does not normalize large artery stiffness in essential hypertension. *Hypertension* 48: 404–410, 2006.

34. **Stöhr EJ**, **Shave RE**, **Baggish AL**, **Weiner RB**. Left Ventricular Twist Mechanics in the Context of Normal Physiology and Cardiovascular Disease: A Review of Studies using Speckle Tracking Echocardiography. *Am J Physiol Heart Circ Physiol* 311: H633–H644, 2016.

35. **Svedlund S**, **Eklund C**, **Robertsson P**, **Lomsky M**, **Gan LM**. Carotid Artery Longitudinal Displacement Predicts 1-Year Cardiovascular Outcome in Patients With Suspected Coronary Artery Disease. *Arterioscler Throm Vas Biol* 31: 1668–1674, 2011.

36. **Taivainen SH**, **Yli-Ollila H**, **Juonala M**, **Kähönen M**, **Raitakari OT**, **Laitinen TM**, **Laitinen TP**. Interrelationships between indices of longitudinal movement of the common carotid artery wall and the conventional measures of subclinical arteriosclerosis. *Clin Physiol Funct Imaging* 37: 305–313, 2017.

37. **Tanaka H**, **Seals DR**, **Monahan KD**, **Clevenger CM**, **DeSouza CA**, **Dinenno FA**. Regular aerobic exercise and the age-related increase in carotid artery intima-media thickness in healthy men. *J Appl Physiol* 92: 1458–1464, 2001.

38. **Tat J**, **Au JS**, **Keir PJ**, **MacDonald MJ**. Reduced common carotid artery longitudinal wall motion and intramural shear strain in individuals with elevated cardiovascular disease risk using speckle tracking. *Clin Physiol Funct Imaging* 37: 106–116, 2017.

39. **Tat J**, **Psaromiligkos IN**, **Daskalopoulou SS**. Carotid atherosclerotic plaque alters the direction of longitudinal motion in the artery wall. *Ultrasound Med Biol* 42: 2114–2122, 2016.

40. **Thein E**, **Hammer C**. Physiologic barriers to xenotransplantation. *Curr Opin Organ Tran* 9: 186–189, 2004.

41. **Thijssen DHJ**, **Cable NT**, **Green DJ**. Impact of exercise training on arterial wall thickness in humans. *Clin Sci* 122: 311–322, 2012.

42. **Touboul PJ**, **Hennerici MG**, **Meairs S**, **Adams H**, **Amarenco P**, **Bornstein N**, **Csiba L**, **Desvarieux M**, **Ebrahim S**, **Fatar M**, **Hernandez Hernandez R**, **Jaff M**, **Kownator S**, **Prati P**, **Rundek T**, **Sitzer M**, **Schminke U**, **Tardif JC**, **Taylor**

A, **Vicaut E**, **Woo KS**, **Zannad F**, **Zureik M**. Mannheim Carotid Intima-Media Thickness Consensus (2004-2006). *Cerebrovasc Dis* 23: 75–80, 2007.

43. **Vinkers CH**, **Tijdink JK**, **Otte WM**. Use of positive and negative words in scientific PubMed abstracts between 1974 and 2014: retrospective analysis. *British Medical Journal* (December 14, 2015). doi: 10.1136/bmj.h6467.

44. **Wagenseil JE**, **Mecham RP**. Vascular Extracellular Matrix and Arterial Mechanics. *Physiol Rev* 89: 957–989, 2009.

45. **Weiner RB**, **Baggish AL**. Acute versus chronic exercise-induced left-ventricular remodeling. *Expert Rev Cardiovasc Ther* 12: 1243–1246, 2014.

46. **Weizsacker HW**, **Lambert H**, **Pascale K**. Analysis of the passive mechanical properties of rat carotid arteries. *J Biomechanics* 16: 703–715, 1983.

47. **Wolinsky H**, **Glagov S**. Structural Basis for the Static Mechanical Properties of the Aortic Media. *Circ Res* 14: 400–414, 1964.

48. **Yli-Ollila H**, **Laitinen T**, **Weckström M**, **Laitinen TM**. Axial and radial waveforms in common carotid artery: An advanced method for studying arterial elastic properties in ultrasound imaging. *Ultrasound Med Biol* 39: 1168–1177, 2013.

49. **Yli-Ollila H**, **Laitinen T**, **Weckström M**, **Laitinen TM**. New indices of arterial stiffness measured from longitudinal motion of common carotid artery in relation to reference methods, a pilot study. *Clin Physiol Funct Imaging* 36: 376–388, 2015.

50. **Yli-Ollila H**, **Tarvainen MP**, **Laitinen TP**, **Laitinen TM**. Principal component analysis of the longitudinal carotid wall motion in association with vascular stiffness: a pilot study. *Ultrasound Med Biol* 42: 2873–2886, 2016.

51. **Yli-Ollila H**, **Tarvainen MP**, **Laitinen TP**, **Laitinen TM**. Transfer function analysis of the longitudinal motion of the common carotid artery wall. *Front Physiol* 7, 2016.

52. **Zahnd G**, **Balocco S**, **Sérusclat A**, **Moulin P**, **Orkisz M**, **Vray D**. Progressive attenuation of the longitudinal kinetics in the common carotid artery: Preliminary in vivo assessment. *Ultrasound Med Biol* 41: 339–345, 2014.

53. **Zahnd G**, **Boussel L**, **Marion A**, **Durand M**, **Moulin P**, **Sérusclat A**, **Vray D**. Measurement of two-dimensional movement parameters of the carotid artery wall for early detection of arteriosclerosis: A preliminary clinical study. *Ultrasound Med Biol* 37: 1421–1429, 2011.

54. **Zahnd G**, **Vray D**, **Sérusclat A**, **Alibay D**, **Bartold M**, **Brown A**, **Durand M**, **Jamieson LM**, **Kapellas K**, **Maple-Brown LJ**, **O'Dea K**, **Moulin P**, **Celermajer DS**, **Skilton MR**. Longitudinal displacement of the carotid wall and cardiovascular risk factors: Associations with aging, adiposity, blood pressure and periodontal disease independent of cross-sectional distensibility and intima-media thickness. *Ultrasound Med Biol* 38: 1705–1715, 2012.

APPENDIX A

COPYRIGHT PERMISSIONS AND LICENCES

A.1 Creative Commons Attribution License 3.0 (Chapter 2)
A.2 Permissions for Personal Use in a Thesis from Elseiver (Chapter 3)

Appendix A.1

Creative Commons Attribution License 3.0

(Chapter 2)

Creative Commons Legal Code

Attribution 3.0 Unported

CREATIVE COMMONS CORPORATION IS NOT A LAW FIRM AND DOES NOT PROVIDE LEGAL SERVICES. DISTRIBUTION OF THIS LICENSE DOES NOT CREATE AN ATTORNEY-CLIENT RELATIONSHIP. CREATIVE COMMONS PROVIDES THIS INFORMATION ON AN "AS-IS" BASIS. CREATIVE COMMONS MAKES NO WARRANTIES REGARDING THE INFORMATION PROVIDED, AND DISCLAIMS LIABILITY FOR DAMAGES RESULTING FROM ITS USE.

License

THE WORK (AS DEFINED BELOW) IS PROVIDED UNDER THE TERMS OF THIS CREATIVE COMMONS PUBLIC LICENSE ("CCPL" OR "LICENSE"). THE WORK IS PROTECTED BY COPYRIGHT AND/OR OTHER APPLICABLE LAW. ANY USE OF THE WORK OTHER THAN AS AUTHORIZED UNDER THIS LICENSE OR COPYRIGHT LAW IS PROHIBITED.

BY EXERCISING ANY RIGHTS TO THE WORK PROVIDED HERE, YOU ACCEPT AND AGREE TO BE BOUND BY THE TERMS OF THIS LICENSE. TO THE EXTENT THIS LICENSE MAY BE CONSIDERED TO BE A CONTRACT, THE LICENSOR GRANTS YOU THE RIGHTS CONTAINED HERE IN CONSIDERATION OF YOUR ACCEPTANCE OF SUCH TERMS AND CONDITIONS.

1. Definitions

a. **"Adaptation"** means a work based upon the Work, or upon the Work and other pre-existing works, such as a translation, adaptation, derivative work, arrangement of music or other alterations of a literary or artistic work, or phonogram or performance and includes cinematographic adaptations or any other form in which the Work may be recast, transformed, or adapted including in any form recognizably derived from the original, except that a work that constitutes a Collection will not be considered an Adaptation for the purpose of this License. For the avoidance of doubt, where the Work is a musical work, performance or phonogram, the synchronization of the Work in timed-relation with a moving image ("synching") will be considered an Adaptation for the purpose of this License.
b. **"Collection"** means a collection of literary or artistic works, such as encyclopedias and anthologies, or performances, phonograms or broadcasts, or other works or subject matter other than works listed in Section 1(f) below, which, by reason of the selection and arrangement of their contents, constitute intellectual creations, in which the Work is included in its entirety in unmodified form along with one or more other contributions, each constituting separate and independent works in themselves, which together are assembled into a collective whole. A work that constitutes a Collection will not be considered an Adaptation (as defined above) for the purposes of this License.
c. **"Distribute"** means to make available to the public the original and copies of the Work or Adaptation, as appropriate, through sale or other transfer of ownership.
d. **"Licensor"** means the individual, individuals, entity or entities that offer(s) the Work under the terms of this License.
e. **"Original Author"** means, in the case of a literary or artistic work, the individual, individuals, entity or entities who created the Work or if no individual or entity can be identified, the publisher; and in addition (i) in the case of a performance the actors, singers, musicians, dancers, and other persons who act, sing, deliver, declaim, play in, interpret or otherwise perform literary or artistic works or expressions of folklore; (ii) in the case of a phonogram the producer being the person or legal entity who first fixes the sounds of a performance or other sounds; and, (iii) in the case of broadcasts, the organization that transmits the broadcast.
f. **"Work"** means the literary and/or artistic work offered under the terms of this License including without limitation any production in the literary, scientific and artistic domain, whatever may be the

mode or form of its expression including digital form, such as a book, pamphlet and other writing; a lecture, address, sermon or other work of the same nature; a dramatic or dramatico-musical work; a choreographic work or entertainment in dumb show; a musical composition with or without words; a cinematographic work to which are assimilated works expressed by a process analogous to cinematography; a work of drawing, painting, architecture, sculpture, engraving or lithography; a photographic work to which are assimilated works expressed by a process analogous to photography; a work of applied art; an illustration, map, plan, sketch or three-dimensional work relative to geography, topography, architecture or science; a performance; a broadcast; a phonogram; a compilation of data to the extent it is protected as a copyrightable work; or a work performed by a variety or circus performer to the extent it is not otherwise considered a literary or artistic work.

g. **"You"** means an individual or entity exercising rights under this License who has not previously violated the terms of this License with respect to the Work, or who has received express permission from the Licensor to exercise rights under this License despite a previous violation.
h. **"Publicly Perform"** means to perform public recitations of the Work and to communicate to the public those public recitations, by any means or process, including by wire or wireless means or public digital performances; to make available to the public Works in such a way that members of the public may access these Works from a place and at a place individually chosen by them; to perform the Work to the public by any means or process and the communication to the public of the performances of the Work, including by public digital performance; to broadcast and rebroadcast the Work by any means including signs, sounds or images.
i. **"Reproduce"** means to make copies of the Work by any means including without limitation by sound or visual recordings and the right of fixation and reproducing fixations of the Work, including storage of a protected performance or phonogram in digital form or other electronic medium.

2. Fair Dealing Rights. Nothing in this License is intended to reduce, limit, or restrict any uses free from copyright or rights arising from limitations or exceptions that are provided for in connection with the copyright protection under copyright law or other applicable laws.

3. License Grant. Subject to the terms and conditions of this License, Licensor hereby grants You a worldwide, royalty-free, non-exclusive, perpetual (for the duration of the applicable copyright) license to exercise the rights in the Work as stated below:

a. to Reproduce the Work, to incorporate the Work into one or more Collections, and to Reproduce the Work as incorporated in the Collections;
b. to create and Reproduce Adaptations provided that any such Adaptation, including any translation in any medium, takes reasonable steps to clearly label, demarcate or otherwise identify that changes were made to the original Work. For example, a translation could be marked "The original work was translated from English to Spanish," or a modification could indicate "The original work has been modified.";
c. to Distribute and Publicly Perform the Work including as incorporated in Collections; and,
d. to Distribute and Publicly Perform Adaptations.

e. For the avoidance of doubt:

i. **Non-waivable Compulsory License Schemes**. In those jurisdictions in which the right to collect royalties through any statutory or compulsory licensing scheme cannot be waived, the Licensor reserves the exclusive right to collect such royalties for any exercise by You of the rights granted under this License;
ii. **Waivable Compulsory License Schemes**. In those jurisdictions in which the right to collect royalties through any statutory or compulsory licensing scheme can be waived, the Licensor waives the exclusive right to collect such royalties for any exercise by You of the rights granted under this License; and,
iii. **Voluntary License Schemes**. The Licensor waives the right to collect royalties, whether individually or, in the event that the Licensor is a member of a collecting society that administers voluntary licensing schemes, via that society, from any exercise by You of the rights granted under this License.

The above rights may be exercised in all media and formats whether now known or hereafter devised. The above rights include the right to make such modifications as are technically necessary to exercise the rights in other media and formats. Subject to Section 8(f), all rights not expressly granted by Licensor are hereby reserved.

4. Restrictions. The license granted in Section 3 above is expressly made subject to and limited by the following restrictions:

a. You may Distribute or Publicly Perform the Work only under the terms of this License. You must include a copy of, or the Uniform Resource Identifier (URI) for, this License with every copy of the Work You Distribute or Publicly Perform. You may not offer or impose any terms on the Work that restrict the terms of this License or the ability of the recipient of the Work to exercise the rights granted to that recipient under the terms of the License. You may not sublicense the Work. You must keep intact all notices that refer to this License and to the disclaimer of warranties with every copy of the Work You Distribute or Publicly Perform. When You Distribute or Publicly Perform the Work, You may not impose any effective technological measures on the Work that restrict the ability of a recipient of the Work from You to exercise the rights granted to that recipient under the terms of the License. This Section 4(a) applies to the Work as incorporated in a Collection, but this does not require the Collection apart from the Work itself to be made subject to the terms of this License. If You create a Collection, upon notice from any Licensor You must, to the extent practicable, remove from the Collection any credit as required by Section 4(b), as requested. If You create an Adaptation, upon notice from any Licensor You must, to the extent practicable, remove from the Adaptation any credit as required by Section 4(b), as requested.

b. If You Distribute, or Publicly Perform the Work or any Adaptations or Collections, You must, unless a request has been made pursuant to Section 4(a), keep intact all copyright notices for the Work and provide, reasonable to the medium or means You are utilizing: (i) the name of the Original Author (or pseudonym, if applicable) if supplied, and/or if the Original Author and/or Licensor designate another party or parties (e.g., a sponsor institute, publishing entity, journal) for attribution ("Attribution Parties") in Licensor's copyright notice, terms of service or by other reasonable means, the name of such party or parties; (ii) the title of the Work if supplied; (iii) to the extent reasonably practicable, the URI, if any, that Licensor specifies to be associated with the Work, unless such URI does not refer to the copyright notice or licensing information for the Work; and (iv) , consistent with Section 3(b), in the case of an Adaptation, a credit identifying the use of the Work in the Adaptation (e.g., "French translation of the Work by Original Author," or "Screenplay based on original Work by Original Author"). The credit required by this Section 4 (b) may be implemented in any reasonable manner; provided, however, that in the case of a Adaptation or Collection, at a minimum such credit will appear, if a credit for all contributing authors of the Adaptation or Collection appears, then as part of these credits and in a manner at least as prominent as the credits for the other contributing authors. For the avoidance of doubt, You may only use the credit required by this Section for the purpose of attribution in the manner set out above and, by exercising Your rights under this License, You may not implicitly or explicitly assert or imply any connection with, sponsorship or endorsement by the Original Author, Licensor and/or Attribution Parties, as appropriate, of You or Your use of the Work, without the separate, express prior written permission of the Original Author, Licensor and/or Attribution Parties.

c. Except as otherwise agreed in writing by the Licensor or as may be otherwise permitted by applicable law, if You Reproduce, Distribute or Publicly Perform the Work either by itself or as part of any Adaptations or Collections, You must not distort, mutilate, modify or take other derogatory action in relation to the Work which would be prejudicial to the Original Author's honor or reputation. Licensor agrees that in those jurisdictions (e.g. Japan), in which any exercise of the right granted in Section 3(b) of this License (the right to make Adaptations) would be deemed to be a distortion, mutilation, modification or other derogatory action prejudicial to the Original Author's honor and reputation, the Licensor will waive or not assert, as appropriate, this Section, to the fullest extent permitted by the applicable national law, to enable You to reasonably exercise Your right under Section 3(b) of this License (right to make Adaptations) but not otherwise.

5. Representations, Warranties and Disclaimer

UNLESS OTHERWISE MUTUALLY AGREED TO BY THE PARTIES IN WRITING, LICENSOR OFFERS THE WORK AS-IS AND MAKES NO REPRESENTATIONS OR WARRANTIES OF ANY KIND CONCERNING THE WORK, EXPRESS, IMPLIED, STATUTORY OR OTHERWISE, INCLUDING, WITHOUT LIMITATION, WARRANTIES OF TITLE, MERCHANTIBILITY, FITNESS FOR A PARTICULAR PURPOSE, NONINFRINGEMENT, OR THE ABSENCE OF LATENT OR OTHER DEFECTS, ACCURACY, OR THE PRESENCE OF ABSENCE OF ERRORS, WHETHER OR NOT DISCOVERABLE. SOME JURISDICTIONS DO NOT ALLOW THE EXCLUSION OF IMPLIED WARRANTIES, SO SUCH EXCLUSION MAY NOT APPLY TO YOU.

6. Limitation on Liability. EXCEPT TO THE EXTENT REQUIRED BY APPLICABLE LAW, IN NO EVENT WILL LICENSOR BE LIABLE TO YOU ON ANY LEGAL THEORY FOR ANY SPECIAL, INCIDENTAL, CONSEQUENTIAL, PUNITIVE OR EXEMPLARY DAMAGES ARISING OUT OF THIS LICENSE OR THE USE OF THE WORK, EVEN IF LICENSOR HAS BEEN ADVISED OF THE POSSIBILITY OF SUCH DAMAGES.

7. Termination

a. This License and the rights granted hereunder will terminate automatically upon any breach by You of the terms of this License. Individuals or entities who have received Adaptations or Collections from You under this License, however, will not have their licenses terminated provided such individuals or entities remain in full compliance with those licenses. Sections 1, 2, 5, 6, 7, and 8 will survive any termination of this License.
b. Subject to the above terms and conditions, the license granted here is perpetual (for the duration of the applicable copyright in the Work). Notwithstanding the above, Licensor reserves the right to release the Work under different license terms or to stop distributing the Work at any time; provided, however that any such election will not serve to withdraw this License (or any other license that has been, or is required to be, granted under the terms of this License), and this License will continue in full force and effect unless terminated as stated above.

8. Miscellaneous

a. Each time You Distribute or Publicly Perform the Work or a Collection, the Licensor offers to the recipient a license to the Work on the same terms and conditions as the license granted to You under this License.
b. Each time You Distribute or Publicly Perform an Adaptation, Licensor offers to the recipient a license to the original Work on the same terms and conditions as the license granted to You under this License.
c. If any provision of this License is invalid or unenforceable under applicable law, it shall not affect the validity or enforceability of the remainder of the terms of this License, and without further action by the parties to this agreement, such provision shall be reformed to the minimum extent necessary to make such provision valid and enforceable.
d. No term or provision of this License shall be deemed waived and no breach consented to unless such waiver or consent shall be in writing and signed by the party to be charged with such waiver or consent.
e. This License constitutes the entire agreement between the parties with respect to the Work licensed here. There are no understandings, agreements or representations with respect to the Work not specified here. Licensor shall not be bound by any additional provisions that may appear in any communication from You. This License may not be modified without the mutual written agreement of the Licensor and You.
f. The rights granted under, and the subject matter referenced, in this License were drafted utilizing the terminology of the Berne Convention for the Protection of Literary and Artistic Works (as amended on September 28, 1979), the Rome Convention of 1961, the WIPO Copyright Treaty of 1996, the WIPO Performances and Phonograms Treaty of 1996 and the Universal Copyright Convention (as revised on July 24, 1971). These rights and subject matter take effect in the relevant jurisdiction in which the License terms are sought to be enforced according to the corresponding provisions of the implementation of those treaty provisions in the applicable national law. If the standard suite of rights granted under applicable copyright law includes additional rights not granted under this License, such additional rights are deemed to be included in the License; this License is not intended to restrict the license of any rights under applicable law.

Creative Commons Notice

Creative Commons is not a party to this License, and makes no warranty whatsoever in connection with the Work. Creative Commons will not be liable to You or any party on any legal theory for any damages whatsoever, including without limitation any general, special, incidental or consequential damages arising in connection to this license. Notwithstanding the foregoing two (2) sentences, if Creative Commons has expressly identified itself as the Licensor hereunder, it shall have all rights and obligations of Licensor.

Except for the limited purpose of indicating to the public that the Work is licensed under the CCPL, Creative Commons does not authorize the use by either party of the trademark "Creative Commons" or any related trademark or logo of Creative Commons without the prior written consent of Creative Commons. Any permitted use will be in compliance with Creative Commons' then-current trademark usage guidelines, as may be published on its website or otherwise made available upon request from time to time. For the avoidance of doubt, this trademark restriction does not form part of this License.

Creative Commons may be contacted at https://creativecommons.org/.

Appendix A.2

Guidelines for Personal Use in a Thesis from Elseiver

(Chapter 3)

ELSEVIER

SEARCH CART MENU

Personal use

Authors can use their articles, in full or in part, for a wide range of scholarly, non-commercial purposes as outlined below:

- Use by an author in the author's classroom teaching (including distribution of copies, paper or electronic)
- Distribution of copies (including through e-mail) to known research colleagues for their personal use (but not for Commercial Use)
- Inclusion in a thesis or dissertation (provided that this is not to be published commercially)
- Use in a subsequent compilation of the author's works
- Extending the Article to book-length form
- Preparation of other derivative works (but not for Commercial Use)
- Otherwise using or re-using portions or excerpts in other works

These rights apply for all Elsevier authors who publish their article as either a subscription article or an open access article. In all cases we require that all Elsevier authors always include a full acknowledgement and, if appropriate, a link to the final published version hosted on Science Direct.